NEAR TR 430

April 20, 1991

COMPUTATIONAL ANALYSIS OF HIGH-SPEED EJECTION SEATS

by

Steven C. Caruso

Michael R. Mendenhall

under

SBIR Phase I

Contract No. N62269-90-C-0264

for

Naval Air Development Center

Thomas J. Marquette, Code 6032

Warminster, PA 18974-5000

Nielsen Engineering & Research, Inc.

510 Clyde Avenue

Mountain View, CA 940943-2287

Telephone: (415)968-9457 • Facsimile: (415)968-1410

SECURITY CLASSIFICATION OF THIS PAGE

REPORT DOCUMENTATION PAGE

1a. REPORT SECURITY CLASSIFICATION UNCLASSIFIED	1b. RESTRICTIVE MARKINGS NONE
2a. SECURITY CLASSIFICATION AUTHORITY N/A	3. DISTRIBUTION/AVAILABILITY OF REPORT
2b. DECLASSIFICATION/DOWNGRADING SCHEDULE N/A	
4. PERFORMING ORGANIZATION REPORT NUMBER(S) NEAR TR 430	5. MONITORING ORGANIZATION REPORT NUMBER(S)
6a. NAME OF PERFORMING ORGANIZATION NIELSEN ENGINEERING AND RESEARCH, INC.	6b. OFFICE SYMBOL (If applicable)
6c. ADDRESS (City, State, and ZIP Code) 510 CLYDE AVENUE MOUNTAIN VIEW, CA 94043-2287	7a. NAME OF MONITORING ORGANIZATION NAVAL AIR DEVELOPMENT CENTER AIR VEHICLE AND CREW SYSTEMS
	7b. ADDRESS (City, State, and ZIP Code) CODE 6032 WARMINSTER, PA 18974-5000
8a. NAME OF FUNDING/SPONSORING ORGANIZATION Naval Air Development Center	8b. OFFICE SYMBOL (If applicable) Code 6032
8c. ADDRESS (City, State, and ZIP Code) Warminster, PA 18974-5000	9. PROCUREMENT INSTRUMENT IDENTIFICATION NUMBER
	10. SOURCE OF FUNDING NUMBERS

PROGRAM ELEMENT NO.	PROJECT NO.	TASK NO.	WORK UNIT ACCESSION NO.

11. TITLE (Include Security Classification)

Computational Analysis of High-Speed Ejection Seats

12. PERSONAL AUTHOR(S)
Caruso, S. C. and Mendenhall, M. R.

13a. TYPE OF REPORT	13b. TIME COVERED	14. DATE OF REPORT (Year, Month, Day)	15. PAGE COUNT
TECHNICAL	FROM 91 AUG 20 TO 91 APR 20	91 April 20	85

16. SUPPLEMENTARY NOTATION

Technical Monitor: Thomas J. Marquette

17. COSATI CODES		
FIELD	GROUP	SUB-GROUP
01	03.03	
23	06	

18. SUBJECT TERMS (Continue on reverse if necessary and identify by block number)
Ejection Seats
Computational Fluid Dynamics
Aerodynamics
Flow Field
Transonic Flow

19. ABSTRACT (Continue on reverse if necessary and identify by block number)

This final report documents the results of a study demonstrating the use of analytical computational fluid dynamics methods to predict the aerodynamic characteristics and flowfield details of a typical ejection seat with an occupant. This feasibility study was limited to two-dimensional flow around a configuration defined by a longitudinal plane of symmetry through the center of the ejection seat. Navier-Stokes codes were used to predict the steady and time-dependent transonic and supersonic flow characteristics for a series of ejection seats for which wind tunnel data are available, and comparisons of measured and predicted forces and moments are presented to show the trends produced by the analysis techniques. Structured and unstructured grids were considered in the calculations to demonstrate the capability of the method and to guide the planning for a future three-dimensional approach. The report concludes with recommendations for a program leading to the development of a three-dimensional CFD analysis code applicable to the study of windblast loads and minimum drag design of modern ejection seats.

20. DISTRIBUTION/AVAILABILITY OF ABSTRACT	21. ABSTRACT SECURITY CLASSIFICATION
☒ UNCLASSIFIED/UNLIMITED ☐ SAME AS RPT. ☐ DTIC USERS	UNCLASSIFIED
22a. NAME OF RESPONSIBLE INDIVIDUAL	22b. TELEPHONE (Include Area Code) / 22c. OFFICE SYMBOL

DD FORM 1473, 84 MAR 83 APR edition may be used until exhausted. All other editions are obsolete

SECURITY CLASSIFICATION OF THIS PAGE
UNCLASSIFIED

U.S. Government Printing Office: 1985—507-047

TABLE OF CONTENTS

SUMMARY

This final report documents the results of a study demonstrating the use of analytical computational fluid dynamics methods to predict the aerodynamic characteristics and flowfield details of a typical ejection seat with an occupant. This feasibility study was limited to two dimensional flow around a configuration defined by a longitudinal plane of symmetry through the center of the ejection seat. Navier-Stokes codes were used to predict the steady and time-dependent transonic and supersonic flow characteristics for a series of ejection seats for which wind tunnel data are available, and comparisons of measured and predicted forces and moments are presented to show the trends produced by the analysis techniques. Structured and unstructured grids were considered in the calculations to demonstrate the capability of the method and to guide the planning for a future three-dimensional approach. The report concludes with recommendations for a program leading to the development of a three-dimensional CFD analysis code applicable to the study of windblast loads and minimum drag design of modern ejection seats.

INTRODUCTION

Operational requirements of modern tactical aircraft often involve high speed flight at low altitude; therefore, the ejection seat performance envelope must be expanded to include these flight regimes if pilot and crew survival rates are to be maintained or improved. Reference 1 notes that the performance envelope of escape systems in current fighter aircraft is deficient with respect to the aircraft flight envelope. Supporting statistics seem to show a declining trend in survival rate by 1980 (Ref. 2), and recent statistics indicate a high probability of injury at high speeds (Ref. 3). There is still a major problem with safe ejection at moderate to high speeds. For example, the injury rate caused by aerodynamic windblast effects exceeds 10% at 375 knots, but the major and fatal injury rate is nearly 50% when ejection speed increases to 500 knots (Refs. 4 and 5). Significant advances in ejection seat design are required if safe escape at 700+ knots is the desired goal.

Pilot ejection at low altitude and high speed places the seat and pilot in an environment of high dynamic pressure and subsequent high loads. The sources of injury to the pilot are (1) the deceleration forces caused by the high drag of the ejection seat, (2) windblast or aerodynamic loads on the pilot (shock waves may be important at 700 knots), and (3) high rotation rates caused by an aerodynamically unstable ejection seat. The first of these injury sources may be the most difficult to eliminate because of the physical constraints on ejection seat design dictated by the requirements of the airframe. The solution to the latter two sources may not be compatible with the deceleration problem, and it is possible that design modifications to reduce these effects will actually aggravate the deceleration loads by increasing drag.

Currently, most improvements in ejection seat design are based on evolutionary changes to configurations for which there is a knowledge base of information. This information is typically generated from parametric modifications in scale model tests in wind tunnels (Refs. 6 through 9). As the speed range for safe ejection increases toward the 725-knot goal, the resulting transonic speeds present other difficulties for consideration. First, transonic flow creates special problems in wind tunnel testing because of the unsteady nature of the flow; therefore, measurements in this speed regime are difficult and frequently

inaccurate. Second, the high loads in this speed range dictate stronger and more expensive models, a significant disadvantage considering the large number of models or variations required for parametric testing. Finally, the cost and time required for a comprehensive wind tunnel investigation of a new ejection seat concept can be a limiting factor in the number of possible configurations included in the program, thus increasing the chances that an optimum ejection seat configuration will not be found.

As discussed in Reference 10, there is substantial variation in aerodynamic behavior between different types of ejection seats; therefore, it is impossible to predict ejection seat performance using knowledge of the performance of another seat. This simply means that the performance of a new ejection seat configuration is not known until an experimental program is completed. At this point in the development of a new ejection seat, a large investment in cost and time has been made with little guarantee that the new seat will be successful.

Recent advances in the capabilities of computational fluid dynamics (CFD) provide an opportunity to study ejection seat designs and identify possible configuration improvements prior to wind tunnel testing. As demonstrated in the aircraft industry (Ref. 11), CFD can be used to analyze a number of potential configurations prior to wind tunnel testing. The total number of candidate configurations which can be studied numerically is much larger than the number which can be tested experimentally; therefore, it is possible to eliminate the poor or marginal configurations prior to testing. As a consequence, the wind tunnel test can be dedicated to the detailed study of a small number of possible configurations in the search for the optimum.

The purpose of this report is to describe a feasibility study which demonstrates an analytical CFD capability to predict the detailed fluid mechanics of ejection seats in transonic flows at high dynamic pressures. Since drag reduction and separated flows are key interest points for analysis, it is necessary to obtain solutions of the Navier-Stokes equations for these complex configurations. Such solutions require the generation of detailed computational grids. These and other problems associated with the development of an analytical procedure are described in the following sections. The goal of the proposed

analytical prediction method is to provide information on the detailed fluid mechanic characteristics of the flow around an ejection seat such that design and analysis of safety improvements can be investigated prior to verification by experimental testing.

GENERAL APPROACH

TECHNICAL OBJECTIVE

The technical objective of the Phase I investigation reported herein is to perform a feasibility study which will demonstrate an analytic computational fluid dynamic capability to predict the aerodynamic characteristics of an ejection seat in transonic flow at high dynamic pressure. This demonstration is a necessary first step in the development of a CFD capability which can be applied to the improvement of ejection seat designs in those critical areas involving aerodynamic forces and moments, particularly in the area of drag reduction. Specifically, the CFD methods can be applied to the prediction of the aerodynamic coefficients and stability derivatives of the seat configuration and the flowfield around the seat and pilot. This will permit the prediction of the aerodynamic pressure distribution on the pilot and the resulting forces on the head and limbs.

The above technical objective is accomplished through the coupling of a number of available technologies. An existing code to solve the Navier-Stokes equations for the transonic flow around a complex ejection seat and pilot configuration is used. For demonstration purposes, the code is applied initially to a two-dimensional longitudinal cross section in the plane of symmetry of the configuration to investigate various critical computational parameters, such as, (1) grid requirements, (2) flow stability, (3) transient loads, and (4) possible flow control. Results of these preliminary calculations are compared with wind tunnel data on existing ejection seat configurations to verify trends in the predicted pressure distributions (Ref. 12) and flowfields (Ref. 7).

Although the preliminary calculations are restricted to two-dimensional flow because of the limited scope of the feasibility study, the knowledge gained in the study will permit

the formulation of a plan for the development of a three-dimensional CFD analysis code in a Phase II investigation. Such a plan is presented in a later section of this report. The ultimate objective of this advanced effort is a computational technique for the complete aerodynamic analysis of ejection seats with a crew member. The method will not be dependent on a priori knowledge of the aerodynamic coefficients and, as such, will be a true prediction method. The method will have application to configuration design changes for the purpose of minimizing some flow characteristic such as drag and/or windblast loads.

PROPOSED METHOD

With the development of modern computer hardware and software technology, more powerful analytical methods are being developed which can be applied to the problem of ejection seat analysis. Current research in computational fluid dynamics is aimed at achieving accurate predictions of complex flowfields; therefore, the primary objective of this work is to develop a flowfield prediction method which can be used for basic understanding of the unsteady, time-dependent transonic flow about ejection seat configurations. CFD technology is currently available in the analytical community; therefore, the proposed effort is an application of existing technology, not a development of new technology.

First, an existing Navier-Stokes solution procedure and code which is applicable to complex two-dimensional configurations in unsteady transonic flow is required. Although the present feasibility study is restricted to two-dimensional flow, eventual extension to three dimensions for a future effort is a prime consideration in the selection of a method. Second, a procedure to produce a solution grid around an ejection seat with an occupant is necessary. Because of the complex nature of this configuration and the desire to modify the grid easily, an unstructured grid is anticipated to be the best choice. Again, extension to three dimensions without major difficulty is the prime concern.

The components of the proposed prediction method must be consistent with a CFD analysis method applicable to preliminary design; that is, the final method should be easy to use, require a minimum of time to set up or modify a configuration, and produce reliable

results which are easily interpreted. The latter requirement is particularly important for CFD methods which generate large quantities of information on the solution of a problem.

The initial or prototype method developed to demonstrate the feasibility of the proposed approach is verified by comparison with available experimental test cases where possible. Since the method is two dimensional, the comparisons must be qualitative in most cases; however, it will be important to see that trends in forces and moments and pressure distributions are predicted, particularly unsteady or transient phenomena. The predicted results are examined for consistency and physical realism to provide some validation for the preliminary method in a later section.

TECHNICAL APPROACH

A detailed description of the technical approach employed to investigate the feasibility of a computational method to predict ejection seat aerodynamic characteristics is presented. Since computational fluid dynamics is still in the early stages of use for practical aerodynamic analyses of complex configurations, it is necessary to outline the technical approach in detail and provide some of the deliberations which were essential to the method selection process. A careful build-up of the methods involved was made to assist in the identification of possible problem areas which could be critical to the final method.

For this initial study, calculations are restricted to two-dimensional flows in the ejection seat longitudinal plane of symmetry. The following sections describe the several components of the method beginning with a brief discussion of the background of the approach. This is followed by details of the computational mesh development and the flowfield calculation techniques. In a later section, preliminary results from two-dimensional Navier-Stokes calculations are corrected for three-dimensional effects and compared with experimental data to validate the methods and demonstrate the feasibility of the technical approach.

BACKGROUND

Ejection seats present particularly difficult geometries for computational analysis, and they require unconventional mesh approaches to suitably perform flowfield predictions. For this reason, both conventional and unconventional grid generation methods were considered. A previously-developed, unstructured mesh approach (Ref. 13) for iced airfoils was suggested as being appropriate for application to ejection seat models; however, as the research in this project proceeded, a different technical approach emerged. An outline of this process is described next.

With conventional structured mesh methods, a single grid is usually created which meshes the entire flowfield, extending from the surface of the configuration out to the far field boundaries. This approach may be difficult to implement if the configuration geometry is complex; for example, in the procedure designed for iced airfoils (Ref. 13), the difficulty posed by the geometry is attacked by decomposing the flow domain into two or more regions which are each easily meshed using conventional structured mesh approaches. Then, mesh points of all the component grids are merged to create a complete mesh that is unstructured and which represents the entire flowfield.

Since ejection seats are a new application for mesh generation methods, a structured mesh generation technique was used for a single two-dimensional grid whose domain covered the flowfield in the immediate vicinity of a typical ejection seat configuration in the longitudinal plane of symmetry. It was relatively simple to generate a single, conventional structured mesh possessing good mesh qualities which covers the entire flowfield, extending from the surface of the ejection seat to the far field flow boundary. This is possible because conventional ejection seat geometries (those without radical protuberances) are not particularly complex in the longitudinal plane of symmetry. It is unlikely that a single, complete structured mesh can be created if, for example, either the two-dimensional configuration is in relative motion to a fixed surface or if the fully three-dimensional configuration is being modeled. Such cases require a more complex meshing strategy like the unstructured approach.

Navier-Stokes codes for unstructured meshes are in early stages of development, and an unstructured mesh Navier-Stokes flow code was not generally available at the initiation of this effort. An Euler code was available, but an Euler code cannot be expected to produce realistic results for the bluff body flowfields typical with ejection seats because of the dominant effect of flow separation. Navier-Stokes codes using structured meshes are readily available. Therefore, the initial computations performed in this investigation were made with a conventional structured mesh approach to demonstrate the capability of CFD to predict ejection seat flowfields. An unstructured mesh code, which became available late in the investigation, was used for a limited number of additional calculations to illustrate the capability of the unstructured mesh approach and to demonstrate the similarity and differences between the results.

COMPUTATIONAL GRID DEVELOPMENT

Structured Mesh

Conventional meshes in common usage today are usually structured; that is, the connectivity pattern of the mesh is uniform and easily described. Generally, the connectivity pattern is a rectangular array of points. For example, each point in a two-dimensional mesh can be identified by a unique pair of integer indices (i,j), and all its immediate neighbors can be identified simply by incrementing these indices, i.e., $(i\pm1,j\pm1)$. This structured nature of the mesh permits certain efficiencies to be obtained in performing operations on the mesh (fast solution algorithms for example). However, because it is structured, it is limited in its ability to adapt to changes in its boundaries and its own complexity. The mesh in the vicinity of a time varying boundary must be locally deformed to conform to the movement of the boundary. If the deformation is too severe, a completely new structured mesh must be constructed in order to avoid grid-induced inaccuracies.

Unstructured Mesh

In contrast to a structured mesh, an unstructured mesh has no obvious structure in its connectivity pattern; consequently, it can adapt its boundaries and its complexity much more easily than a structured mesh by undergoing a local restructuring. The connectivity pattern is first determined when the mesh is generated and stored, usually in the form of lists of neighboring grid points and volumes for later use. To accomplish a grid restructuring, points or cells are added, removed, or repositioned, then linked to the existing pattern through an updating of the neighbor lists. During an unsteady ejection seat computation, for example, individual triangular elements could be removed and repositioned to accommodate the movement of the configuration boundary with respect to the oncoming stream.

Mesh Generation

All computational meshes used in this study were created using a hyperbolic grid generation code (Ref. 14), a conventional structured mesh generator. This program creates a mesh by solving hyperbolic partial differential equations for the coordinates of the grid points. The program requires an input description of the configuration is terms of (x,y) coordinates. A mathematical description of the surface of the configuration is constructed by computing cubic-spline polynomials from the input (x,y) pairs. An initial grid point distribution along the surface is created by interpolation using the cubic splines. These initial grid point locations are then "marched away" from the surface in a stepwise manner by solving the hyperbolic governing equations at each step. Clustering of the mesh can be provided in directions both normal and circumferential to the surface as needed.

FLOWFIELD PREDICTION

Methods

Advanced Navier-Stokes methods for aerodynamic applications are generally based on structured meshes and can be grouped into two broad categories: finite difference and finite volume methods. Finite element methods are not considered here because they are not as well-developed for CFD applications, and since most CFD codes are based on the former methods, the technology developed in this work can be more readily adapted to existing codes.

Finite difference methods for Navier-Stokes computations are often based on a solution of the governing equations in a transformed, general curvilinear coordinate system. It is important that the computational grid be regular and the coordinate lines as nearly orthogonal as possible so that the grid does not induce inaccuracies in the finite difference equations. However, a good grid is difficult to generate when the domain is geometrically complex, as is the case of fully three-dimensional ejection seats with an occupant. For unsteady ejection seat problems, the relation of one boundary surface (the seat) to another (the airframe) can be time varying, and the mesh must be adjusted accordingly. For a finite difference mesh, this usually requires regenerating the entire grid, an expensive and time consuming problem.

For finite volume methods, the Navier-Stokes equations are solved in integral form. Grids can be generated in the same manner as for finite difference methods, but they are no longer required to be orthogonal, and the mesh cells can be constructed as general quadrilaterals. Although the finite volume mesh is somewhat more flexible than the finite difference mesh, both are limited in their ability to deal with complex geometries and time varying boundaries. The difficulty arises from two inherent characteristics of these grids. First, the underlying geometrical form for each mesh, the quadrilateral, is not necessarily optimal for complex geometries. Secondly, triangular mesh structures, often used in finite element methods, can be more easily applied to difficult topologies.

Codes

The NASA Ames Research Center code, ARC2D (Ref. 15), is used to compute the structured-mesh ejection seat flowfields. ARC2D has been widely tested and is used throughout the aerodynamic engineering community, and it has been shown to produce excellent agreement with experimental results for a variety of configurations over a wide range of Mach numbers and angles of attack.

ARC2D solves the two-dimensional Euler and thin-layer Navier-Stokes equations by using a conventional implicit finite-difference scheme. Calculations can be made in either a time-accurate mode for unsteady flowfields, or in a time-inaccurate mode to compute steady-state solutions efficiently. A complete description of the equations and methods used in ARC2D can be found in Reference 15.

A simplified turbulence model included in ARC2D is appropriate only for attached boundary layers or very simple shear layers. Consequently a turbulence model is not used, and all calculations, considering both structured and unstructured meshes, are made assuming laminar flow. The arguments for neglecting the effects of turbulence are presented below.

The unstructured mesh code, NSU2D, solves the Navier-Stokes equations by using an explicit, finite volume method formulated for triangular meshes. Similar to ARC2D, the code may be run in time-accurate or time-inaccurate modes. NSU2D currently has no turbulence model; therefore, it can only be used to predict laminar flows at this time. A complete discussion of the algorithms employed in NSU2D are presented in Reference 16.

Some comments on the omission of turbulence modeling in the ejection seat flowfield predictions are necessary. A case can be made that turbulence is a secondary effect in ejection seat flows. Since all analyses in this study are approximate due to the two-dimensional limitation, the assumption of laminar flow does not compromise the overall goal of this study to demonstrate the capability of CFD for predicting ejection seat flowfields. Turbulence modeling will certainly be important for obtaining accurate three-

dimensional flowfield predictions. Turbulence will affect the state of the boundary layer on the surface of the configuration and also in the wake. In many cases, flow separation on the ejection seat configuration is due to sharp corners, and not the condition of the boundary layer. Since the average base pressure (on the leeward side of the configuration) is influenced primarily by the separation location, a realistic assessment of ejection seat drag is possible even if turbulence effects are neglected.

Once separated, the wake flow will undergo a rapid transition to turbulence due to the characteristically high Reynolds numbers of these flowfields. Without turbulence modeling, the downstream development of the wake cannot be adequately predicted; however, prediction of the far-field wake is not the primary interest in this initial investigation. It can also be argued that turbulence plays a secondary role in flows which exhibit significant vortex shedding and where the dominant influences are provided by the large scale vortical structures. However, the unsteadiness of the wake can be affected by turbulence, which in turn can feed back into the unsteadiness in the loads on the configuration. Consequently, the accuracy of the time-dependent behavior of the loads (amplitudes and frequencies) is expected to be influenced by the lack of turbulence modeling. Finally, it should be noted that current engineering level turbulence models for strongly separated flows are often inadequate (Ref. 17).

There is also the possibility that the restriction to laminar flow at Reynolds numbers at which flow instabilities may occur could cause unsteadiness in the solutions. This problem area is discussed in more detail in a later section.

Computational Requirements

Computation requirements are limiting factors in any computational analysis. These requirements consist of engineering time to set up an anlysis and the actual computer time required to produce the results. Since this ultimately translates into the cost of the analysis of an ejection seat, it is essential that the real cost of a computation be considered a part of this feasibility study. The following information developed in the course of the investigation is provided to illustrate typical computer requirements.

The hyperbolic mesh generation algorithm is very efficient, and a typical two-dimensional ejection seat mesh can be generated in a few minutes on a VAX 11/780 computer. This would amount to seconds on a supercomputer.

The structured mesh flow code, ARC2D, requires considerably more computer power than the grid generation program. Although it can execute on small mainframes or powerful workstations, ARC2D can be run efficiently only on supercomputers. This is typical of most advanced CFD codes. A single flowfield computation made with ARC2D requires 15-20 cpu hours on a SUN SPARCstation 1 workstation; while the same computation executes in approximately 10-15 cpu minutes on a CRAY X-MP supercomputer.

The unstructured mesh code runs slower than ARC2D, typically by a factor of three to five for a steady state calculation using the same set of mesh points. However, since running times are proportional to the number of grid points, this discrepancy can be reduced because the unstructured mesh approach permits a more efficient use of grid points. It is the fewer number of grid points required by an unstructured mesh that provides the computational advantage in both time and cost.

RESULTS

As discussed in the previous section, many calculations of ejection seat flowfields were made using the structured mesh code to demonstrate the technical approach. Additional results were obtained with an unstructured mesh code to further demonstrate the feasibility of this aspect of the approach. In this section, the structured mesh results are described first, followed by a description of the unstructured mesh results.

STRUCTURED MESH

Three different ejection seat configurations were investigated using the structured mesh flowfield code. The configurations include a reclined ejection seat model (Ref. 8), a F-106 ejection seat model (Ref. 18), and a model of the Navy SIIIS-3ER seat (Ref. 19). The results for each configuration are presented individually.

Reclined Ejection Seat

The first configuration considered is a wind tunnel model of a dummy in a reclined ejection seat (Ref. 8). The test conditions cover a wide range of freestream Mach numbers and angles of attack and yaw (including zero yaw for which two-dimensional simulations are most appropriate).

The surface definition for the profile of the model in the longitudinal plane of symmetry shown in Figure 1 was obtained by digitizing the scaled description presented in Reference 8. Several two-dimensional structured grids were constructed about this configuration using the hyperbolic grid generation code (Ref. 14) described in the previous section. The mesh generation experience gained during this gridding exercise demonstrated the ease with which a single, complete, structured two-dimensional mesh can be generated about this typical ejection seat configuration. The complete grid used in the flowfield calculation and a detail view in the vicinity of the configuration are shown in Figures 2(a) and (b), respectively.

Laminar Navier-Stokes calculations made with this grid were performed at two freestream Mach numbers, 0.6 and 1.2, and at four angles of attack from 35° to 135°. The freestream Reynolds number is 12×10^6 per foot for all cases.

Results for the supersonic freestream flow condition at $\alpha = 35°$ are presented in Figures 3-5. The flowfield results are shown in Figure 3 as computed velocity vectors, contours of the pressure, Mach number, and the stream function fields in the vicinity of the

configuration. For steady flows, the stream function contours are equivalent to streamlines. For all supersonic freestream cases, a steady-state flowfield was obtained.

The following flow features are apparent in the results presented in Figure 3. Forward flow stagnation occurs in the lower leg area on the dummy. A bow shock is located some distance upstream of the model as can be seen in the far field view shown in Figure 3(d). The flow rapidly accelerates, with accompanying pressure drop and Mach number rise, around the helmet and feet areas, followed by a separation at both locations. The wake of the body is very localized and its pressure level is nearly constant as seen in Figure 3(b). The flow outside the near wake undergoes a weak compression, both above and below the wake, as the flow proceeds past the end of the recirculation region. The outer flow compression areas are illustrated by the weak pressure rise, Mach number decrease, and bending of streamlines in the vicinity of the oblique shocks which are located just downstream of the end of the wake.

The pressure coefficient on the surface of the reclined ejection seat configuration is shown in Figure 4. The profile of the seat and occupant is superimposed on the pressure coefficient to illustrate the distribution over the configuration. Notice that the negative pressure on the base or back side of the seat is nearly constant, a common phenomenon in regions of separated flow. The regions of high pressure on the front surface are also uniform. The highest pressure is in the stagnation region on the legs of the dummy, there is a lower pressure where the flow accelerates around the knee region, and the chest and face region has a uniform positive pressure. The predicted surface pressure distribution can be integrated to obtain the components of force and the moments on the configuration.

Measured pressure distributions on the reclined ejection seat are not available for comparison with the predicted results; therefore, validation of the computational method must be accomplished using the measured forces and moments on the configuration. To provide a reasonable comparison between the two-dimensional calculations and three-dimensional experimental results, the computed forces and moments on the configuration must be corrected for three-dimensional effects in some rational manner. Based on the traditional relationship between two-dimensional airfoil and three-dimensional wing

characteristics, the three-dimensional force distribution on the ejection seat was estimated by assuming an elliptical distribution of the loading in the spanwise direction. This presumes the predicted two-dimensional loading acts on the plane of symmetry, and the loading over the width of the configuration varies in an elliptical manner. This assumption is not very good for very low aspect ratio bodies like the ejection seat, but it should provide a reasonable estimate of the trend of the predicted forces and moments.

The estimated three-dimensional loads on the reclined ejection seat are compared with the experimental results in Figure 5 where the normal and axial forces and pitching moment are defined in terms of the axes shown in Figure 1. The reasonable agreement in the magnitude of the normal and axial forces in Figures 5 (a) and (b) is surprising since the flowfield around the actual configuration is highly three-dimensional and the above correction is approximate at best. More importantly, the predicted trend of the forces with angle of attack seems to be in good agreement with the measurements. The comparison of pitching moments in Figure 5 (c) shows much poorer agreement; although, the computed magnitude of pitching moment is not unreasonable. The measured moments appear to be more nonlinear than those calculated, but it must be noted that there are insufficient computed points to resolve the extreme nonlinear behavior exhibited by the experimental results.

The same reclined ejection seat configuration with the same structured grid was considered in subsonic flow ($M_\infty = 0.6$) over the same range of angles of attack. For most angles at which computations were made ($\alpha = 35°, 115°$, and $135°$), the configuration presents a bluff body shape to the flow, and the computed results were found to be unsteady or periodic in nature. The computed normal force and pitching moment coefficients as a function of iteration number or time are shown in Figure 6 for $\alpha = 35°$. These forces and moments have been corrected for three-dimensional effects using the elliptic loading approximation described above. The results indicate a periodic solution and possibly the existence of a very regular pattern of vortex shedding from the ejection seat. The details of the computed unsteadiness can be examined by looking at the predicted flow characteristics at two extreme points in the solution. These points are designated T_1 and T_2 in Figure 6, and they correspond to predicted results at 5,600 and 7,000 iterations,

respectively. Since the calculated flow characteristics have converged to a periodic solution at this stage of the computation, two closer points could have been selected; however, it was numerically more convenient to choose points at the ends of a block of computations. The results will be identical to those at other iterations which have the same force levels because of the regular behavior of the solution.

It should be noted here that for the subsonic freestream calculations, a steady state flowfield was achieved for only a single angle of attack, $\alpha = 75°$. Under this flow condition, the configuration presents a nearly streamlined profile to the oncoming flow vector. Since this flow condition is not as interesting as one which provides unsteady results, the unsteady flow condition at $\alpha = 35°$ is examined in detail below.

The character of the unsteady flowfield can be studied by examining in detail the velocity and pressure fields, the Mach number contours, and the stream function field. Calculated results are presented in Figures 7 through 11 for two times approximately corresponding to the two extremes in the loading curves, T_1 and T_2, in Figure 6. Note that the stream function contours do not represent streamlines because the flow is unsteady; however, they are useful as indicators of vortical flow regions in the wake of the configuration.

In the velocity vector results shown in Figure 7, notice that the large vortex located in the wake aft of the base of the ejection seat has an opposite sense of rotation for the two times. The base flow is not a stationary rotating region, but it is a periodic stream of vortices shed from some location(s) on the configuration. It is apparent from these two examples that separation and subsequent vortex shedding is likely occurring near the dummy's head and feet or other seat edges. The periodic nature of the results indicate that the dominant separation location is changing with time, much like that observed in the wake of a cylinder where a Karman vortex street of alternating vortices is organized by the motion of the separation points on the upper and lower surfaces of the cylinder.

The normalized pressure contours in Figure 8 further illustrate the oscillating or periodic features of the wake flow. The low pressure in the centers of the vortices

originating from the head and feet regions of the configuration is moving from a location above and behind the head to a position nearer the seat and behind the head in the extreme conditions shown in Figures 8 (a) and (b). Similar verification of the periodic motion in the wake region is shown in the Mach number contours in Figure 9 and the stream function values in Figure 10.

Surface pressures on the reclined ejection seat for times T_1 and T_2 are presented in Figures 11 (a) and (b), respectively. The time variation in pressure is seen to be small on the windward side of the configuration, but is large on the leeward side. It is the change in pressure on the lee side of the seat that has the major influence on the forces and moments on the ejection seat. Note also that the unsteady pressure differentials on the configuration are easily determined from plots such as these.

The estimated three-dimensional forces for the subsonic freestream cases are obtained from time-averaging the predicted forces because of the unsteady flow conditions. For these subsonic results, an alternative to the elliptic loading model described previously is employed. In this case, the calculated two-dimensional results are corrected by a factor which relates experimental drag coefficients for a cylinder to that for a two-dimensional flat plate or a plate of small aspect ratio (Ref. 20). The computed results are compared with the experimental data in Figure 12. The agreement between measured and estimated normal force and axial force coefficients is similar to those shown previously. The results at 75° angle of attack, the only steady state result from the subsonic calculations, are generally very good. The overall trend of the measured and predicted forces is similar, providing some credibility to the calculation procedure. The details of the pitching moment characteristics in Figure 12(c) are not in particularly good agreement, but it is well known that pitching moments are much more difficult to predict accurately than forces. Also, there may be too few computed points to properly illustrate the nonlinear behavior shown by the experiments.

As noted above, the qualitative behavior of the predicted wake on the lee side of the ejection seat is similar to experimental results for the subsonic and transonic flow over a cylinder (Refs. 21 and 22). At subcritical Mach numbers, the cylinder wakes exhibit a

regular vortex shedding process similar to the subsonic ejection seat results just described. As the freestream Mach number is increased, the cylinder's wake changes from the periodic shedding to a quasi-steady, necked shape which persists to supersonic speeds. There is definite similarity of the observed cylinder wake shape and the location of the expansion and compression regions for transonic Mach numbers (Ref. 22) with the corresponding ejection seat wake features calculated for low supersonic freestream flows shown above.

The agreement between computed and experimental characteristics is surprising when it is considered that the dummy/ejection seat configuration is a very low aspect ratio, rectangularly-shaped, bluff body at most angles of attack (Fig. 1). However, the two-dimensional results, modified for end effects, provide a qualitative estimate of the body forces and exhibit correct trends with flow angle of attack. Therefore, the reasonable agreement described above is more an indication the computational approach has promise, not that the specific two-dimensional method can represent complex three-dimensional problems.

F-106 Ejection Seat

The second configuration considered is a one-half scale F-106 seat configuration (Ref. 18). Figure 13 shows a sketch of the half scale F-106 seat/dummy configuration from which the surface definition was obtained. A close-up view of the grid in the vicinity of the configuration is shown in Figure 14. Laminar Navier-Stokes calculations using this grid were performed at a single freestream Mach number of 1.2 and at four angles of attack, ±45° and ±135°. The freestream Reynolds number was 12×10^6 per foot for all calculations.

Steady-state flowfields were obtained for all cases as in the previous supersonic results. The predicted flowfields are qualitatively similar to the supersonic-freestream flowfields obtained for the reclined seat configuration described in Figures 3 and 4, and estimated three-dimensional loads were derived from the two-dimensional loads in the same manner as was done for the reclined seat configuration. The approximate three-dimensional forces and moment coefficients are compared with the experimental results in Figure 15. The forces are given in terms of the axes shown in Figure 13.

As was the case with the reclined seat, the trend of the predicted force and moment characteristics is in reasonable agreement with the measured data. Again, the pitching moment seems to be the most difficult to predict accurately because of the sensitivity to the predicted distribution of forces on this complex configuration. These results, coupled with those obtained previously, provide some further verification for the technical approach using a two-dimensional, structured CFD method for estimating complex three-dimensional data trends for ejection seats.

SIIIS-3ER Ejection Seat

The next ejection seat model investigated using the structured mesh is a 0.65-scale SIIIS-3ER configuration (Ref. 19). The surface definition for this seat was developed from a full scale blueprint supplied by the NADC sponsor; however, the description of the seat does not include a complete description of the dummy's profile. Specifically, the dummy's lower torso and lower extremities are not included, and two different positions of the dummy's head and upper torso are indicated on the drawing. To obtain a complete configuration for the CFD work, a profile of the dummy's lower torso and extremities was estimated and combined with one of the upper torso and head positions. The outline of the resulting configuration used for the CFD simulations is indicated by the bold line shown in Figure 16, a reproduction of the seat blueprint. A close-up view of the resulting grid generated about this configuration is shown in Figure 17.

Analysis of the available experimental data for this configuration (Ref. 19) indicates a weak dependence of the three-dimensional loads on subsonic freestream Mach number for the basic configuration (without yaw stabilizers) at a Reynolds number of 1.5×10^6 per foot. Therefore, a single Mach number of 0.75 was selected for the simulation, and calculations were made at four angles of attack from 0° to 40°. The flow was again assumed laminar as in the previous calculations.

Unsteady flowfields were obtained at all angles of attack as described previously for the subsonic reclined ejection seat cases (Figs. 6-11). The estimated three-dimensional loads

were computed and time-averaged using the same procedure employed in all previous cases. However, in this instance, the resulting force coefficients were significantly larger than the experimental values. This result is inconsistent with all previous numerical results which showed reasonable agreement between measured and predicted aerodynamic characteristics. It is possible that certain assumptions made for this seat are contributing to the poor comparisons; for example, uncertainties in geometric details of the configuration may have a significant impact on the predicted force coefficients.

Since it is apparently not possible to systematically estimate the magnitude of the three-dimensional forces on this seat, it is still possible to get meaningful results from the two-dimensional CFD predictions for the SIIIS-3ER configuration. To facilitate comparison with experimental results and provide an indication of trends, the predicted force coefficients are multiplied by a single scaling factor defined as the ratio of the measured three-dimensional experimental and predicted two-dimensional axial force coefficients at 0° angle of attack; that is, ratio = C_X/c_X. This single factor, developed at $\alpha = 0°$, is used to scale both the predicted axial and normal force coefficients at all angles of attack.

Comparison of the scaled computational results and the measured forces is shown in Figure 18. The trend of the axial force coefficient with angle of attack (Fig. 18 (a)) is in reasonable agreement with experiment. The normal force coefficients shown in Figure 18 (b) are not in as good agreement. The agreement in axial force coefficient is reasonable to expect since the range of flow angles is relatively small, and the drag due to bluff body separation effects is the primary contributor to C_X. Conversely, the normal force results from pressures acting on irregular surfaces such as the pilot's helmet and lap area and the bottom and angled back of the seat.

There was some concern about the unusual nature of these results; therefore, an additional calculation was performed to identify possible problems with the calculational procedure. If the SIIIS-3ER seat configuration is rotated 10° in the longitudinal plane of symmetry, it is very similar in profile to the reclined seat configuration (compare Figs. 2 and 17). A computation was made for the SIIIS-3ER seat at a supersonic flow condition similar to a previous reclined seat case. The computed pressure distribution around the

SIIIS-3ER seat at a freestream Mach number of 1.2 and 25° angle of attack is shown superimposed on the configuration profile (without rotation) in Figure 19. The corresponding pressure distribution for the reclined seat at the same Mach number, but at 35° angle of attack (to account for the 10° rotation) is shown in Figure 4. The similarity of the two pressure distributions shown in these figures indicates that there is no major irregularity in the SIIIS-3ER calculation procedure, but the sensitivity of the solution to the three-dimensional geometric characteristics may be greater than expected.

There is still some uncertainty regarding the problems with the comparisons of measured and predicted forces on this seat. This anomaly should be studied further when the capability to conduct full three-dimensional calculations is available.

UNSTRUCTURED MESH

A series of calculations using the unstructured mesh flowfield prediction code were made for the SIIIS-3ER ejection seat configuration for the purpose of demonstrating the unstructured mesh capability and to compare its prediction accuracy with the structured mesh code. Results of these calculations are described below.

The unstructured mesh for this series of calculations was derived from the same grid used for the previous structured mesh results. The triangular mesh shown in Figure 20 was obtained from a modification of the structured mesh shown in Figure 17. A single diagonal line splits each rectangular-shaped control volume defined by groups of four neighboring grid points in the structured mesh. Consequently, both structured and unstructured meshes considered for this study use the same set of grid points, making a direct comparison of numerical results meaningful.

Since the ejection seat computations are a new application for the unstructured mesh code and the first calculation is primarily a test case, a supersonic freestream was selected so that a steady state flowfield could be used for comparison purposes. The first calculation was made for a freestream Mach number of 1.2 and 25° angle of attack. A steady solution was obtained, and the predicted surface pressure distribution is shown in Figure 21. Surface

pressures on the windward side of the configuration agree very well with the previous structured mesh results shown in Figure 19. The trends in base pressures also agree; however, the predicted pressure levels are somewhat higher for the unstructured mesh calculation.

A quantitative comparison of steady results from structured and unstructured meshes in supersonic flow is made as follows. The two-dimensional forces calculated for the supersonic unstructured mesh results are corrected for three-dimensional effects using the elliptic loading assumption as done previously for the structured mesh results. The estimated three-dimensional force coefficients are C_x = 0.51 and 0.55 and C_y = -0.11 and -0.12 for unstructured and structured predictions, respectively. There is approximately 8% difference in the results from the two meshes. This is an indication that grid independence has not been achieved; however, it also indicates that numerical differences between the structured and unstructured methods should not produce significantly different results.

It is possible that these differences are a measure of the differences in the two solution algorithms. In addition, the unstructured mesh flowfield code has not been extensively tested with supersonic freestream conditions, and some difficulty was experienced with the code's treatment of the outflow boundary conditions. This problem modified the character of the wake and caused some difference in base pressure levels. A similar problem is not evident for subsonic freestream conditions discussed below; therefore, this minor numerical difficulty is left for future consideration and analysis.

Laminar, unsteady, unstructured mesh results were calculated on the SIIIS-3ER ejection seat at a subsonic freestream Mach number of 0.75 and for four angles of attack from 0° to 40°, the same conditions as used for the previous subsonic structured mesh results. As also seen for the reclined ejection seat in subsonic flow, the calculated subsonic aerodynamic characteristics are unsteady and periodic in nature. The angle of attack range for the SIIIS-3ER seat data is more limited than the reclined seat data, but in the low flow angle regime, the predicted results are very similar.

The computed normal force and axial force coefficients are corrected for three-dimensional effects using the measured axial force coefficient at $\alpha = 0°$ as before, and they are shown as a function of iteration number or time in Figure 22 for $\alpha = 0°$. The periodic solution is evident. Choosing two extreme points in the force results, T_1 and T_2 in Figure 22, the predicted flow characteristics can be examined in detail. The points selected correspond to 16,800 and 18,200 iterations in the solution. It should be noted here that the periodic nature of the solution was well developed prior to these iterations, and similar results will be obtained at corresponding lower iteration numbers.

The character of the unsteady flowfield can be studied by examining the predicted flow parameters obtained from the unstructured mesh calculations. Velocity vectors, pressure fields, and Mach number contours for the two specified times in the solution, T_1 and T_2 defined above, are shown in Figures 23 through 25. The velocity vector results shown in Figure 23 illustrate interesting differences at the two times. At the earlier time (Fig. 23(a)) corresponding to the lower forces on the seat, there is a strong vortical flow region near the feet on the lee side and another larger vortical flow region of opposite sign directly behind the seat. In contrast, the flow corresponding to the higher forces is shown in Figure 23(b) where the flow in the feet region has changed direction and is not as strong a vortical flow as before. The large vortex behind the seat has moved downstream to be replaced by a weaker vortical region of opposite sign near the seat. The flow in the region of the head is very different at the two times shown. This indication of unsteadiness near the pilot's head could have serious consequences on the seat occupant during ejection at these flow conditions.

The normalized pressure contours in Figure 24 further illustrate the changing flow patterns on the lee side of the seat. The low pressures in the centers of the vortices give some indication of the motion of the vortices described in the previous figures. Notice that the pressures in the head and base regions have changed significantly between the two times, but there is little change on the windward side of the configuration. This will be better illustrated in a later figure showing surface pressures on the seat.

The Mach number contours shown in Figure 25 illustrate a strong shock wave near the head, particularly when the force is lowest in Figure 25(a). The results show a shock present near the head in Figure 25(b), but it appears to be weaker and slightly farther away from the head. The flow on the windward side is nearly stagnated over the entire body area.

Surface pressure coefficients on the SIIIS-3ER ejection seat configuration are shown in Figure 26 at the two extremes of the predicted normal forces. As noted above, the pressure on the windward side is nearly constant at the stagnation level for both times. However, there is a significant change in the pressure distribution on the base side of the seat at the different times. In Figure 26(a) the predicted pressures on the lee side indicate rapidly changing pressures near the corners. Notice also that the low pressure region switches from the head to the feet region between the times shown.

The overall forces on this configuration are obtained from a time average of the unsteady forces. The approximate three-dimensional results on this seat were obtained by correcting the two-dimensional results using the experimental value of axial force coefficient as described for the previous results for this seat. The measured and predicted axial force and normal force coefficients are shown in Figures 27 (a) and (b), respectively. For these comparisons, the structured mesh results from Figure 18 are also shown. In Figure 27(a), the axial force coefficients from the unstructured mesh calculations are in good agreement with the trend of the experimental data and the predicted results from the structured mesh.

The normal force coefficients in Figure 27(b) have a different character. The unstructured mesh results exhibit the same trend as the measurements up to higher angles of attack; however, the structured mesh results do not show the same trends or quality of agreement. It is not clear why the observed discrepancy in structured and unstructured mesh results exists in the normal force coefficient. The possible problem areas are grid-dependent solutions, different solution algorithms, accuracy of the unsteady solutions, and sensitivity of the results to small perturbations in the predicted flowfield. A complete investigation of these problem areas were beyond the scope of this feasibility study; however, a discussion of these topics is presented in the next section.

CONCLUSIONS

The Phase I study to demonstrate the feasibility of applying modern computational fluid dynamic techniques to the analysis of ejection seat configurations is described herein. Under the assumption of two-dimensional flow, it is shown that CFD methods have the capability of providing detailed aerodynamic and flowfield characteristics for a wide range of flow conditions and ejection seat configurations. Specific problem areas of interest in the study are grid generation, unsteady transonic flow, flow transients, separation effects, and validation with experimental data. Some concluding remarks on each of these topics are presented as follows.

Since this study may be one of the first applications of CFD to complex ejection seat configurations, a systematic computational process was selected to identify problem areas and assist in the evaluation of the technical approach. Beginning with two-dimensional flow to keep the computational requirements within reason, the ejection seat is modeled in profile through its longitudinal plane of symmetry. Three different seat/occupant configurations based on wind tunnel models are examined with the traditional structured grid or mesh approach. Contrary to initial thoughts, it proved to be a very simple task to generate a practical structured mesh around each of the configurations using standard gridding techniques.

Though the development of a structured mesh for these complex two-dimensional configurations is important, it is expected that it will be much more difficult to generate a similar structured mesh for a three-dimensional ejection seat configuration. Therefore, an unstructured grid was investigated for the two-dimensional shapes in anticipation that an unstructured grid will be required to adequately model the three-dimensional configurations. Unstructured meshes and their generation are still in the research phase of development, and they are not commonly used for CFD applications; however, there is considerable interest in their capabilities and uses, and they are rapidly becoming more available for applications. Complex gridding techniques for unstructured grids were investigated, but it was determined that a very good computational grid could be

developed from the existing structured meshes. For purposes of this feasibility study, unstructured grids were generated for one ejection seat configuration with little difficulty.

A readily available and well tested two-dimensional Navier-Stokes code (ARC2D) was applied to the three configurations represented by structured grids. Results are presented for subsonic and transonic flow conditions for a wide range of angles of attack. Since the flows are dominated by separation effects, only laminar results are calculated to avoid possible problems and uncertainties associated with turbulence modeling.

A newer two-dimensional Navier-Stokes code, NSU2D, was selected for the unstructured grid computations. It was applied for a range of angles of attack at both subsonic and supersonic speeds, and in each case, reasonable aerodynamic characteristics were obtained without major difficulty. As before, only laminar results are available from this initial study.

The comparisons between the structured and unstructured grid methods illustrate qualitative agreement for similar flow conditions. In supersonic flow, results are steady for both methods, and in general, both the structured and unstructured grids produce similar aerodynamic characteristics for the entire range of flow conditions. There are some minor differences caused by a boundary condition problem in the unstructured code, but these can be resolved in a future effort.

At subsonic speeds, unsteady flow results are obtained from both structured and unstructured methods; however, some details of the predicted aerodynamic characteristics are different for the two methods. For example, near $\alpha = 0°$, both methods are in good agreement for both axial and normal force coefficients. However, as angle of attack increases, the axial force results from the two methods begin to exhibit some disagreement, but the normal force coefficients become significantly different. The trend of the normal force obtained from the unstructured grid is in reasonable agreement with the measurements, but the overall result is that the predicted forces are very sensitive to the solution procedure and the resulting unsteady flowfield. Unsteady flows are difficult to

calculate accurately, and it is known that unsteady algorithms are less well developed than steady algorithms.

Flow separation from the configurations has a dominant influence on the predicted aerodynamic characteristics, but it appears that each method has the ability to compute the effects of this phenomenon in laminar flow. It is not clear at this time that similar unsteady behavior is being predicted by both the structured and unstructured methods, and this is an area for future investigation. In addition, the effects of turbulence must be included. The difficulties of predicting details of separation in turbulent flows are well known, but the necessary technology is available to include an appropriate turbulence model in the unstructured method so that separation effects can be modeled more accurately.

As noted above, there are several areas for concern regarding the calculations described in this report. One of these areas is in the comparison of computational results with experimental data. In these comparisons, agreement is adequate for supersonic flow, which is steady; the agreement is not adequate for subsonic flows which are generally unsteady. A major source of error is the approximation of three-dimensional results from two-dimensional computations.

A second area of concern is the appearance of unsteady flow at subsonic speeds. It is quite natural for the flow to be unsteady because of asymmetric vortex shedding, but it is possible that the use of a laminar flow model at a Reynolds number at which flow instabilities could occur is giving rise to a spurious unsteadiness. Unsteady flows, especially at transonic speeds have not been extensively studied, and there are a number of important research issues. For example, unsteady flows may not be unique; that is, for a given set of boundary conditions, several solutions may exist; turbulence is one such example. Another aspect is that the flow can be ill conditioned; that is, a small change in some flow parameter can lead to a large change in aerodynamic forces; an example of this is shown in Reference 23.

The third area of concern is the disagreement between the solutions for the structured and the unstructured grid methods for subsonic flow. The fact that there is adequate

agreement (8%) between the two methods for steady (supersonic) flow indicates that the numerical differences as such, do not contribute significantly to the discrepancy for the unsteady (subsonic) cases, although it should be noted that grid independence has not been achieved. However, the numerical differences could cause a large difference if the subsonic flow is ill conditioned, and the comparison in Figure 27 would seem to indicate that this is the case.

The objective of this Phase I feasibility study has been accomplished. Based on the results presented in this final report, it is apparent that a three-dimensional computational fluid dynamics prediction method for ejection seat configurations can be developed using technology currently available. Such a method could be developed to be applicable for preliminary design and configuration optimization analyses. For example, it would be possible to perform an analytical evaluation of a number of new ejection seat designs prior to wind tunnel testing to reduce the actual number of configurations which must be tested. Important characteristics such as drag and windblast loads could be examined for proposed configurations, and modifications and improvements to minimize such characteristics could be carried out prior to model fabrication and testing. A brief outline of a proposed plan to accomplish a three-dimensional CFD design and analysis capability is described in the next section.

RECOMMENDATIONS

In general it is suggested by this study that the subsonic flows around ejection seats are unsteady and that the nature of the unsteadiness can change dramatically due to small changes in the boundary conditions or the solution algorithm because the flow is ill conditioned. If this suggestion is in fact physically true, then it has immense implications for the design of ejection seats because it would indicate that control is very difficult because of the sensitivity of the forces to small control applications. It should also be noted that the unsteady flow, with shocks, could cause substantial injuries to the occupant. It is therefore essential to eliminate the flow unsteadiness if possible, and if not possible to eliminate it, then it is important that some means of analysis be available. Given appropriate

computational methods, new seat designs or modifications can be investigated on a systematic basis prior to testing. The ultimate objective of this added capability is increased safety for the seat occupant over a wide range of ejection flow conditions.

The demonstration of the feasibility of using computational fluid dynamic techniques to solve the detailed aerodynamic characteristics of two-dimensional ejection seat configurations has formed the basis for extending the analysis procedure to actual three-dimensional configurations. Building upon the techniques and results described above, the technology is available to assemble a preliminary design CFD code for modern ejection seats. The extensions and modifications necessary to develop this complete prediction and analysis method are briefly presented below.

The first step is to extend the unstructured grid techniques to complex three-dimensional configurations. Fully automatic grid generation for general CFD problems is difficult for complex three-dimensional geometries such as ejection seats. The primary reason for this is the unavailability of robust automatic mesh algorithms which not only create the mesh, but also create the desired mesh (Ref. 24). A desirable mesh possesses qualities, such as, (1) sufficient resolution of the surface geometry, (2) fine grid resolution near complex-shape surfaces and in regions where there is expected to be large flowfield variations, (3) smooth variation of mesh spacing between fine and coarse mesh regions, and (4) triangles as nearly equilateral as possible. Although a fully automatic grid generation technique for ejection seats may be difficult to achieve at this time, current efforts at NEAR and other organizations will soon provide practical schemes which minimize the amount of user input to create the necessary meshes.

A turbulence model must be used with the Navier-Stokes equations to permit calculations on ejection seats at practical Reynolds numbers. Algebraic turbulence models like the Cebeci-Smith (Ref. 25) or the Baldwin and Lomax (Ref. 26) model cannot be applied in a straightforward manner to unstructured meshes because these models rely on the existence of coordinate lines normal to the thin shear layers, which, of course, are not available with unstructured meshes. Because of the difficulty of applying an algebraic turbulence model on unstructured grids, it is expected that the κ-ε turbulence model (Ref.

27) will present the most practical solution. The κ-ε model does not rely on any inherent mesh coordinate directions and can be easily implemented using the same Runge-Kutta relaxation scheme as is used for the Euler and Navier-Stokes equations. This turbulence model has met with good success in base flow computations at NEAR as reported in Reference 28. Use of this turbulence model is almost certainly required to predict the drag on an ejection seat dominated by base flow separation effects observed in the two-dimensional results described above.

The two-dimensional prediction techniques and methods described herein also demonstrate the importance of transient flows in the unsteady results obtained in the high subsonic and transonic flow regimes. The three-dimensional method must be capable of including the transient effects on ejection seats under extreme ejection conditions. Another form of transient flow behavior must be considered when developing a three-dimensional approach, and that is the unsteadiness caused by the development of the flow when the seat is ejected into an airstream from an aircraft. There will be a transient in the flow before some equilibrium condition is reached. If some form of stagnation zone is desired as pilot protection, then there may be flow instabilities whose transient behavior may be detrimental to the safety of the pilot. All these complex time-dependent effects must be considered in the final design and analysis method.

Even though there are a number of difficult technical tasks to be accomplished, it is feasible to develop a computational fluid dynamics method for the analysis of complex three-dimensional ejection seat configurations. The method could be used to optimize the design of ejection seats to reduce drag and minimize windblast loads by permitting efficient analysis of the effects of geometric modifications on the aerodynamic and flowfield characteristics prior to experimental testing. The obvious advantage of such an approach is the reduction of the number of potential configurations requiring expensive wind tunnel analysis, and thus the added advantage of permitting the use of limited resources for testing of those configurations most likely to provide increased safety to the pilot.

Previously, the use of modern CFD codes was restricted to the advanced computer analyst because of the research nature and continuous development of such codes. The

state-of-the-art of computational techniques has developed to a point that production codes for general usage are now possible. With the advent of expert systems pre- and post-processors, it is now possible to develop a CFD code for ejection seat analysis that can be used easily and successfully by the design engineer. Given this capability, a CFD code for ejection seat analysis could be considered another design tool for use in the search for safer ejection seats.

REFERENCES

1. Jines, L. A. and Roberts, E. O.: Enhanced Ejection Seat Performance with Vectored Thrust Capability. AFWAL-TR-84-3026, August 1985.

2. White, B. J.: USAF Crew Escape State-of-the-Art for Technology Advancement. AFWAL-TR-82-3089, December 1982.

3. Delgado, R. C.: Limb Flail Injuries in USAF Ejections: 1979-1985. 24th SAFE Symposium Proceedings, December 1986, pp. 1-3.

4. Specker, L. J.: Flow Stagnation as an Advanced Windblast Protection Technique. 23rd SAFE Association Symposium Proceedings, December 1985, pp.12-17.

5. Belk, W. F.: Limb Flail Injuries and the Effect of Extremity Restraints in USAF Ejections: 1971-1978. SAFE Journal, 1980.

6. Bull, J. O., Ther, D. T., and Yruczyk, R. R.: Advanced Ejection Seat for High Dynamic Pressure Escape Wind Tunnel Test Report. AFWAL-TR-80-3084, August 1980.

7. Reichenau, D. E. A.: Wake Properties Behind an Ejection Seat Escape System and Aerodynamic Characteristics With Stabilization Parachutes at Mach Numbers From 0.6 to 1.5. AEDC-TR-71-30, February 1971.

8. Brister, J. G. and Yruczyk, R. F.: Reclined Ejection Seat Development Wind Tunnel Test Report. AFWAL-TR-81-3100, August 1981.

9. Hawker, F. K. and Euler, A. J.: Extended Measurements of Aerodynamic Stability and Limb Displacement Forces With the ACES II Ejection Seat. AMRL-TR-75-15, July 1975.

10. Specker, L. J.: Comparison of F-101 Ejection Seat and ACES II Static Aerodynamic Coefficients. 23rd SAFE Symposium Proceedings, December 1985, pp. 41-46.

11. Rubbert, P. and Goldhammer, M.: CFD in Design: An Airframe Perspective. AIAA 89-0092, January 1989.

12. Maynard, S. T. and Swanson, D. E.: The CREST Windblast Protection System Design. 24th SAFE Symposium Proceedings, December 1986, pp. 44-47.

13. Caruso, S. C.: Development of an Unstructured Mesh/Navier-Stokes Method for Aerodynamics of Aircraft with Ice Accretions. NEAR TR-405, September 1989.

14. Klopfer, G. H.: Solution Adaptive Meshes with a Hyperbolic Grid Generator. In Numerical Grid Generation in Computational Fluid Mechanics '88, ed. by S. Sengupta, J. Hauser, P. R. Eiseman, and J. F. Thompson, Pineridge Press Limited, Swansea, 1988.

15. Pulliam, T.: Euler and Thin Layer Navier-Stokes Codes ARC2D and ARC3D, Notes for Computational Workshop, The University of Tennessee Space Institute, Tullahoma, TN, March, 1984.

16. Mavriplis, D. J., Jameson, A. and Martinelli, L.: Multigrid Solution of the Navier-Stokes Equations on Triangular Meshes, AIAA 89-0129, January 1989.

17. Wu, J. and Sankar, L.: Evaluation of Three Turbulence Models for the Prediction of Steady and Unsteady Airloads, AIAA 89-0609, January 1989.

18. White, B. J.: Aeromechanical Properties of Ejection Seat Escape Systems, AFFDL-TR-74-57, April 1974.

19. Ayoub, P. and Yost, P.: Wind Tunnel Tests of a 0.65 Scale Ejection Seat With and Without Yaw Stabilizers, NADC-84093-60, April 1984.

20. Hoerner, S. F.: Fluid-Dynamic Drag, Hoerner, 1958.

21. Dyment, A., Gryson, P., and Ducruet, C.: Self-induced Unsteady Separation on a Fixed Body in Subsonic and Transonic Flow, I.M.F. Lille, France, No. 80/44, October 1980.

22. Van Dyke, M.: An Album of Fluid Motion, The Parabolic Press, Stanford, CA., 1982.

23. Dengel, P. and Fernholz, H. H.: A Study of the Sensitivity of an Incompressible Turbulent Boundary Layer on the Verge of Separation. Paper 1-4, Seventh Symposium on Turbulent Shear Flows, Stanford University, August 21-23, 1989.

24. Cheng, J. H., Finnigan, P. M., Hathaway, A. F., Kela, A. and Schroeder, W. J.: Quadtree/Octree Meshing with Adaptive Analysis. In Numerical Grid Generation in Computational Fluid Mechanics '88, ed. by S. Sengupta, J. Hauser, P. R. Eiseman, and J. F. Thompson, Pineridge Press Limited, Swansea, 1988.

25. Cebeci, T. and Smith, A. M. O.: Analysis of Turbulent Boundary Layers. Academic Press, 1974.

26. Baldwin, B. S. and Lomax, H.: Thin Layer Approximation and Algebraic Model for Separated Turbulent Flows. AIAA 78-0257, 1978.

27. Launder, D. E. and Spalding, D. B.: The Numerical Computation of Turbulent Flows. Computer Methods in Applied Mechanics and Engineering, Vol. 3, 1974, pp. 269-289.

28. Caruso, S. C. and Childs, R. E.: Aspects of Grid Topology for Reynolds-Averaged Navier-Stokes Base Flow Computations. AIAA 88-0523, January 1988.

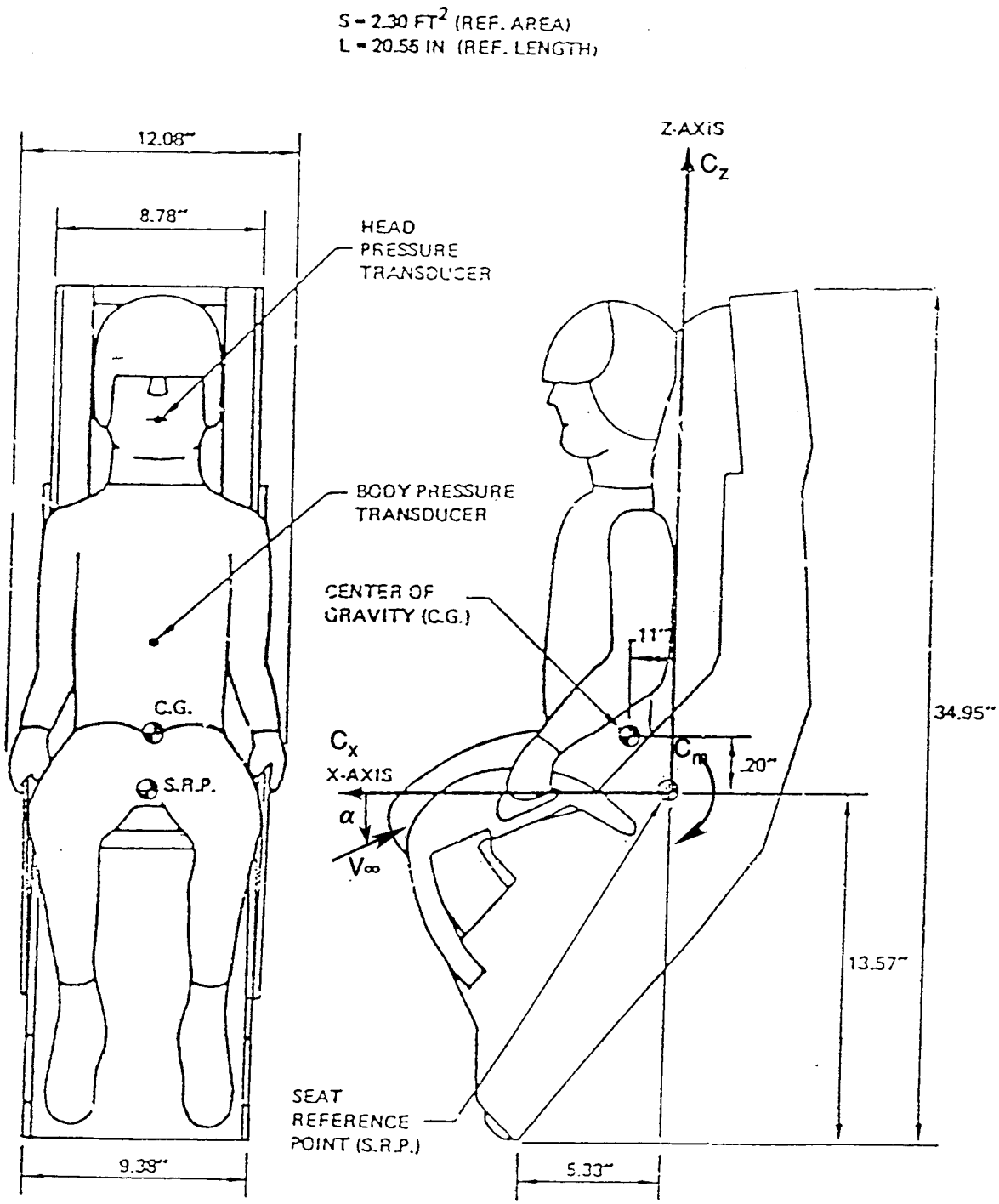

Figure 1. - Reclined Seat Configuration

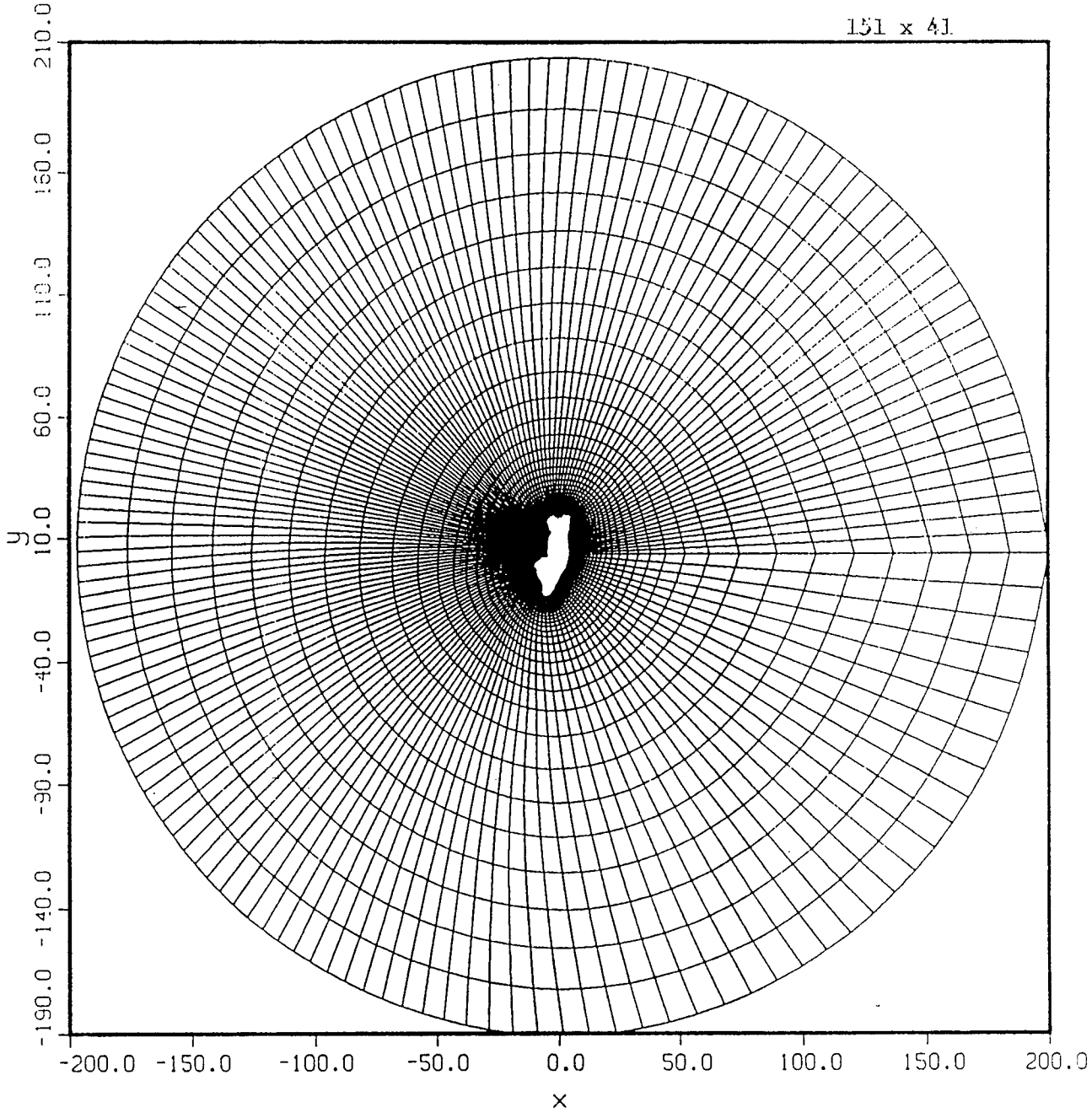

(a) Complete grid

Figure 2. - Structured grid for the reclined ejection seat.

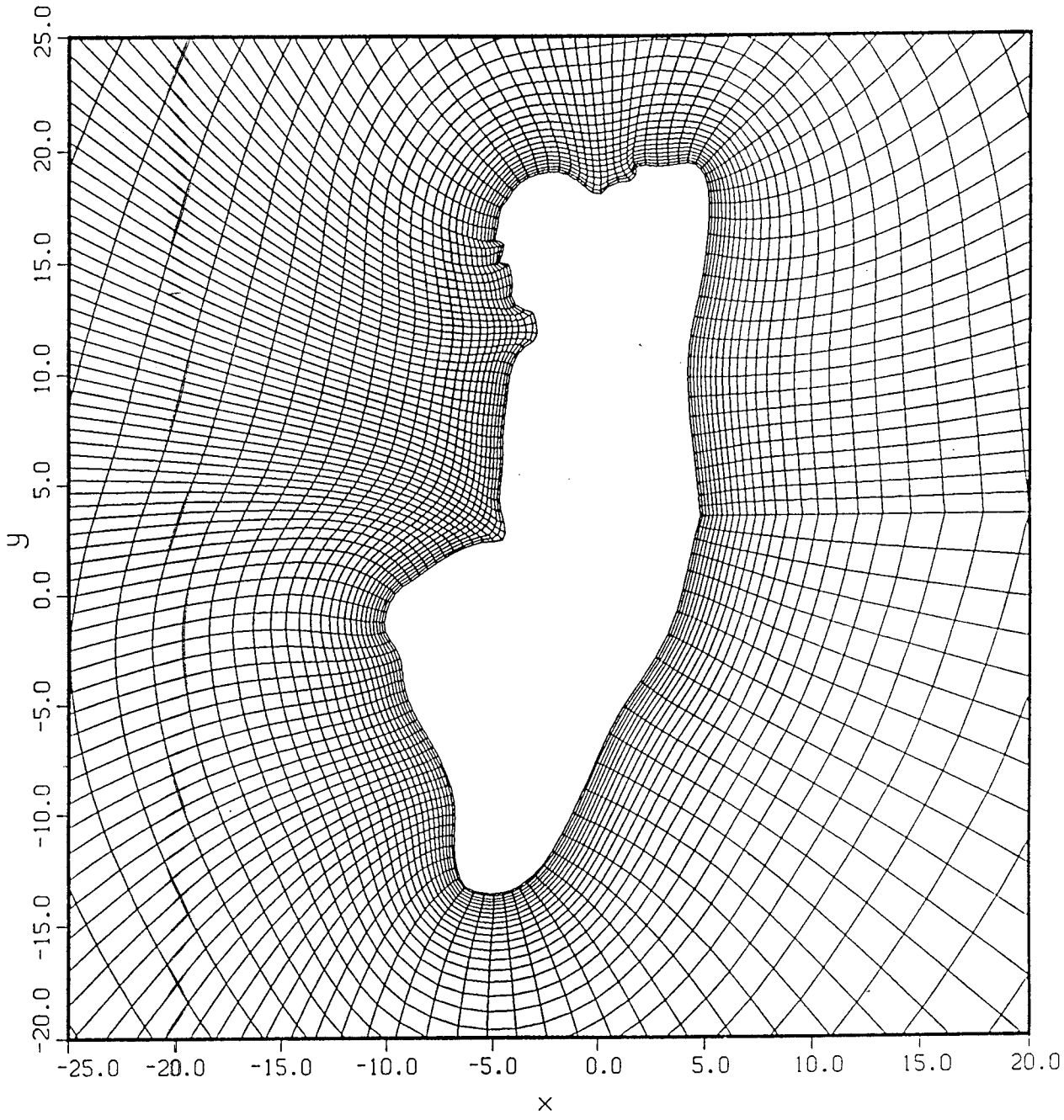

(b) Near field grid

Figure 2. - Concluded.

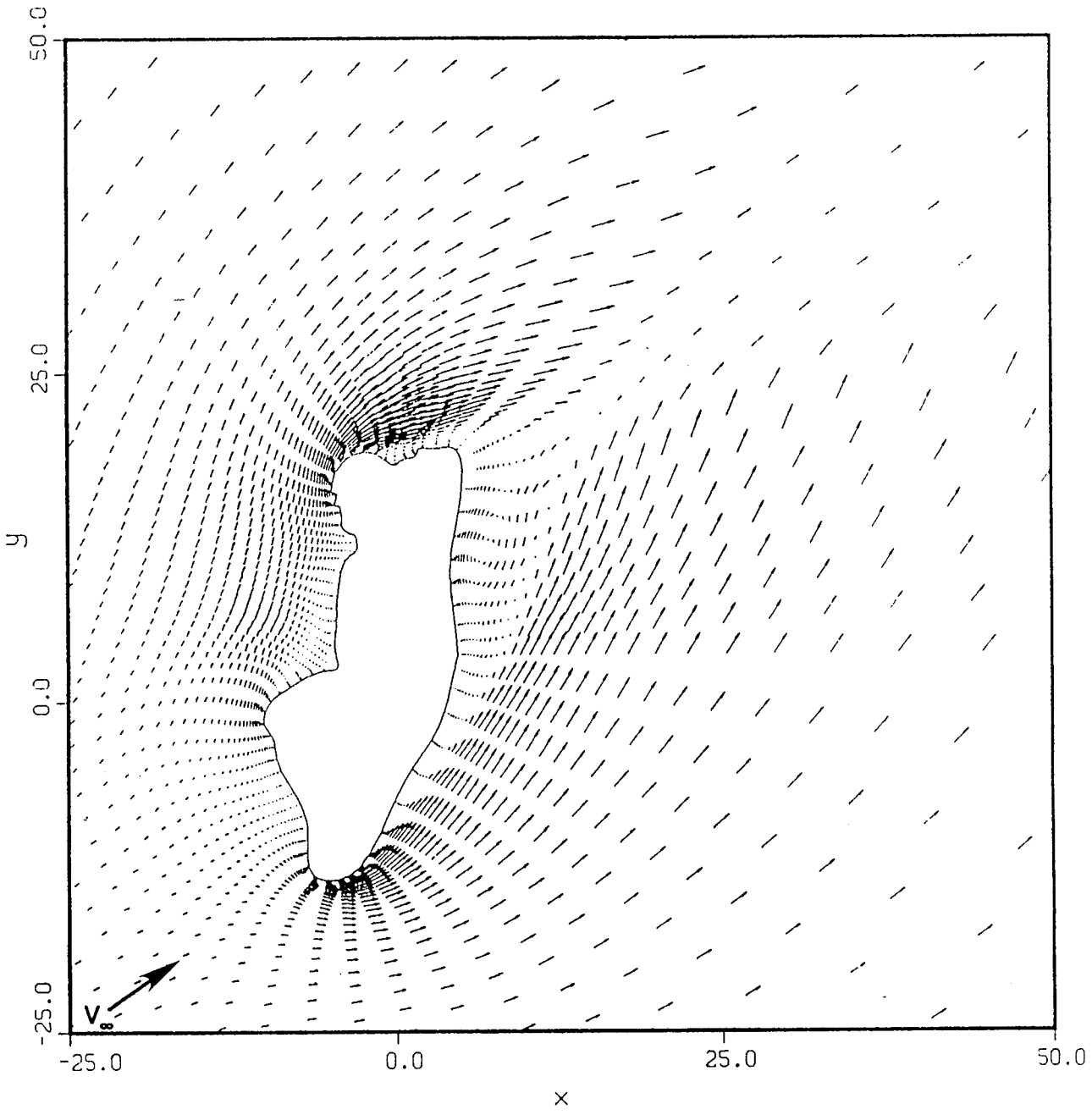

(a) Velocity vectors

Figure 3. - Predicted flowfield characteristics of reclined ejection seat, M = 1.2, $\alpha = 35°$.

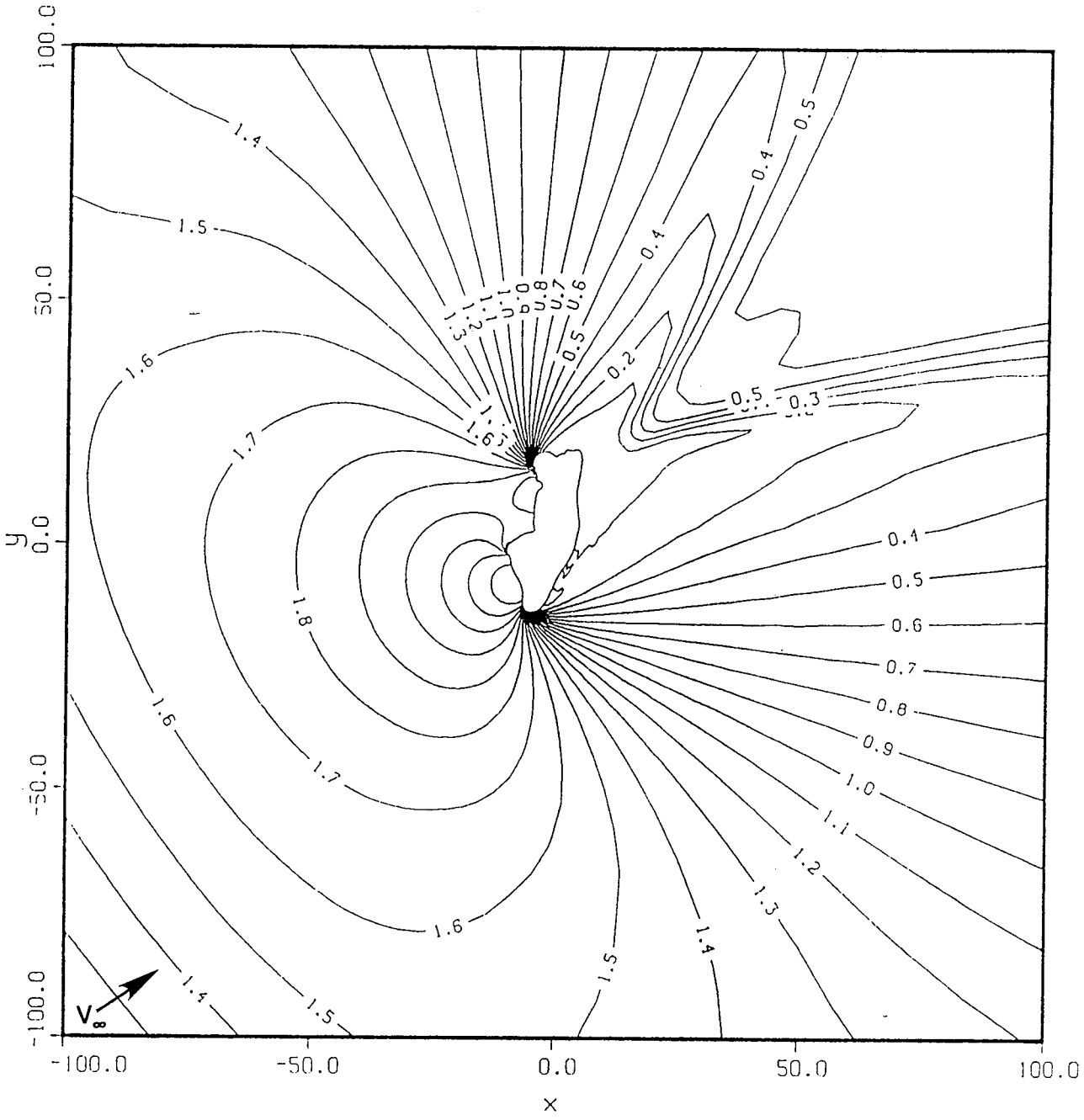

(b) Pressure contours, p/p_∞

Figure 3. - Continued.

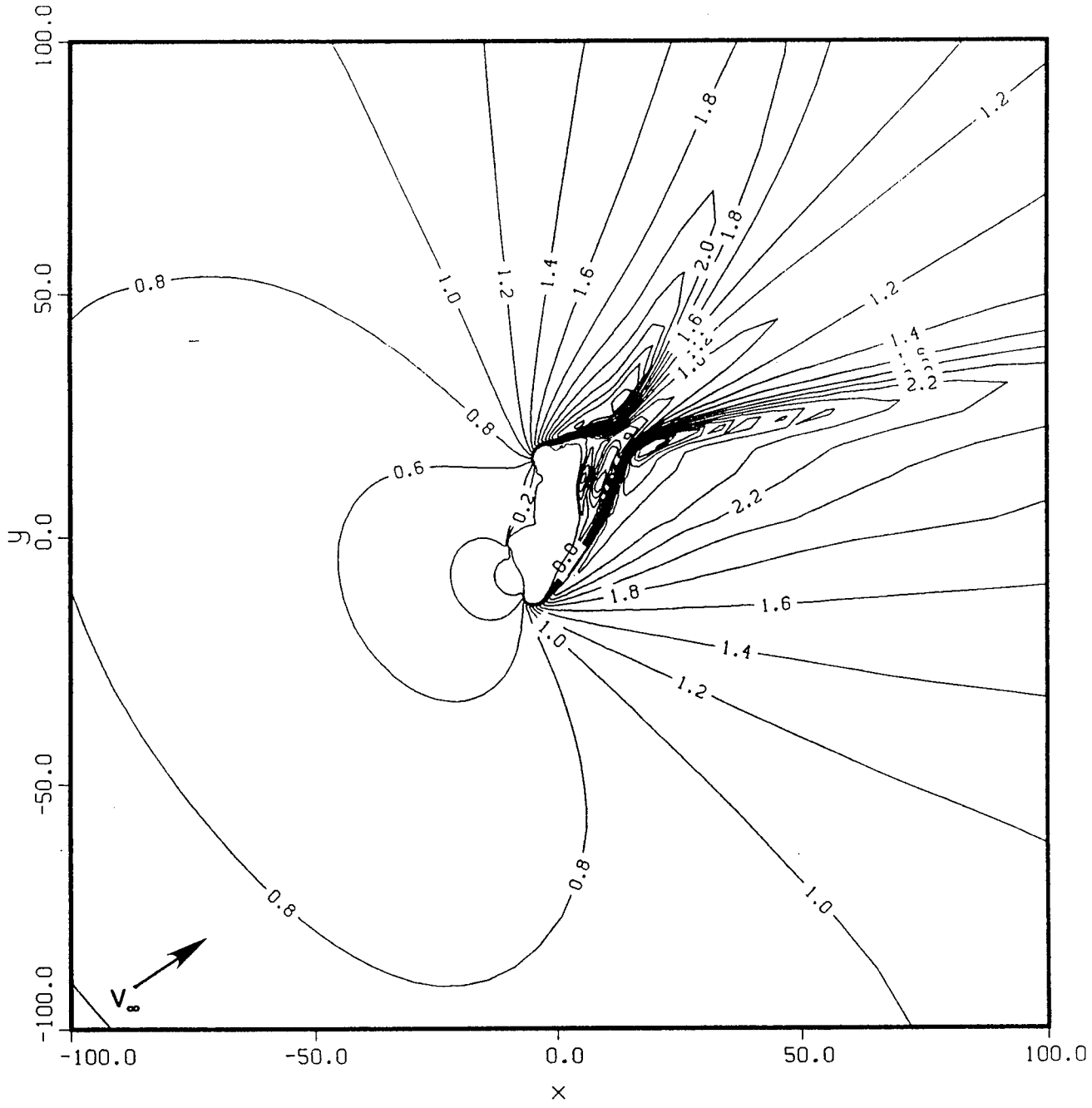

(c) Mach contours, near field

Figure 3. - Continued.

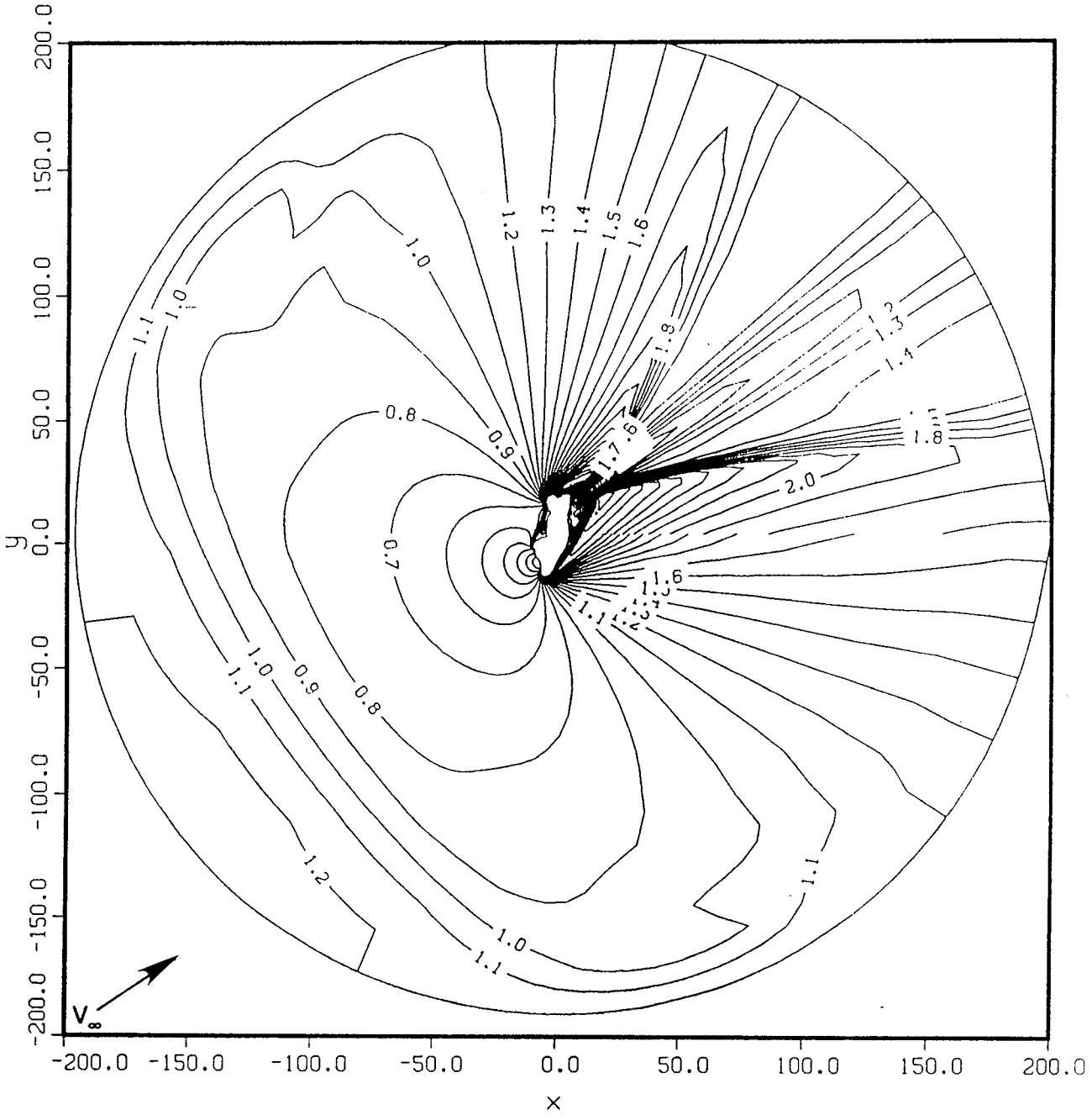

(d) Mach contours, far field

Figure 3. - Continued.

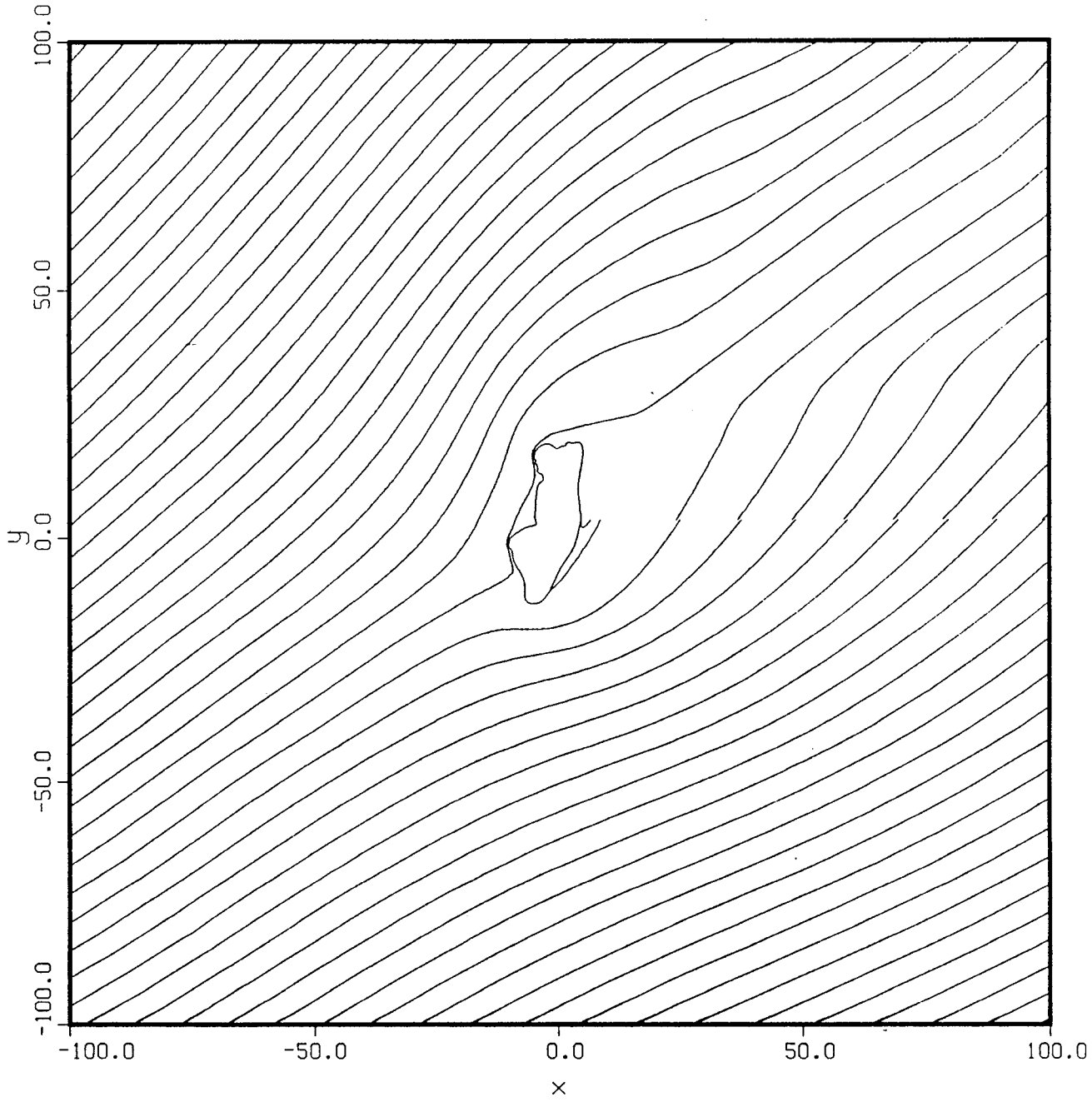

(e) Stream function

Figure 3. - Concluded.

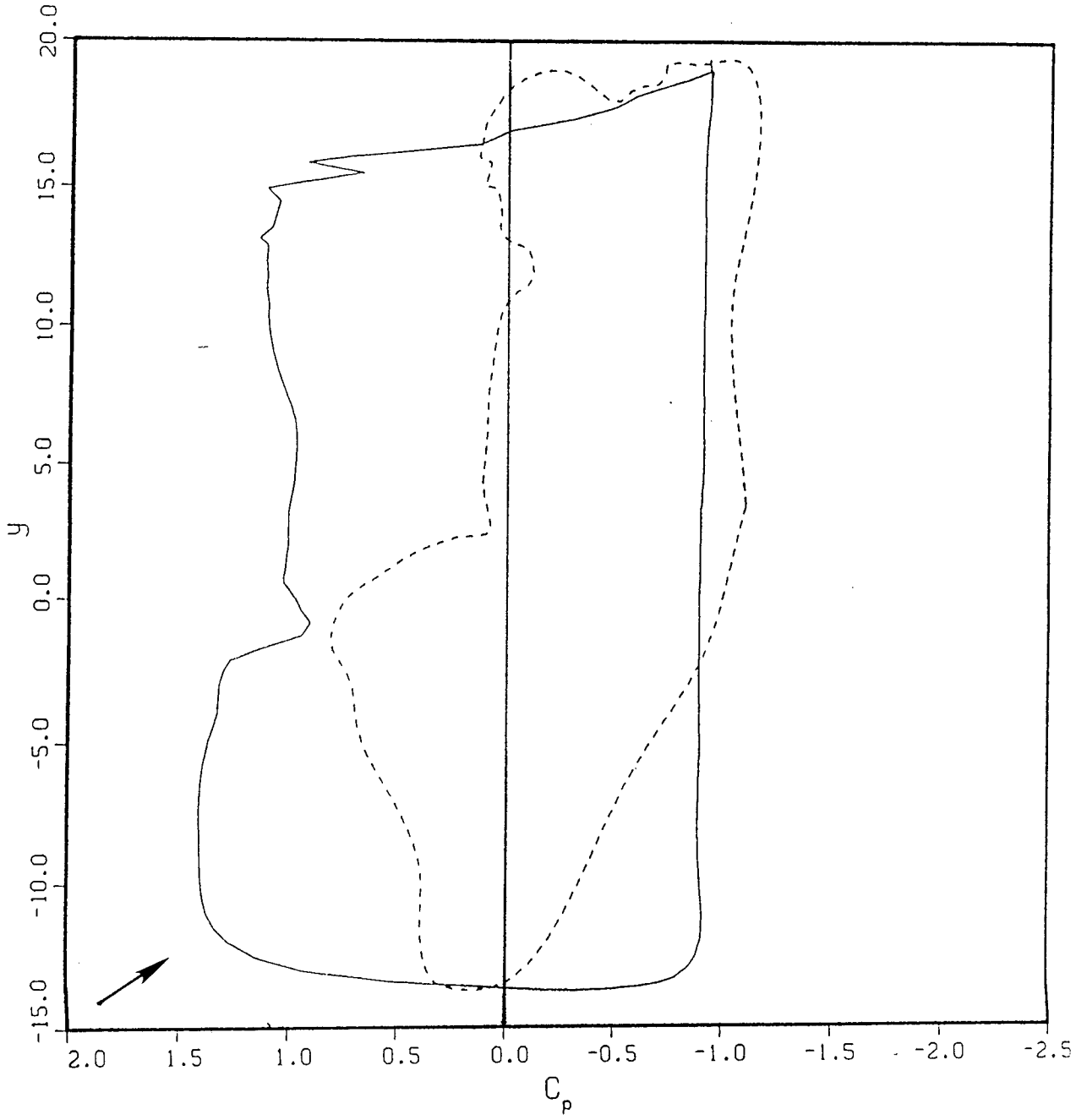

Figure 4. - Predicted surface pressure distribution on the reclined ejection seat, $M_\infty = 1.2$, $\alpha = 35°$.

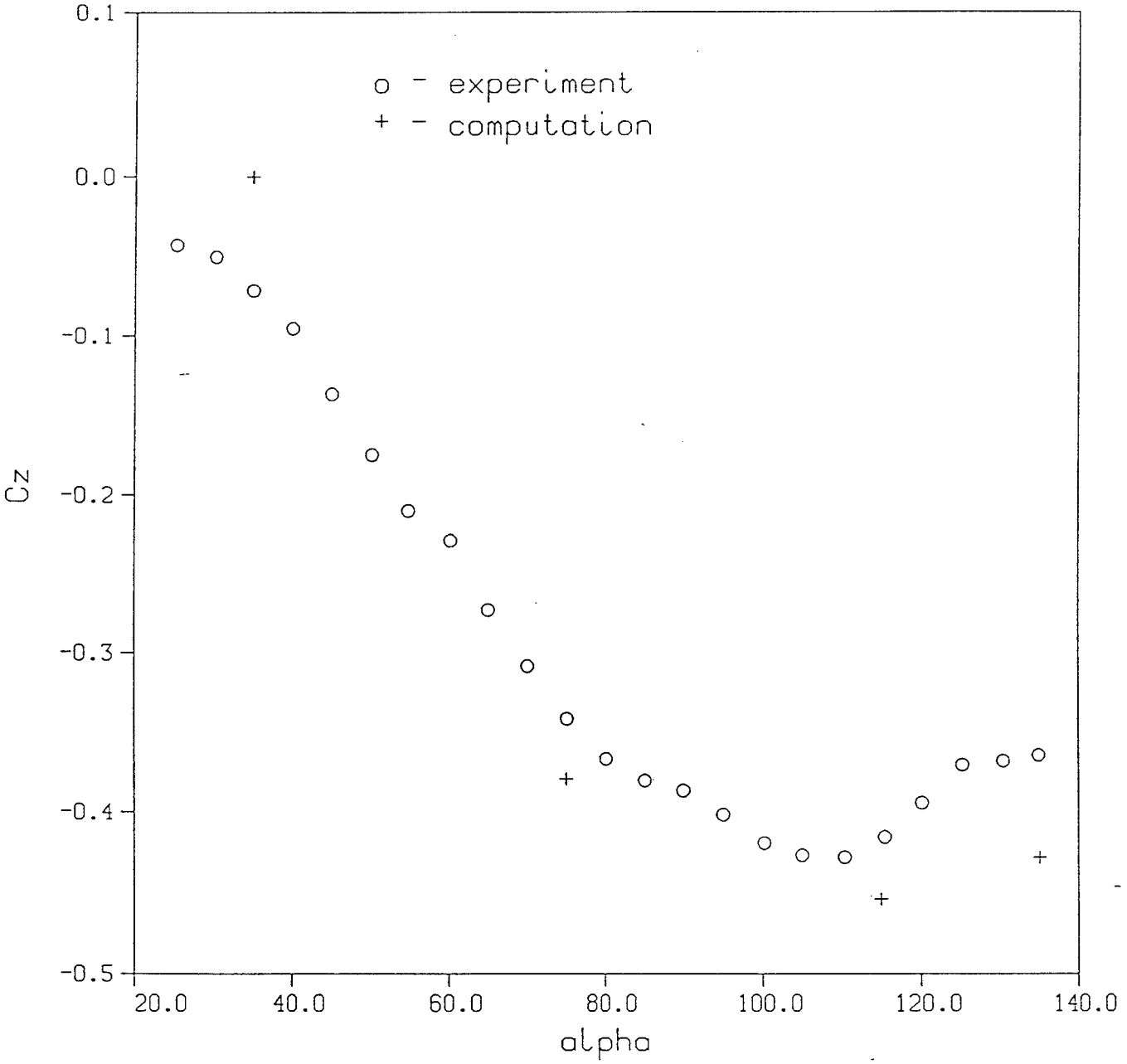

(a) Normal force coefficient

Figure 5. - Measured and predicted force and moment coefficients in the reclined ejection seat, $M_\infty = 1.2$.

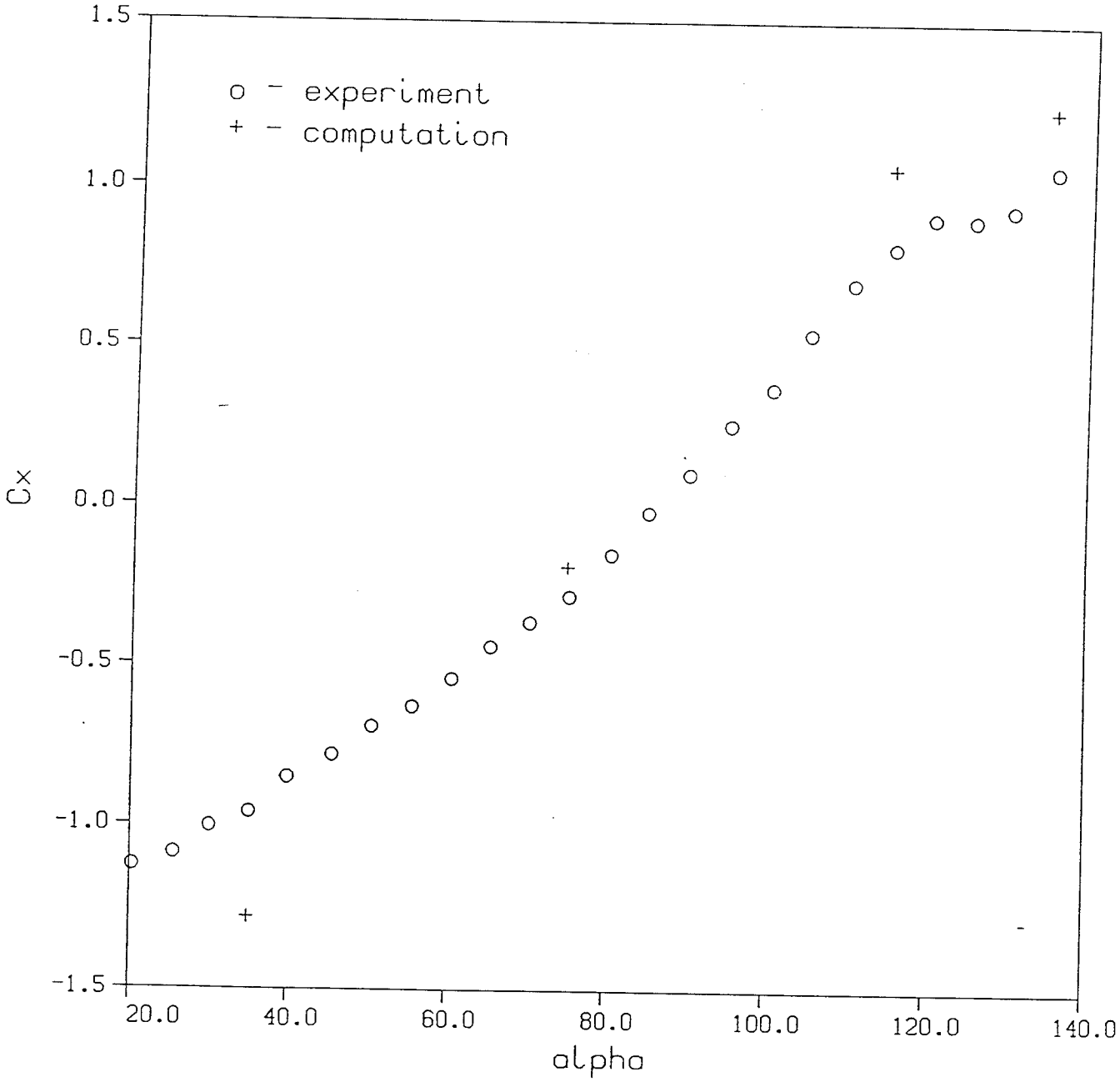

(b) Axial force coefficient

Figure 5. - Continued.

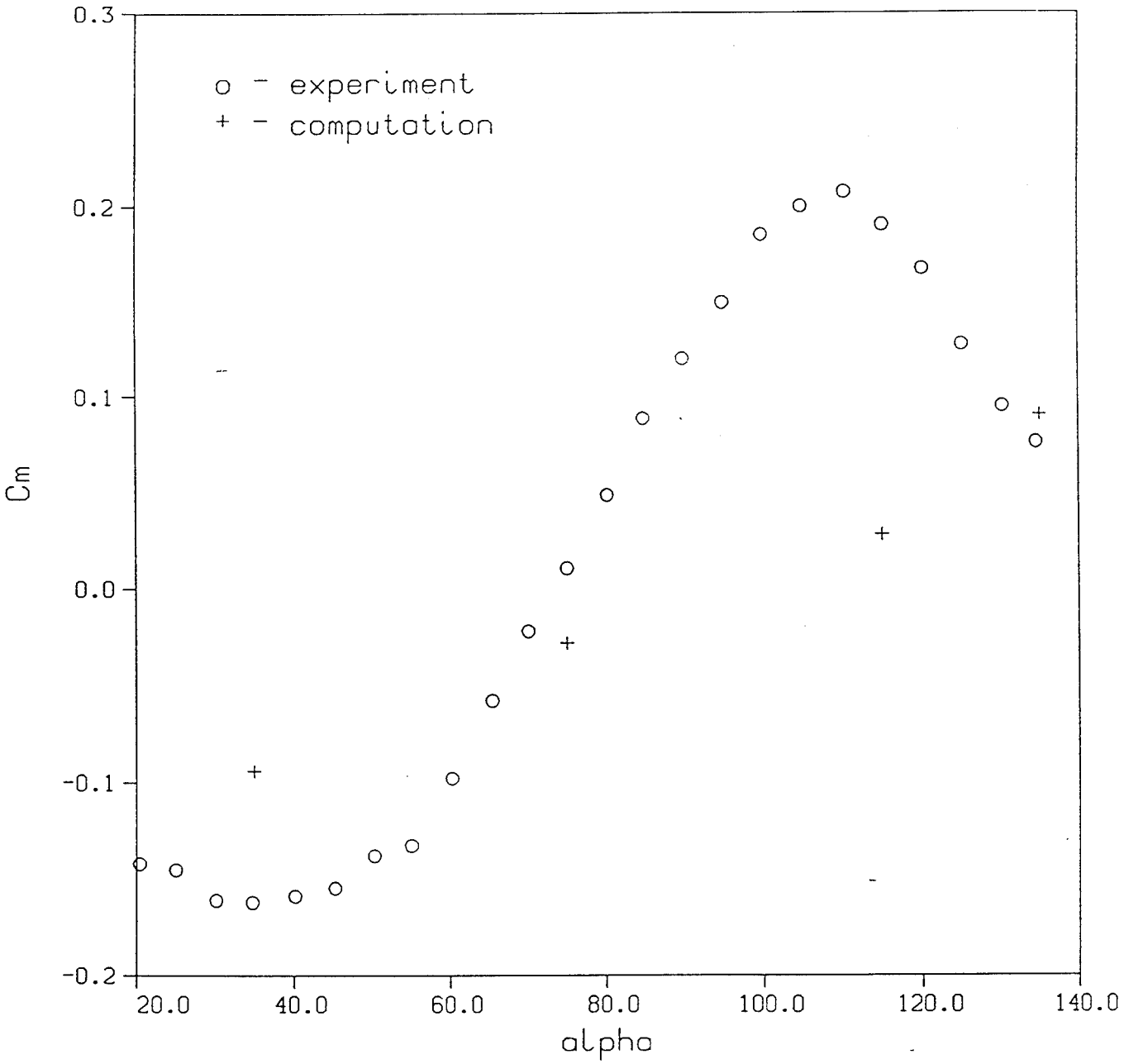

(c) Pitching moment coefficient

Figure 5. - Concluded.

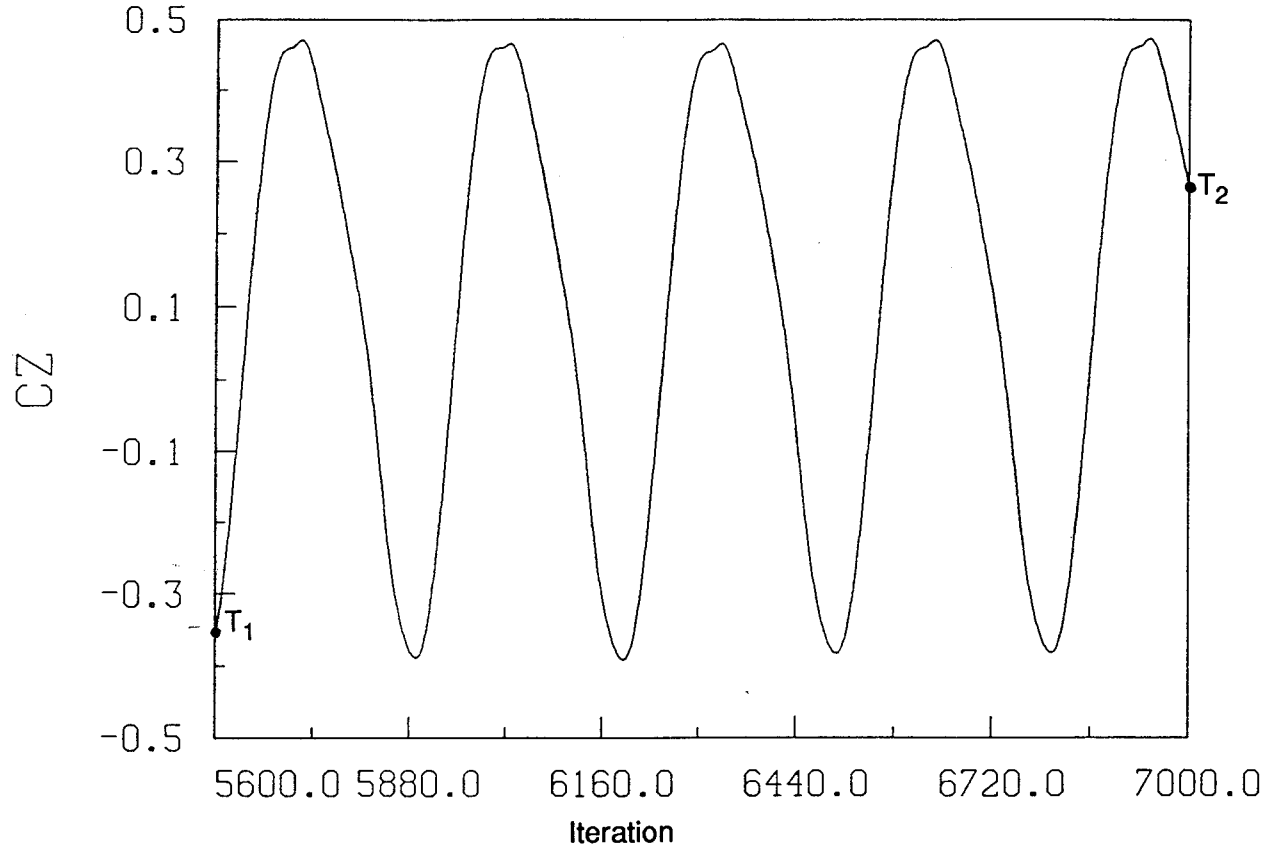

(a) Normal force coefficient

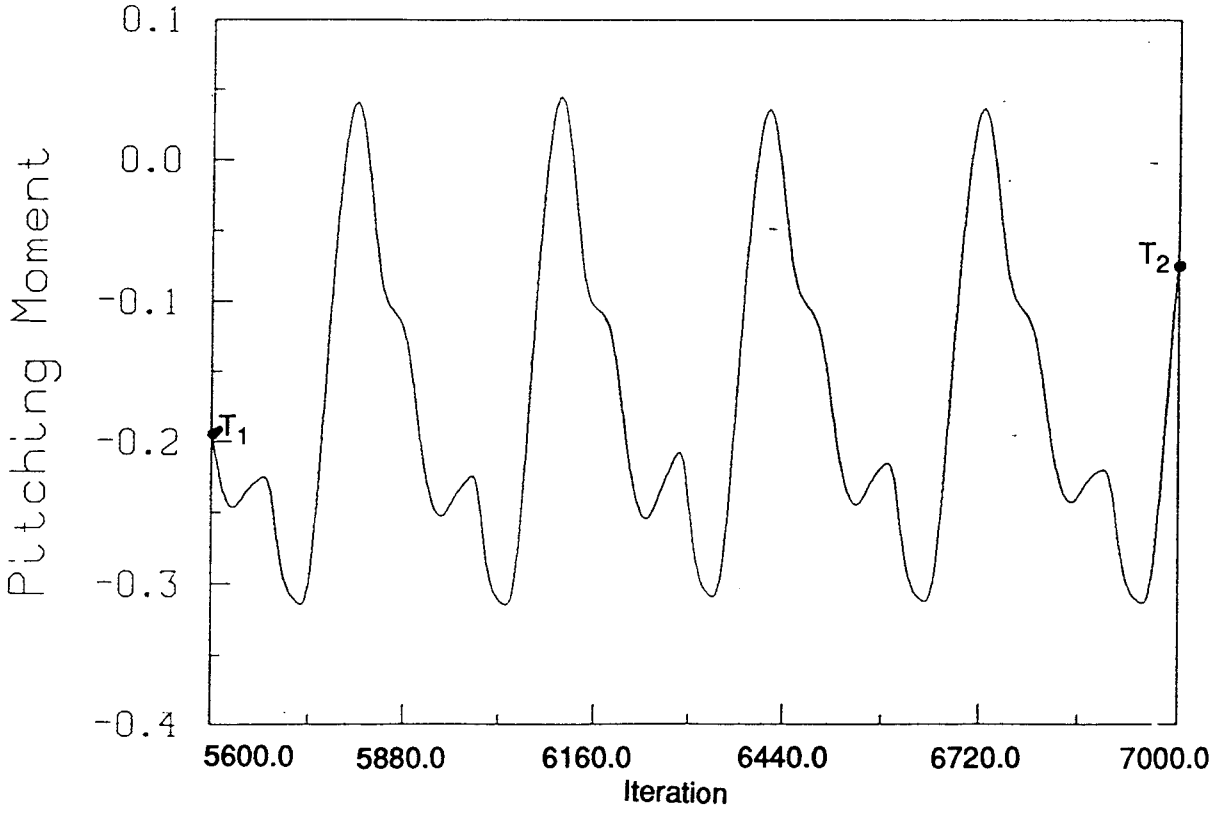

(b) Pitching moment coefficient

Figure 6. - Predicted unsteady forces and moments on the reclined ejection seat, $M_\infty = 0.6$, $\alpha = 35°$.

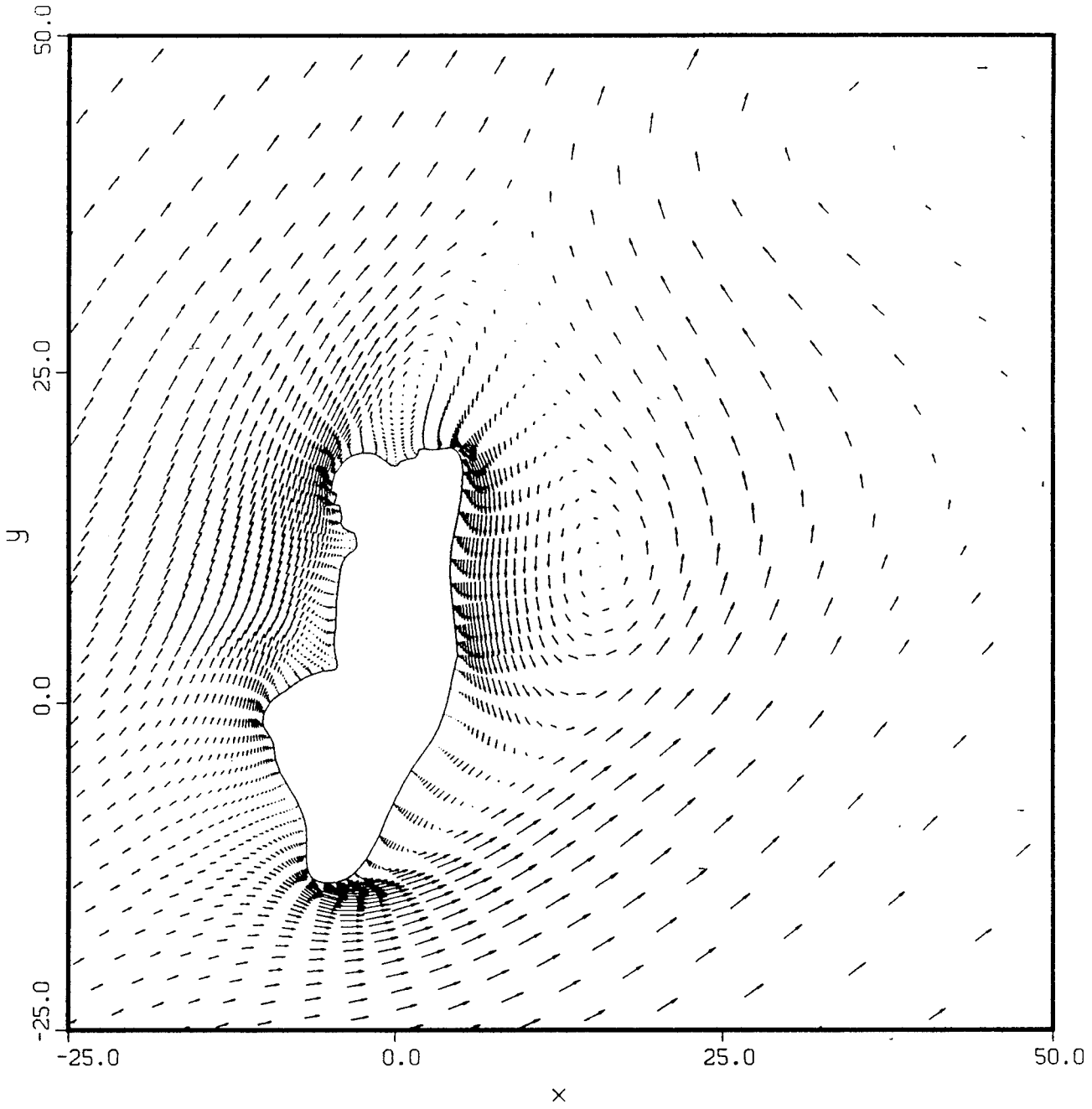

(a) Iteration 5600

Figure 7. - Predicted velocity field near the reclined ejection seat, $M_\infty = 0.6$, $\alpha = 35°$.

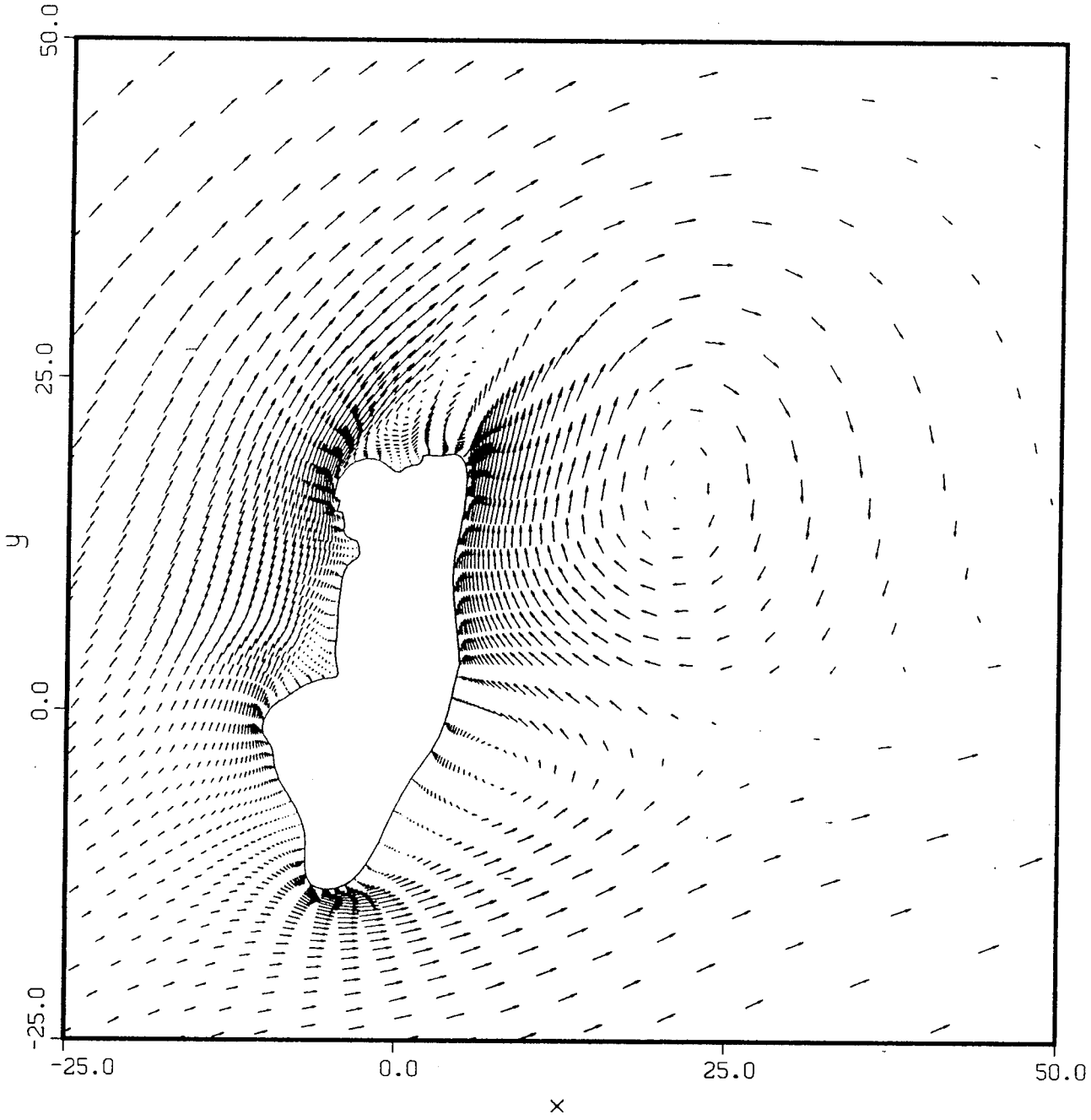

(b) Iteration 7000

Figure 7. - Concluded.

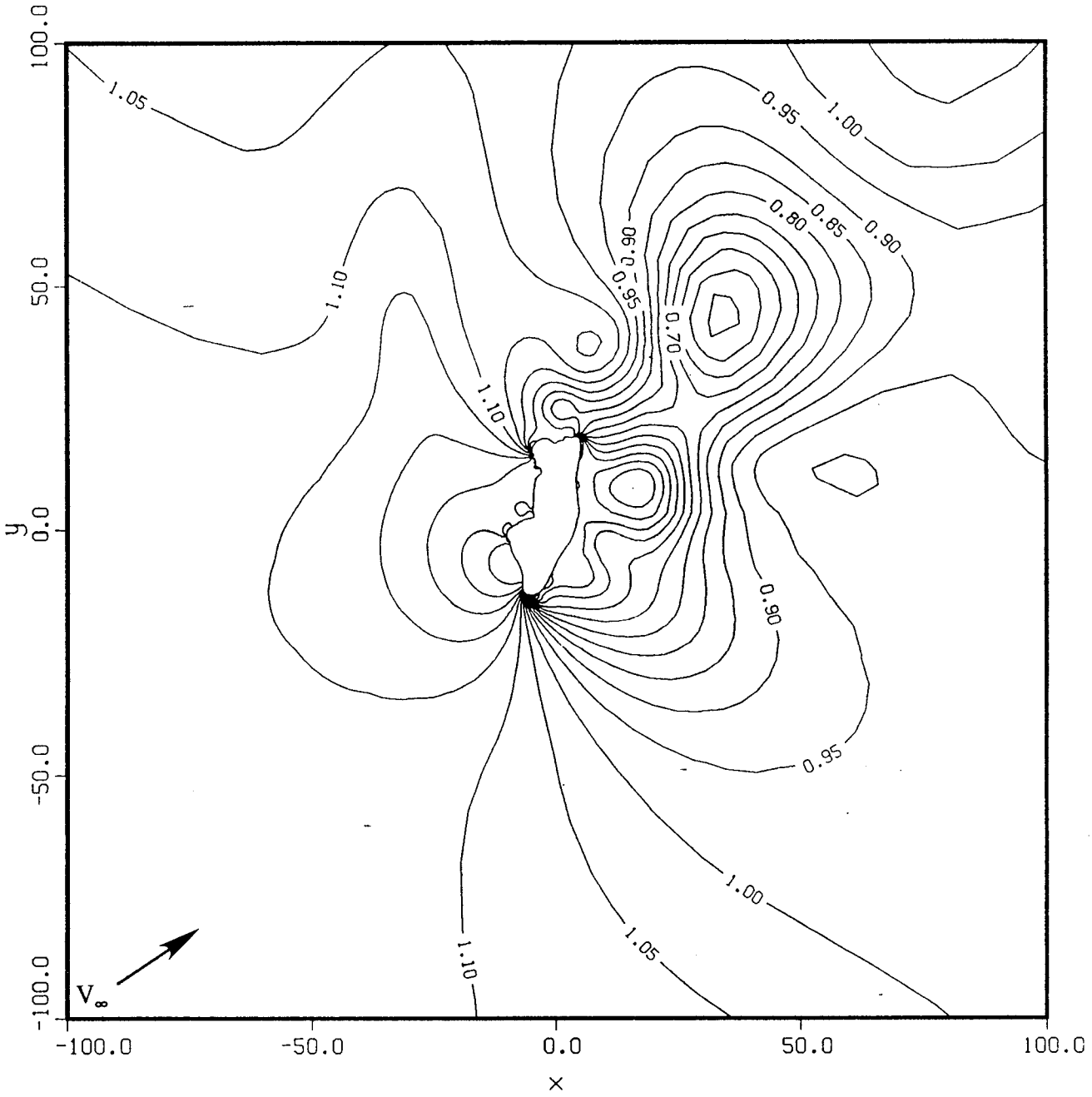

(a) Iteration 5600

Figure 8. - Predicted pressure contours near the reclined ejection seat, $M_\infty = 0.6$, $\alpha = 35°$.

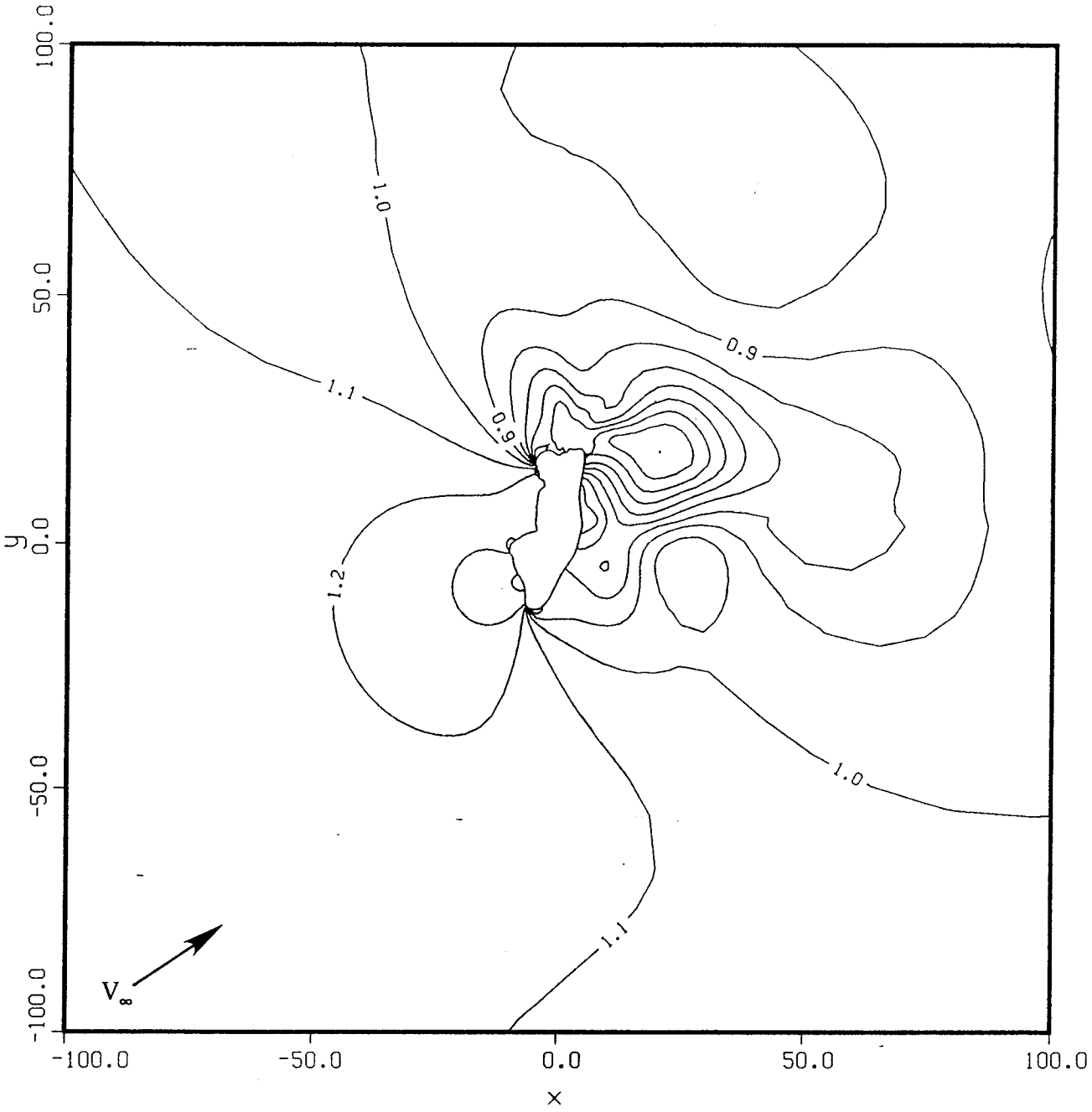

V_∞

(b) Iteration 7000

Figure 8. - Concluded.

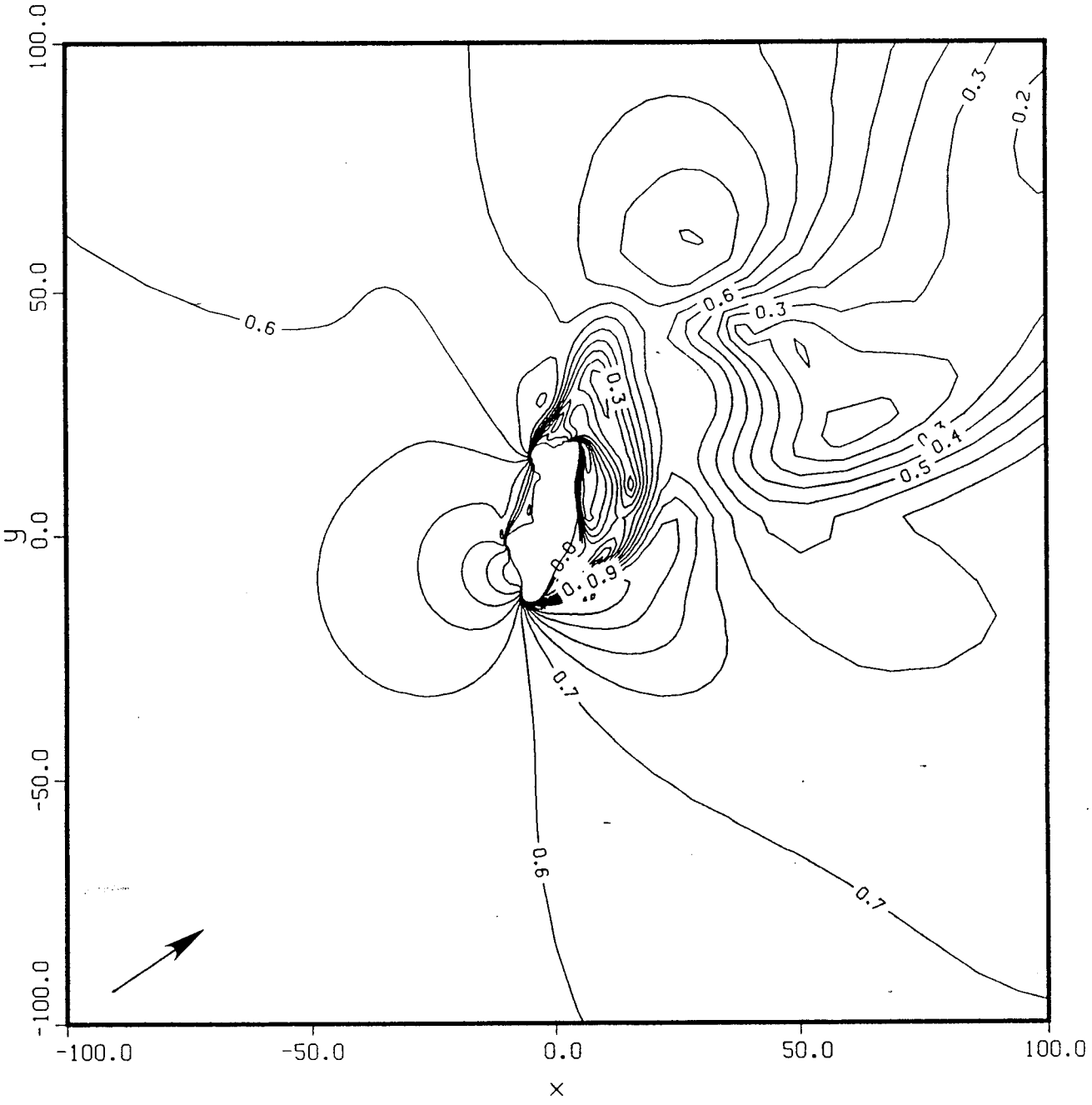

(a) Iteration 5600

Figure 9. - Predicted Mach number contours near the reclined ejection seat, $M_\infty = 0.6$, $\alpha = 35°$.

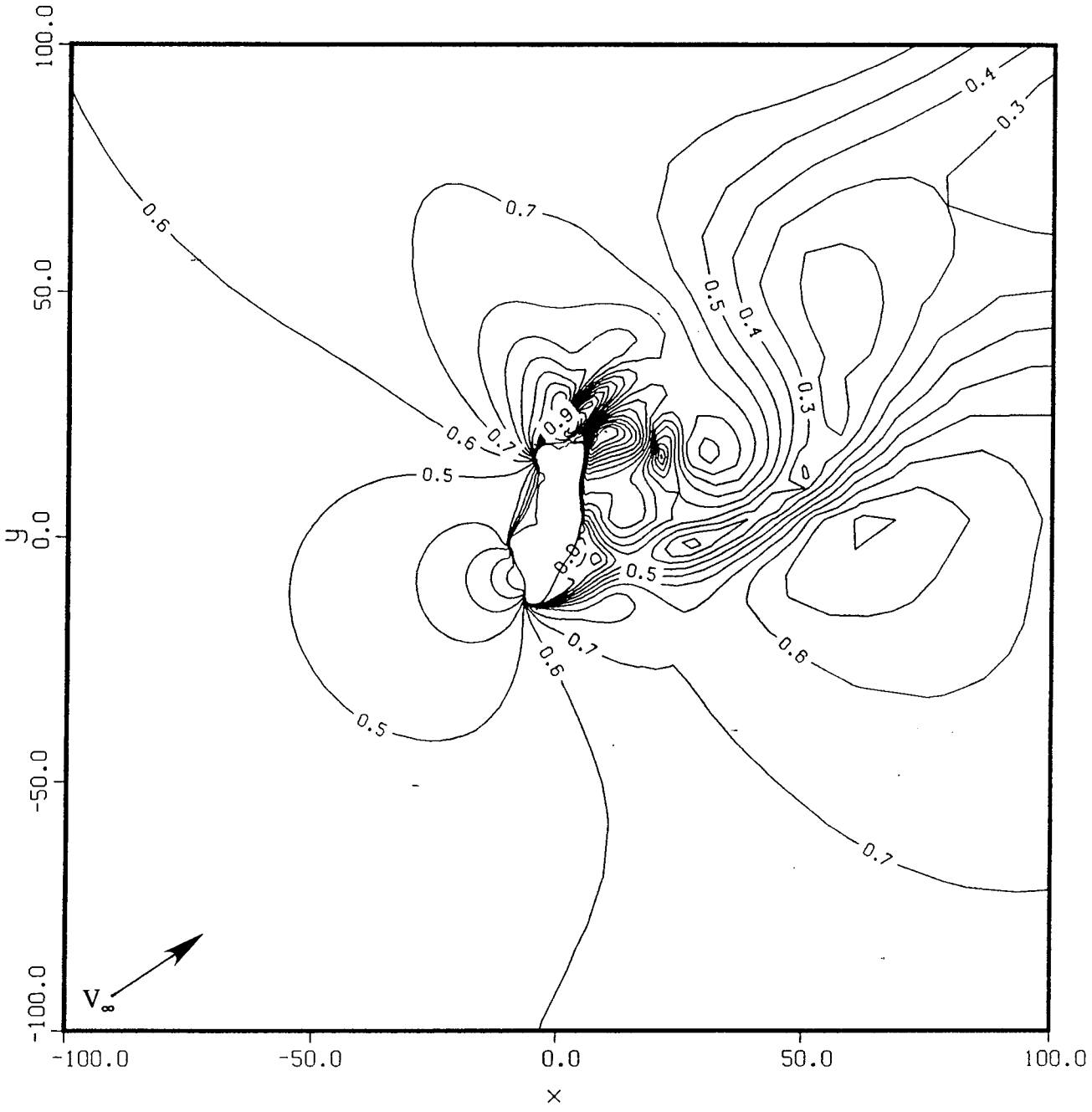

(b) Iteration 7000

Figure 9. - Concluded.

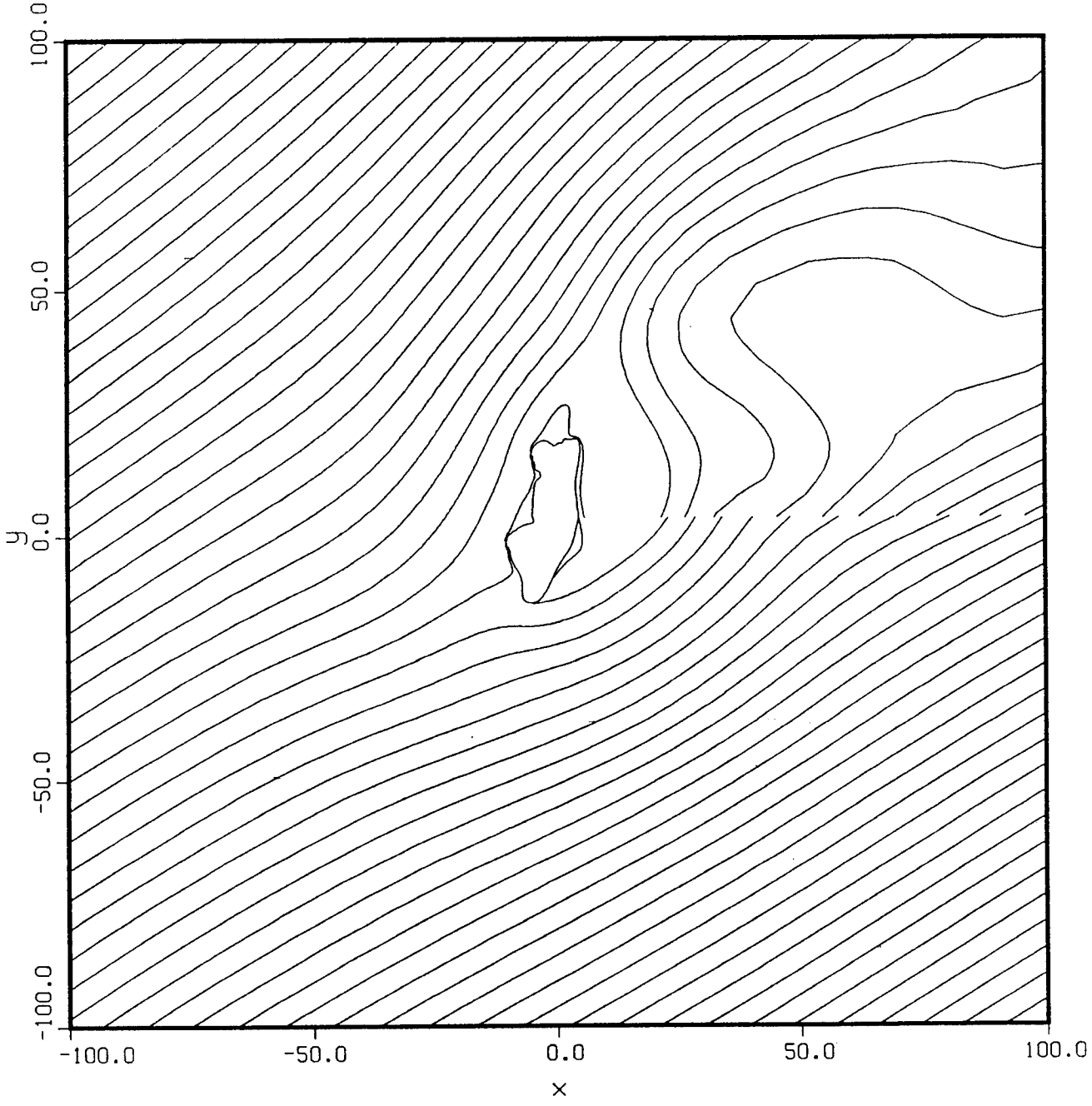

(a) Iteration 5600

Figure 10. - Predicted stream function field near the reclined ejection seat, $M_\infty = 0.6$, $\alpha = 35°$.

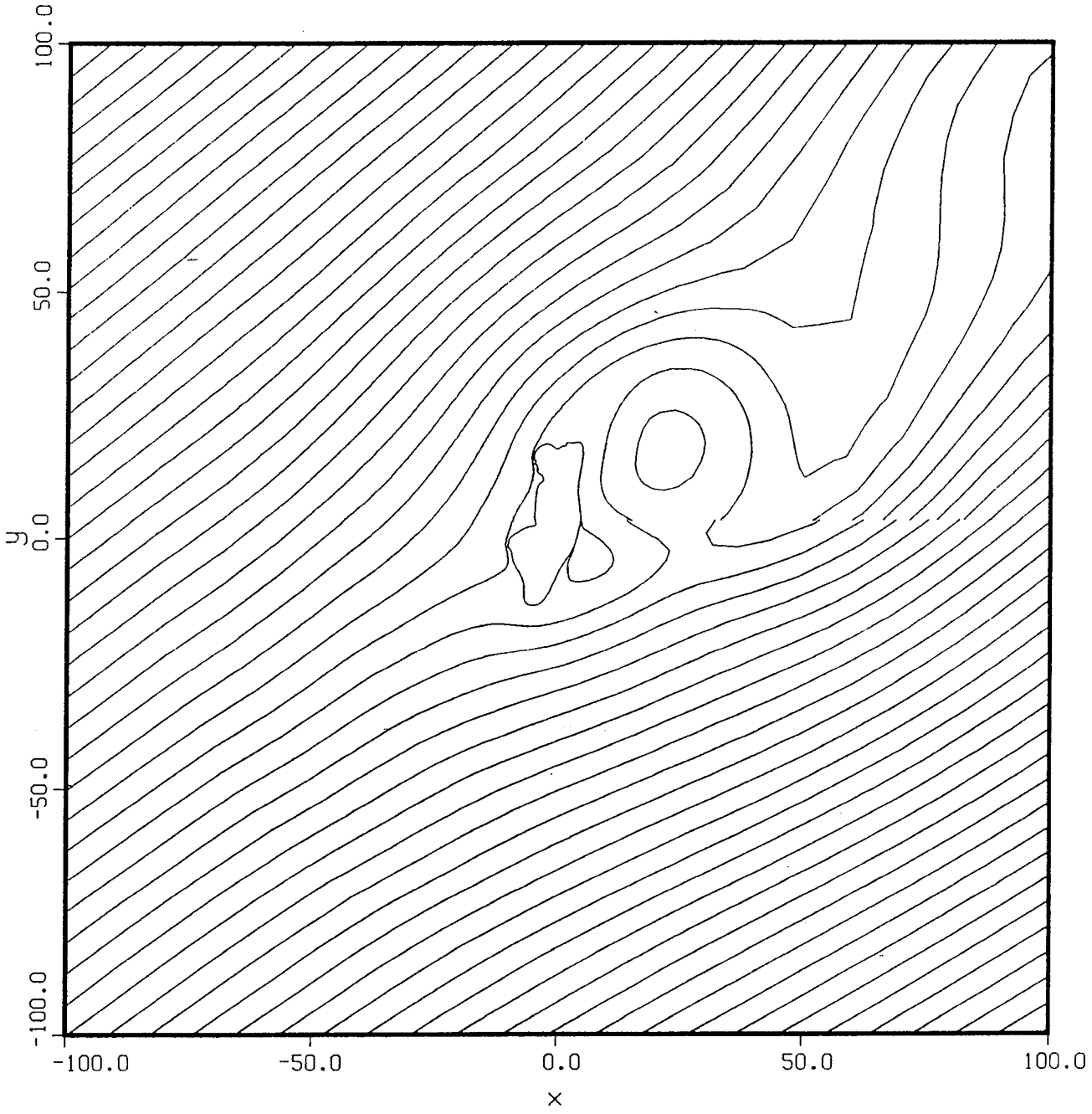

(b) Iteration 7000

Figure 10. - Concluded.

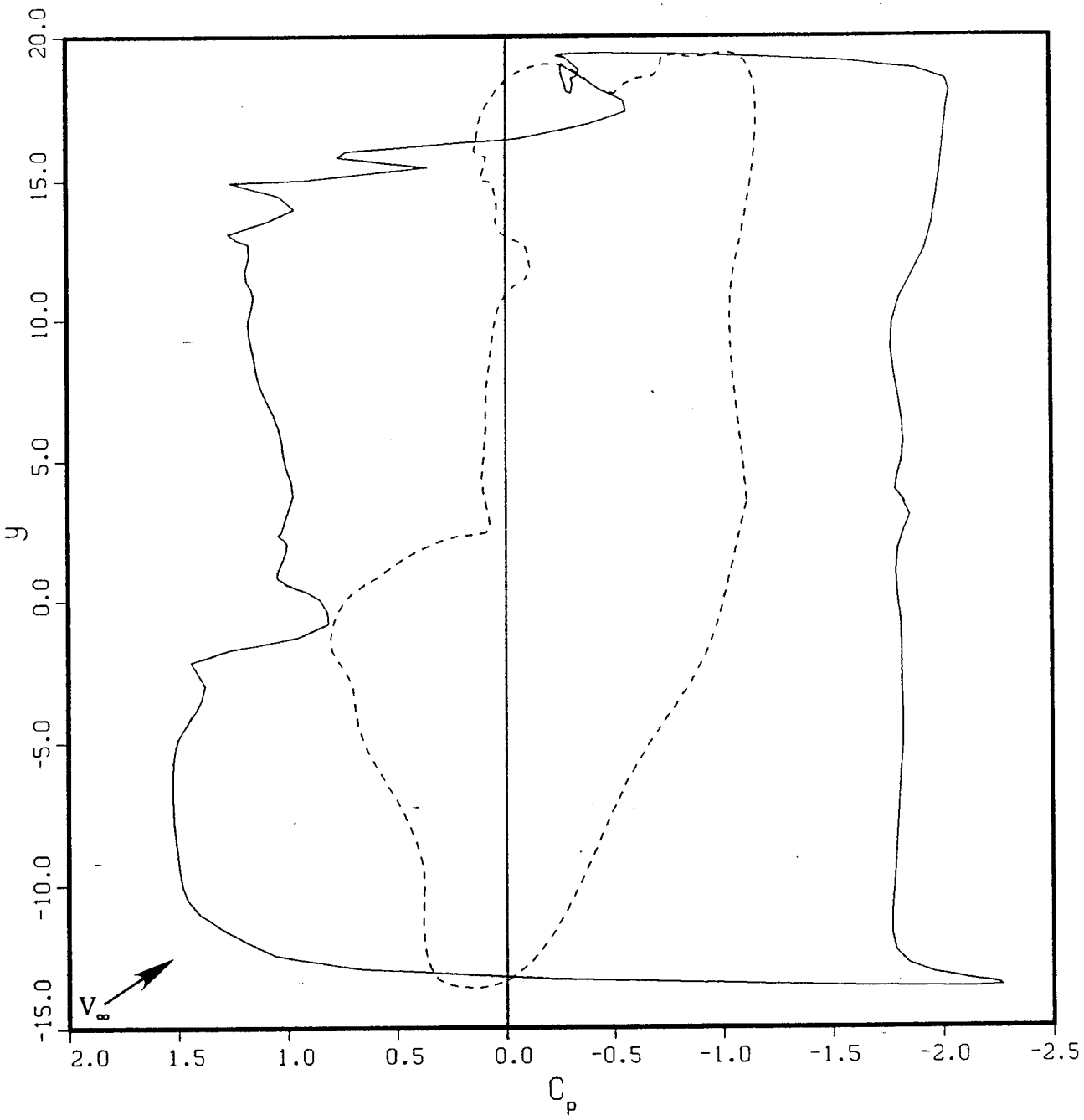

(a) Iteration 5600

Figure 11. - Predicted surface pressure distribution on the reclined ejection seat, $M_\infty = 0.6$, $\alpha = 35°$.

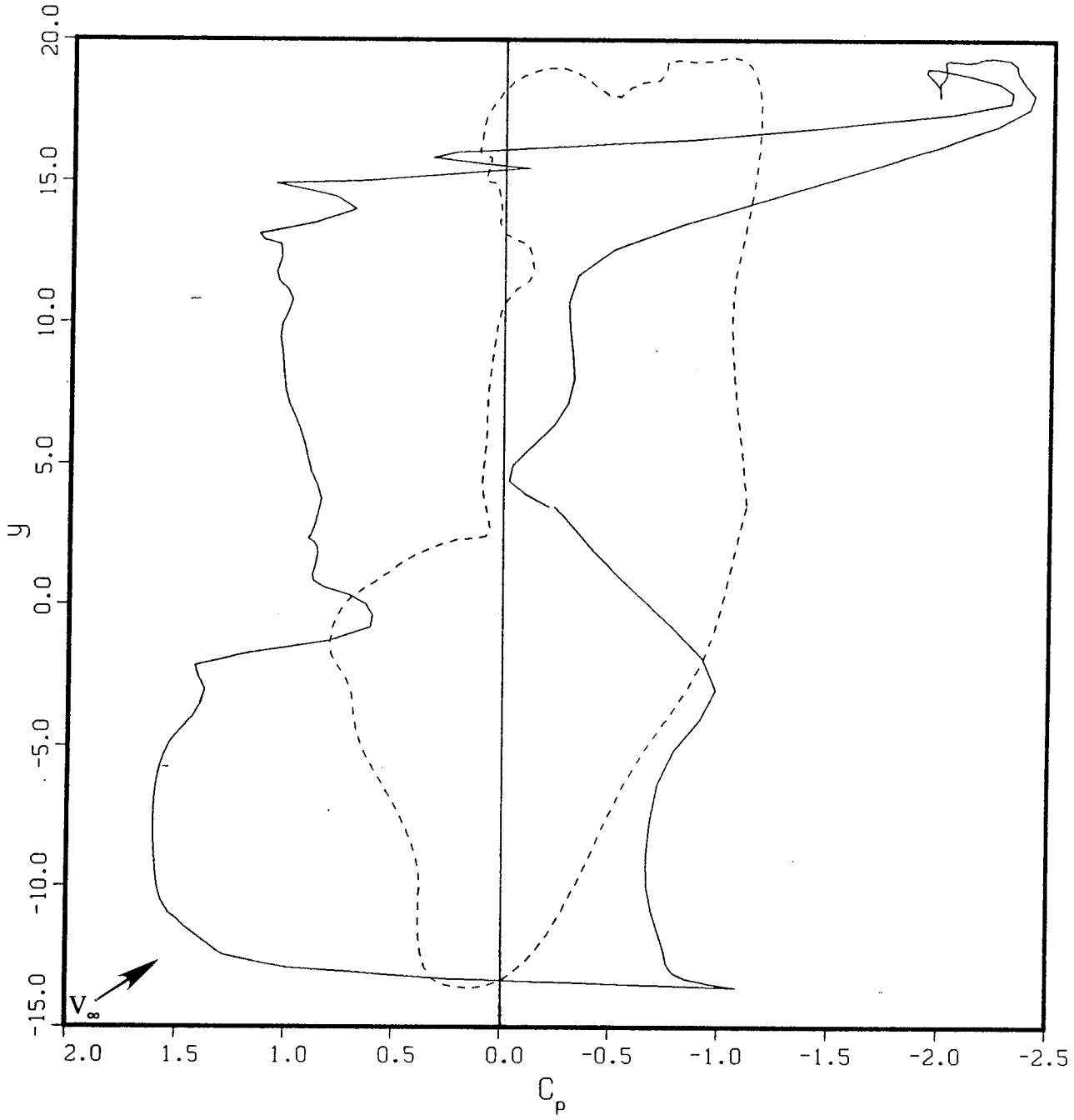

(b) Iteration 7000

Figure 11. - Concluded.

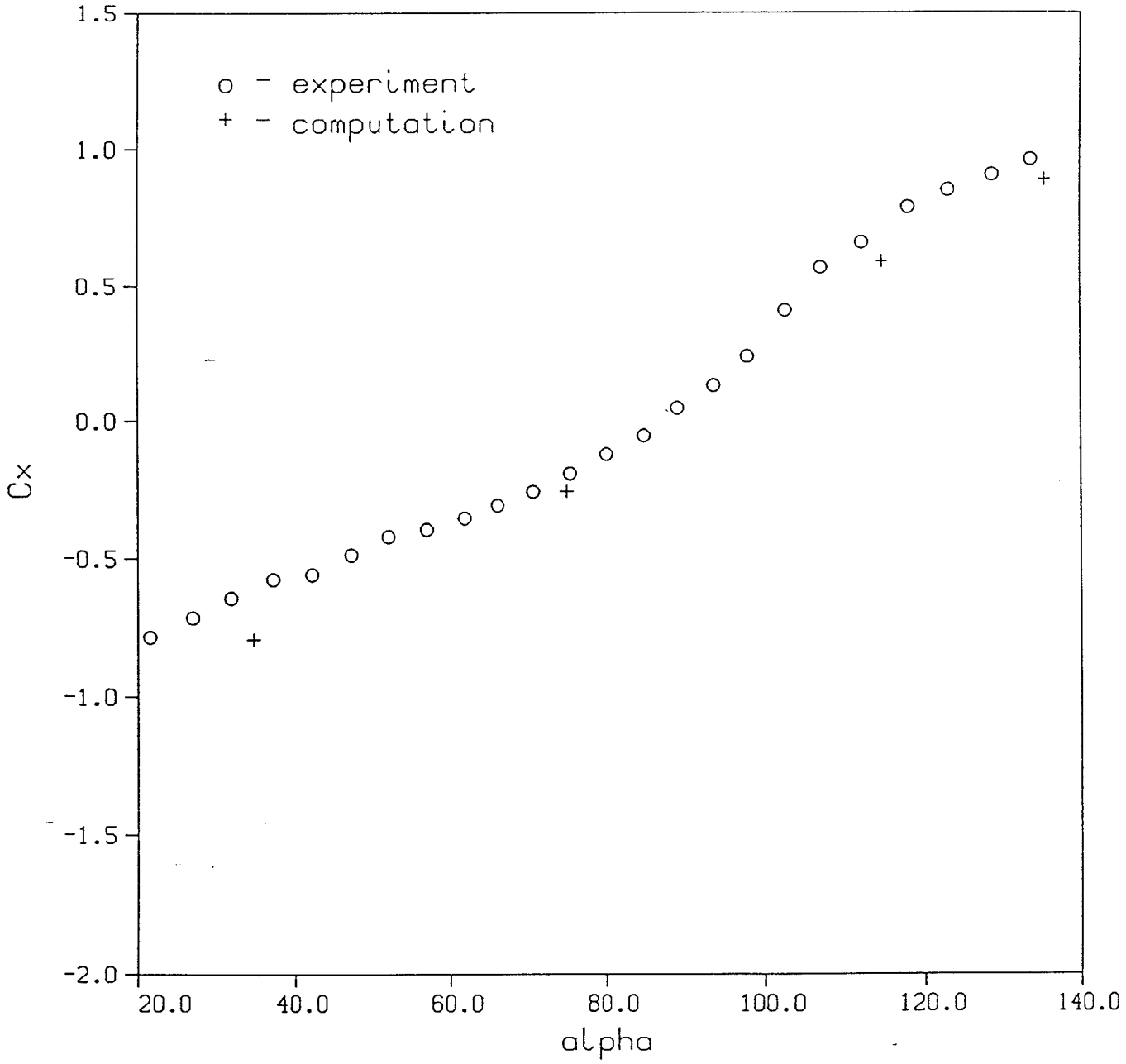

(a) Axial force coefficient

Figure 12. - Measured and predicted force and moment coefficients on the reclined ejection seat, $M_\infty = 0.6$.

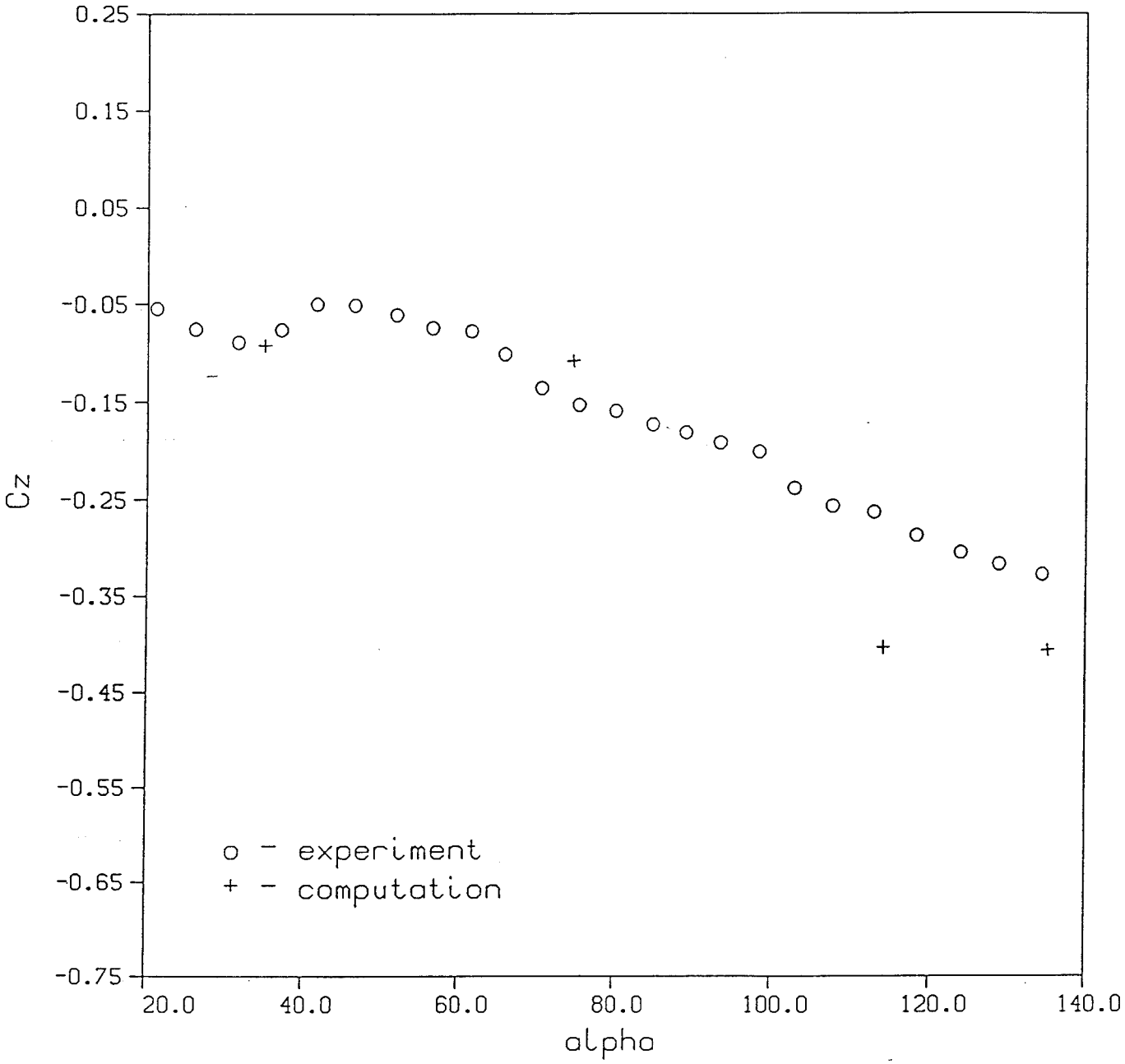

(b) Normal force coefficient

Figure 12. - Continued.

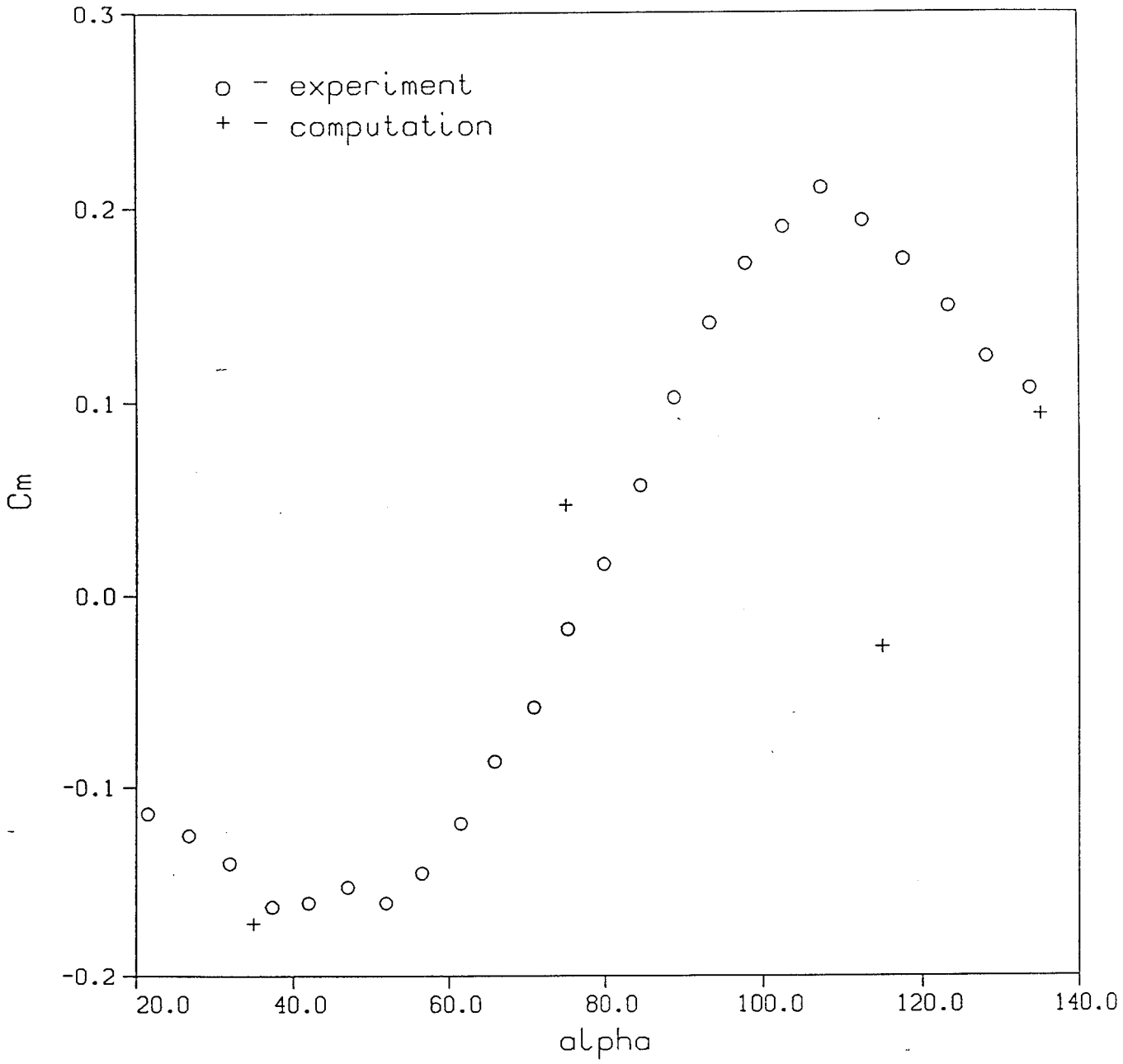

(c) Pitching moment

Figure 12. - Concluded.

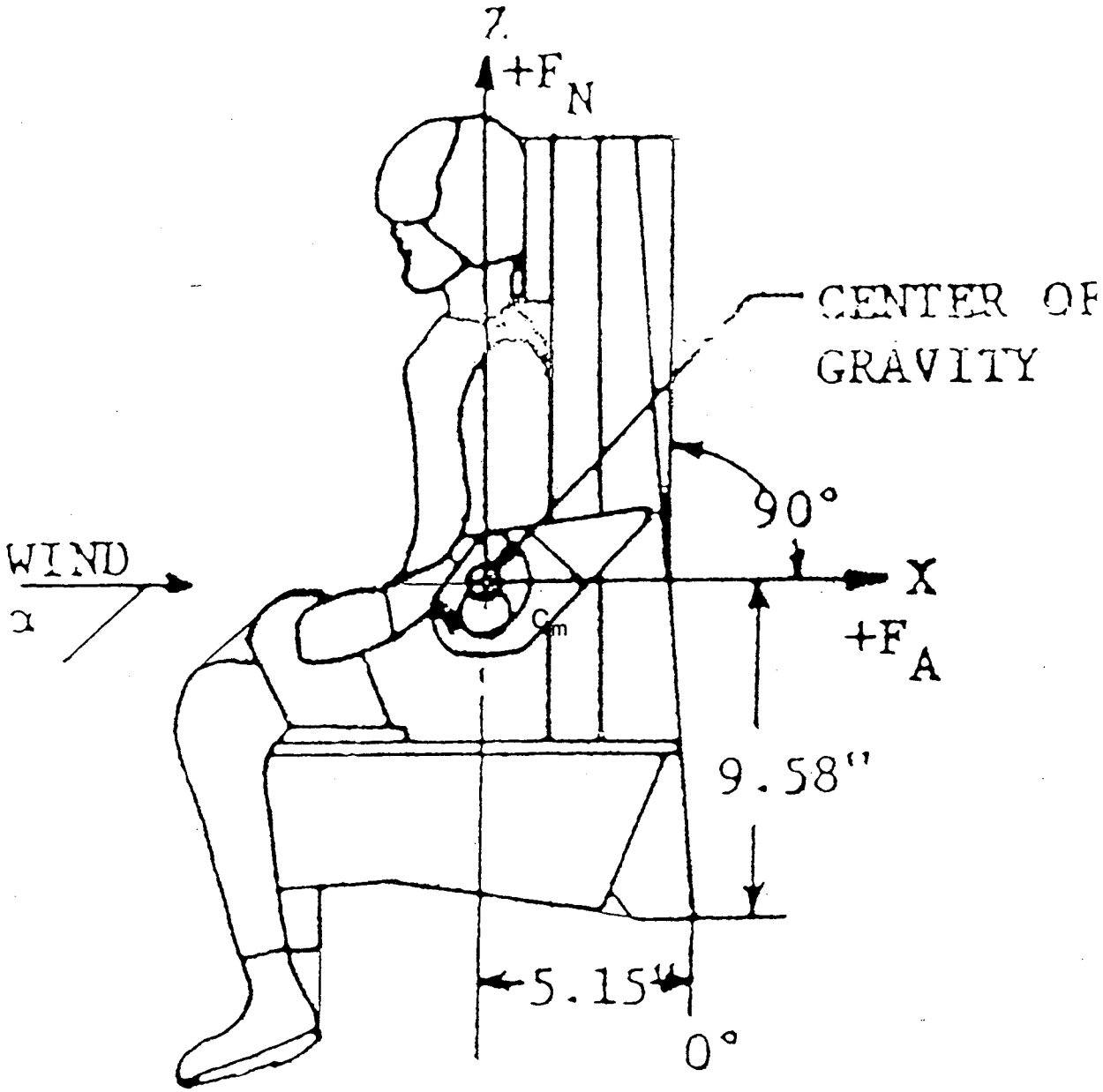

Figure 13. - Half-scale F-106 seat configuration.

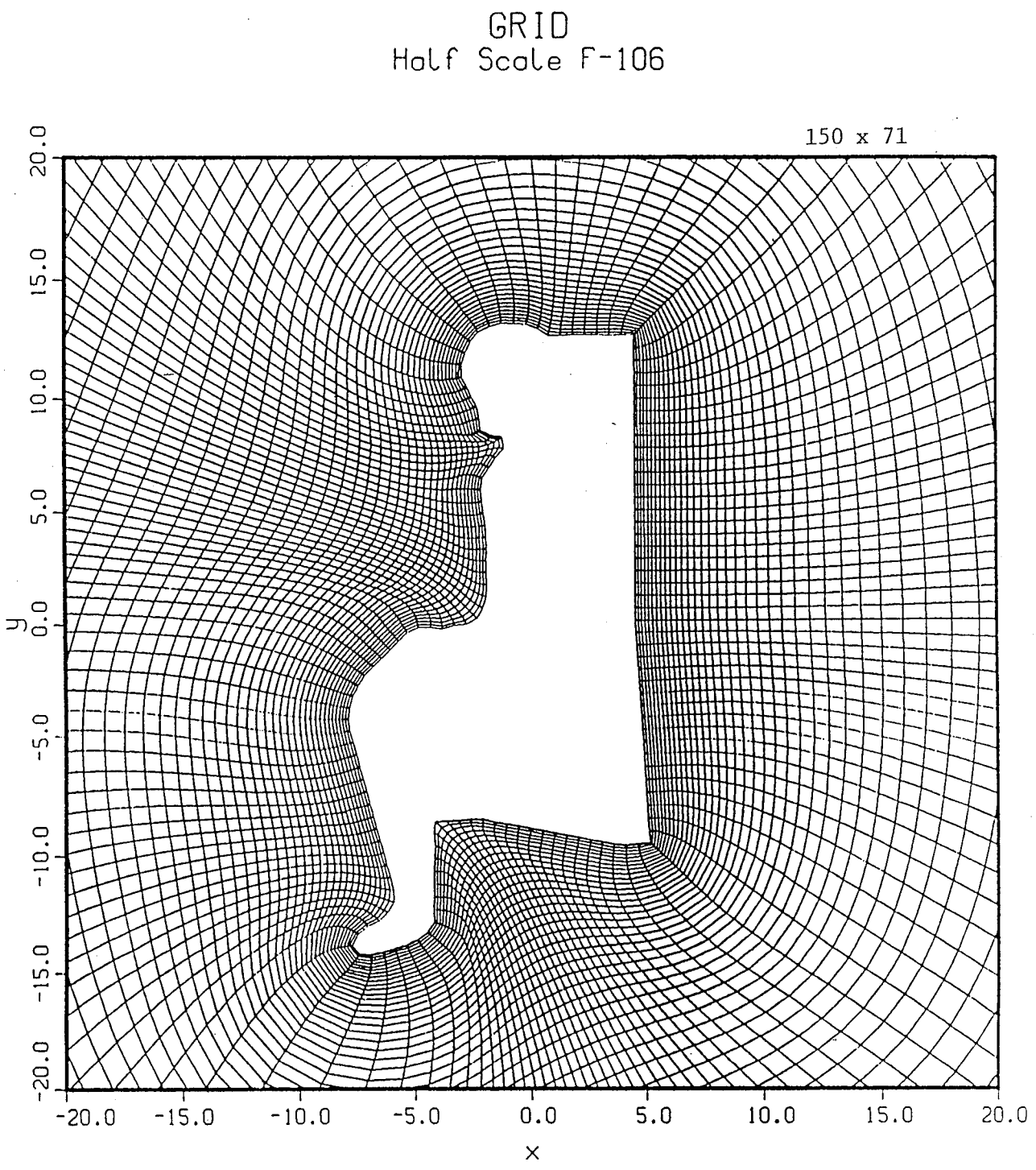

Figure 14. - Structured grid in the vicinity of the F-106 ejection seat model.

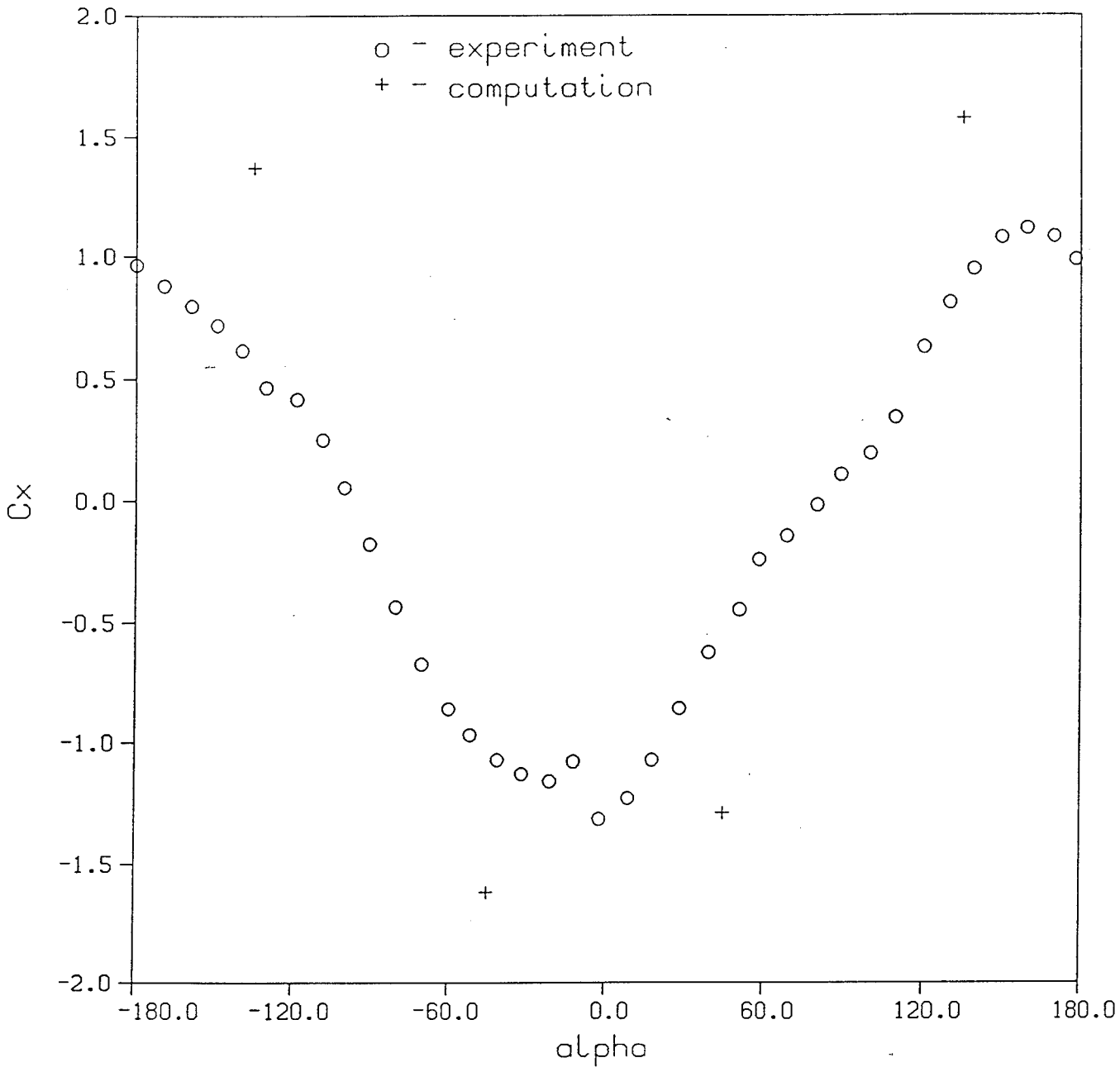

(a) Axial force coefficient

Figure 15. - Measured and predicted forces and moments on the F-106 ejection seat model, $M_\infty = 1.2$.

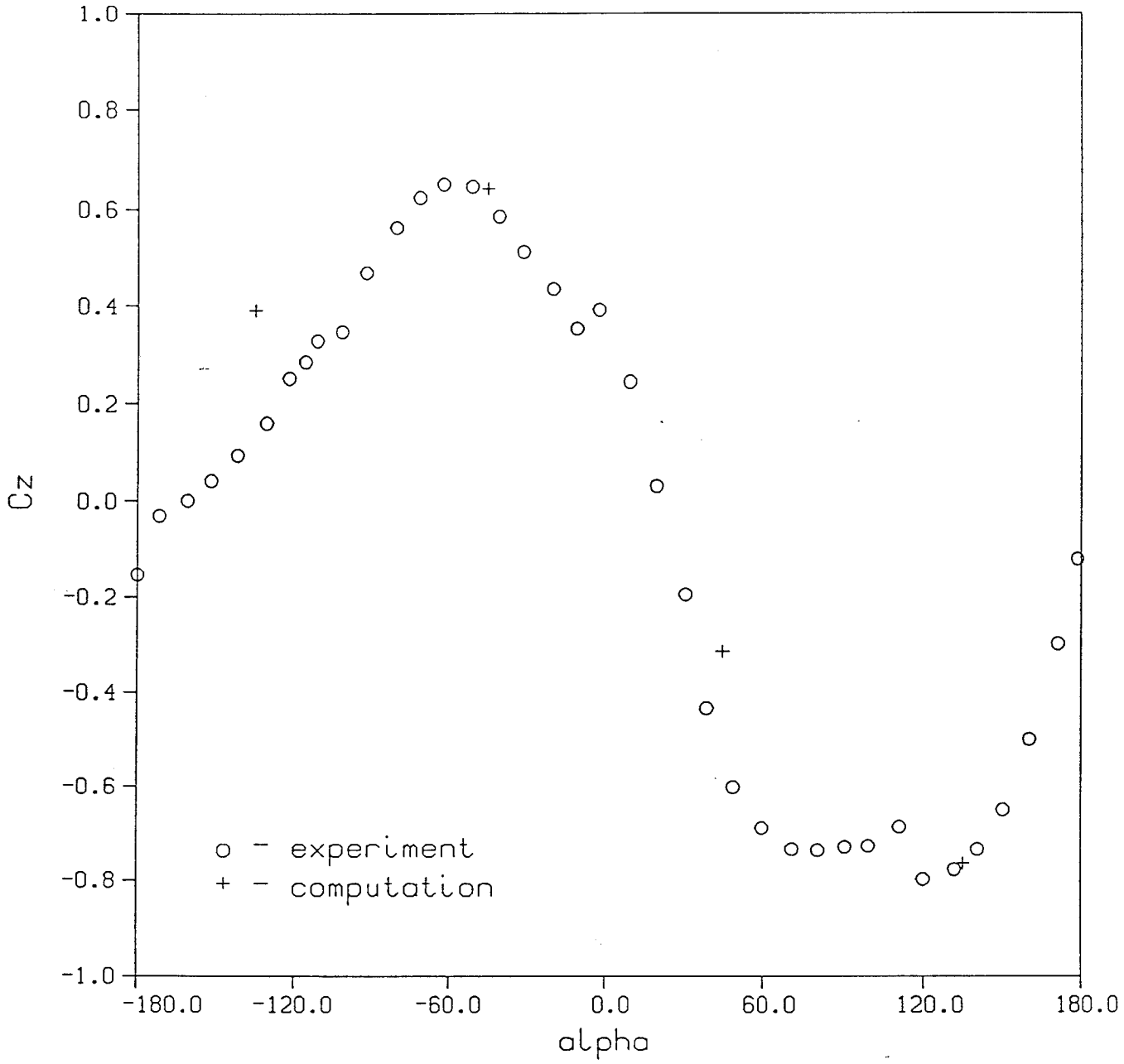

(b) Normal force coefficient

Figure 15. - Continued.

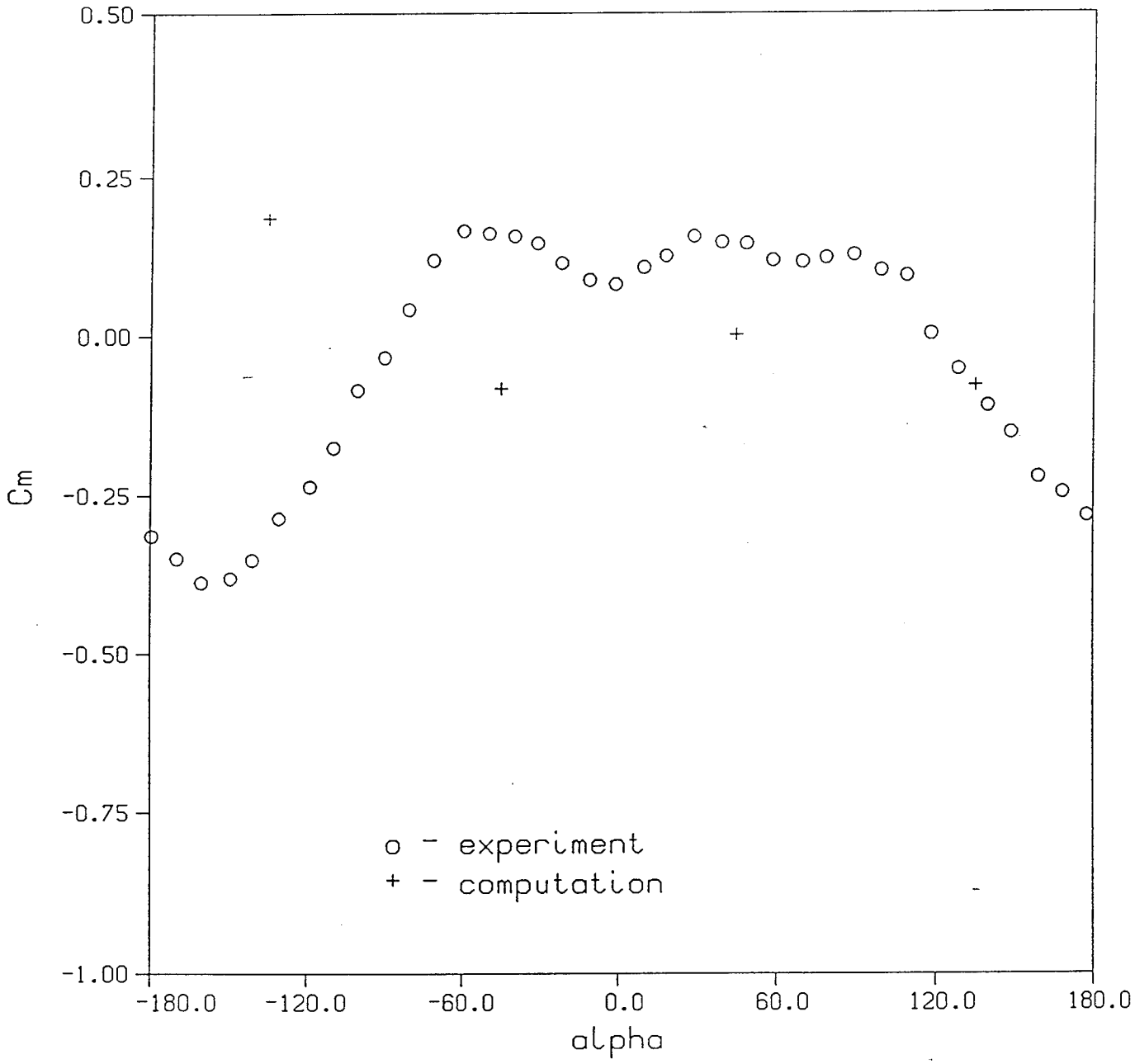

(c) Pitching moment coefficient

Figure 15. - Concluded.

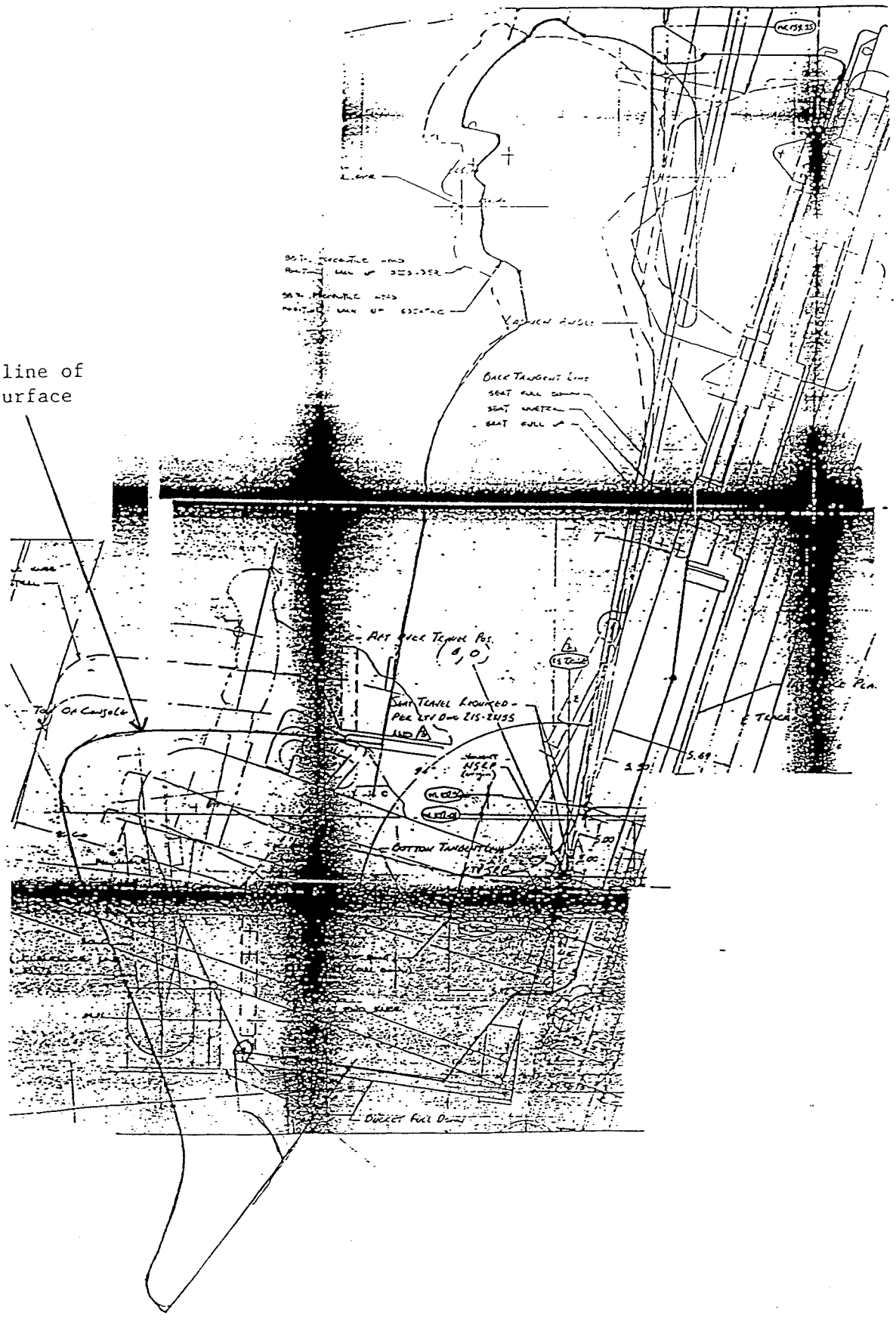

Figure 16. - 0.65 Scale SIIIS-3R Configuration.

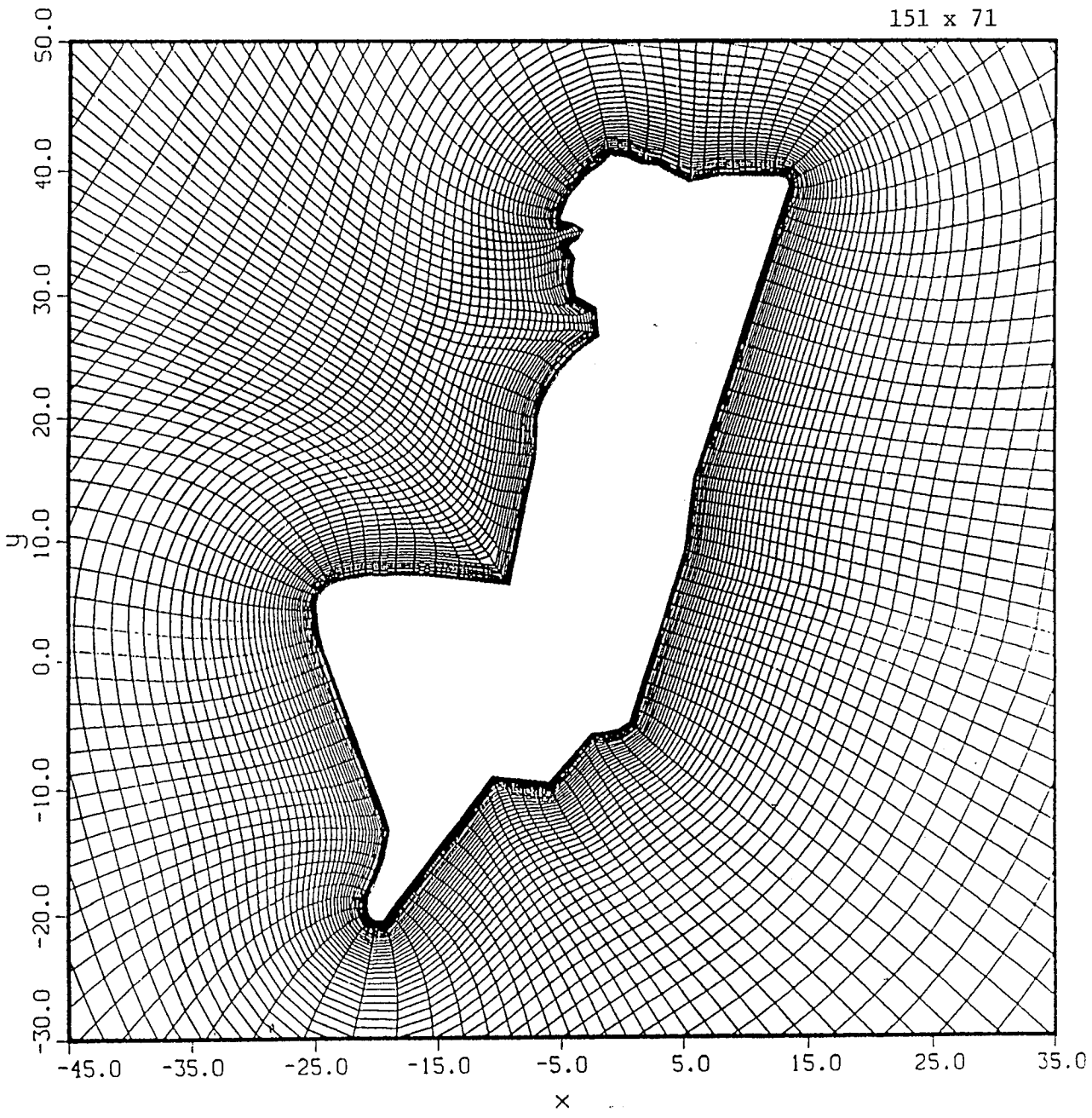

Figure 17. - Near field structured grid for the SIIIS-3ER ejection seat model.

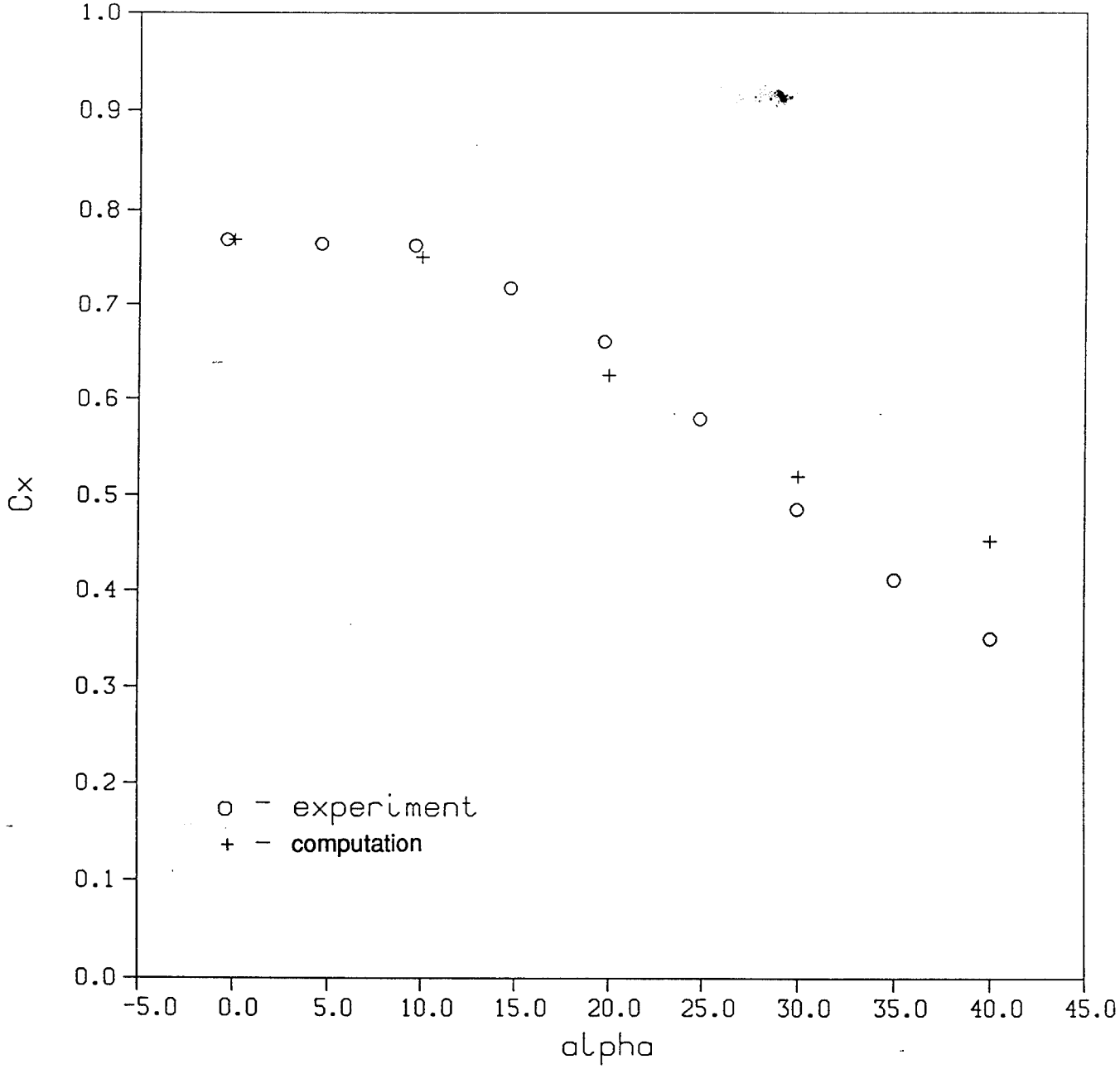

(a) Axial force coefficient

Figure 18. - Measured and predicted forces and moments on the SIIIS-3R ejection seat model, $M_\infty = 0.75$.

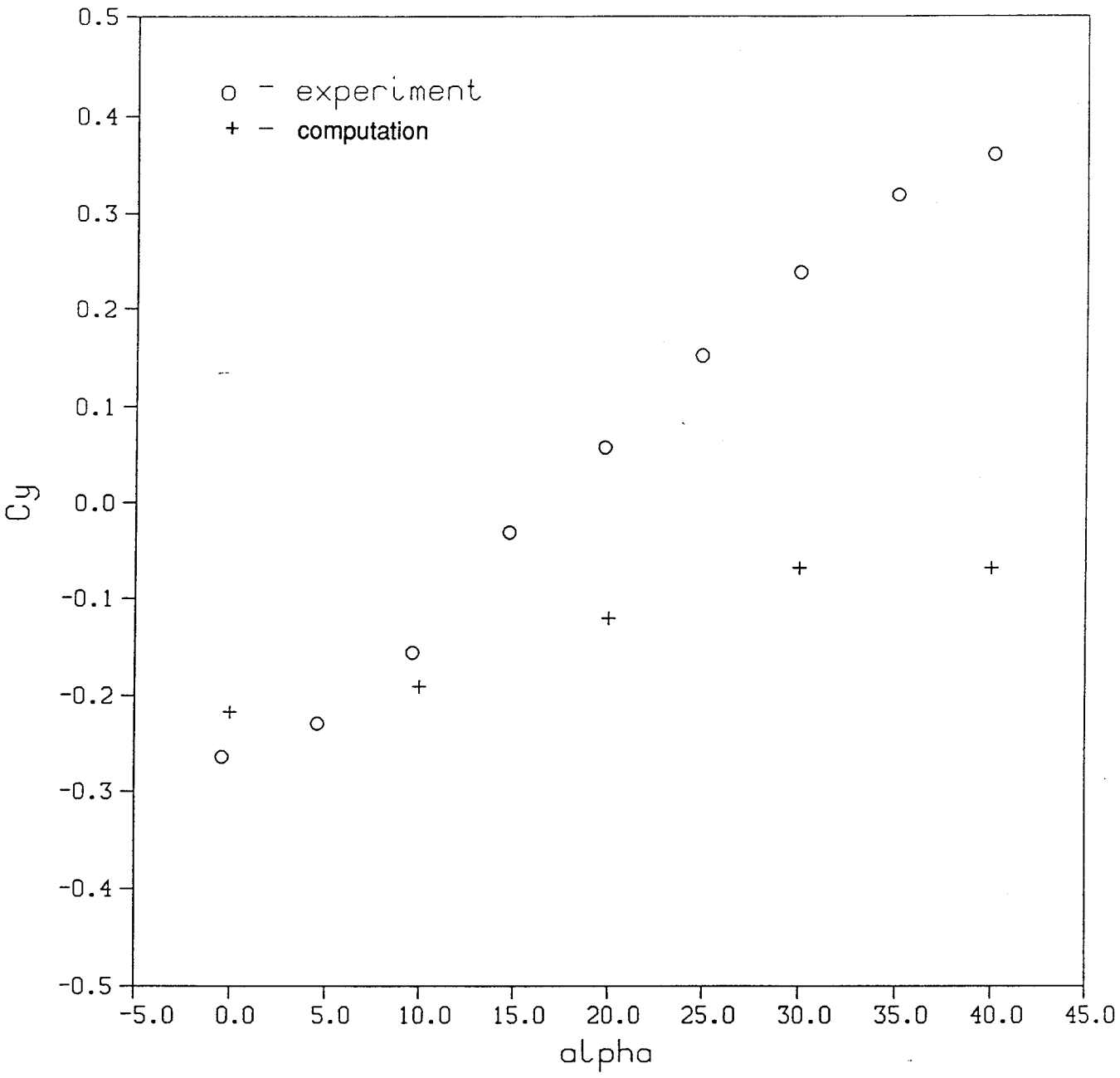

(b) Normal force coefficient

Figure 18. - Concluded.

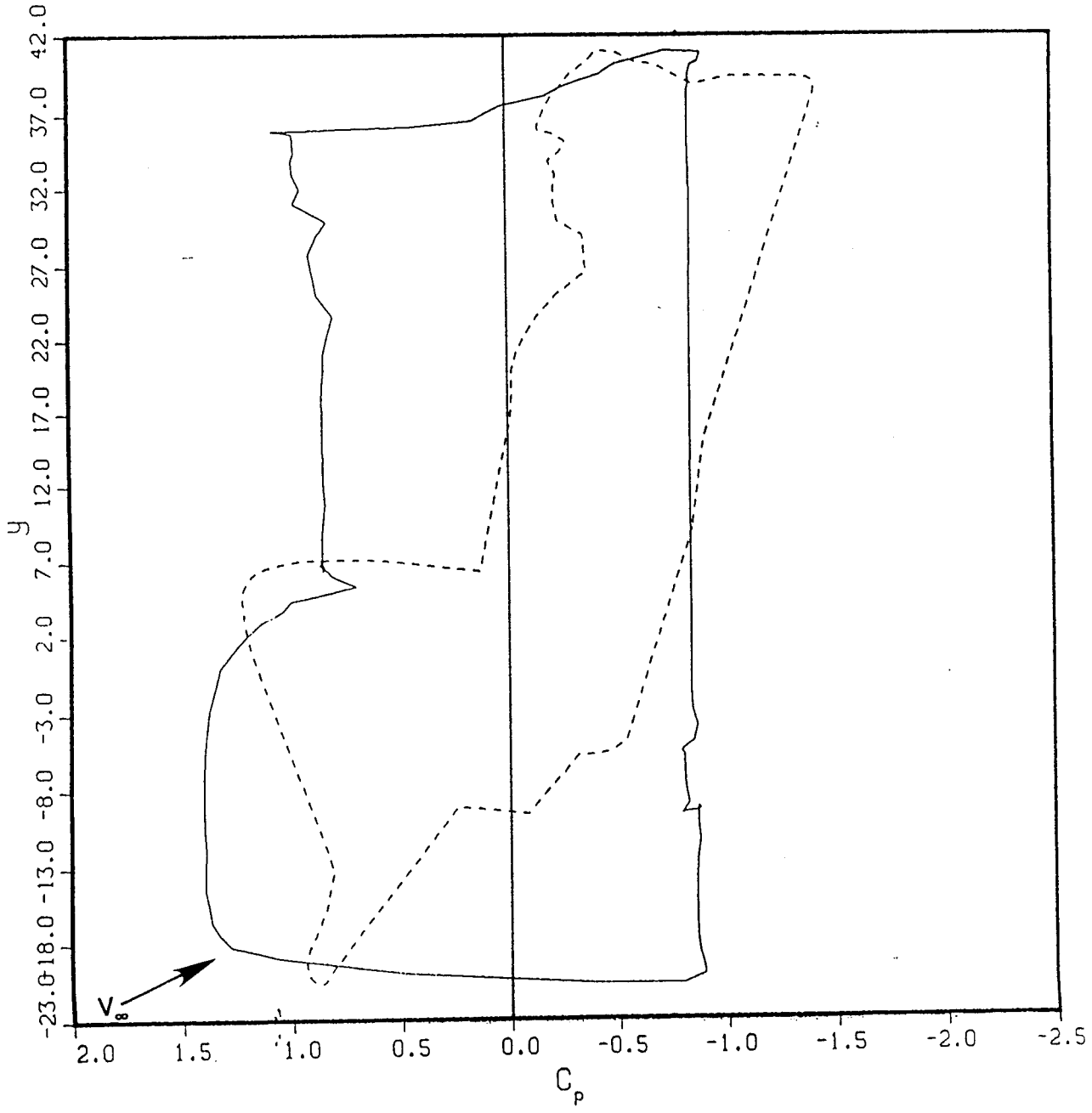

Figure 19. - Predicted surface pressure distribution on the SIIIS-3ER ejection seat model, $M_\infty = 1.2$, $\alpha = 25°$.

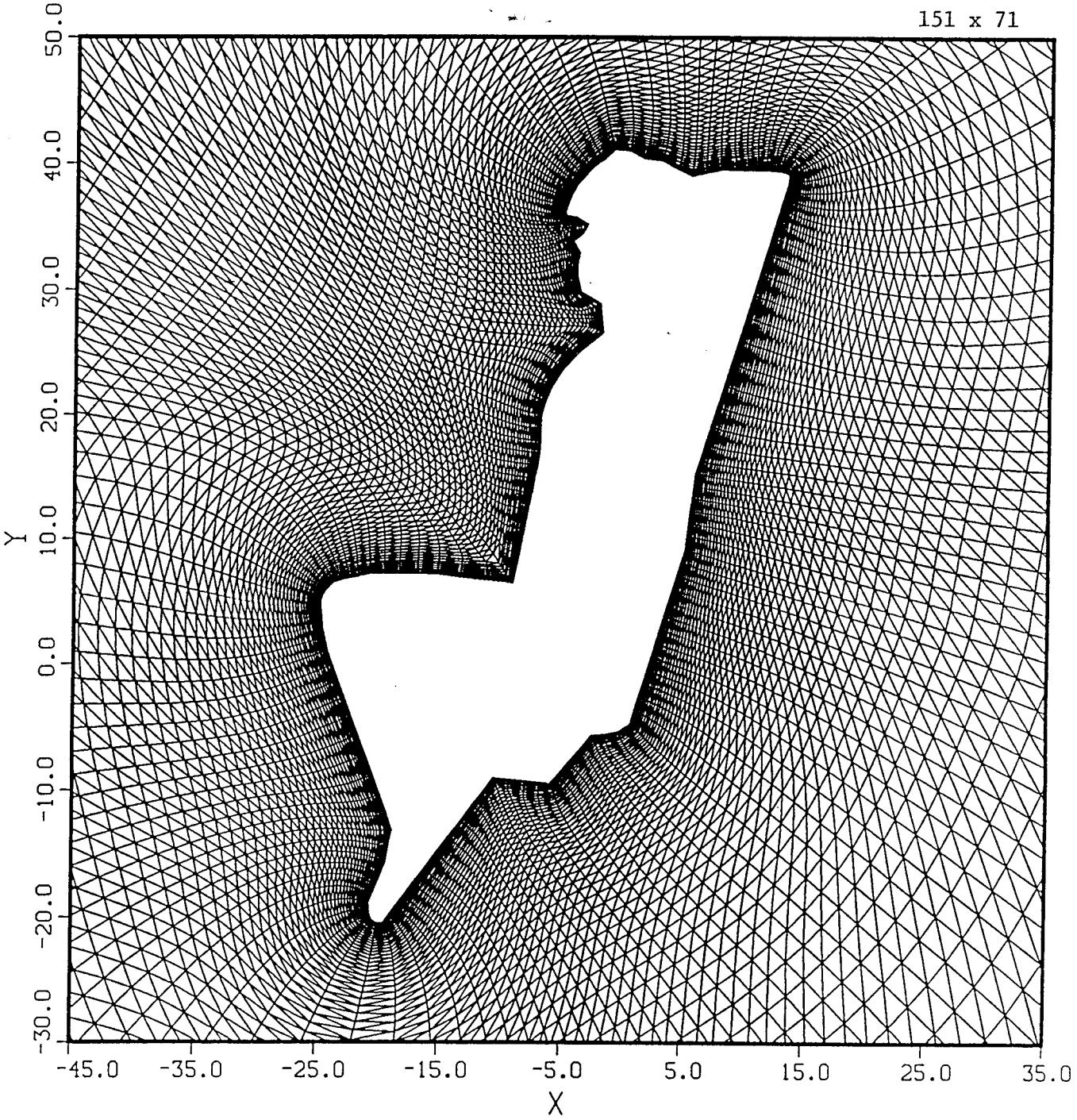

Figure 20. - Unstructured mesh near the SIIIS-3ER ejection seat.

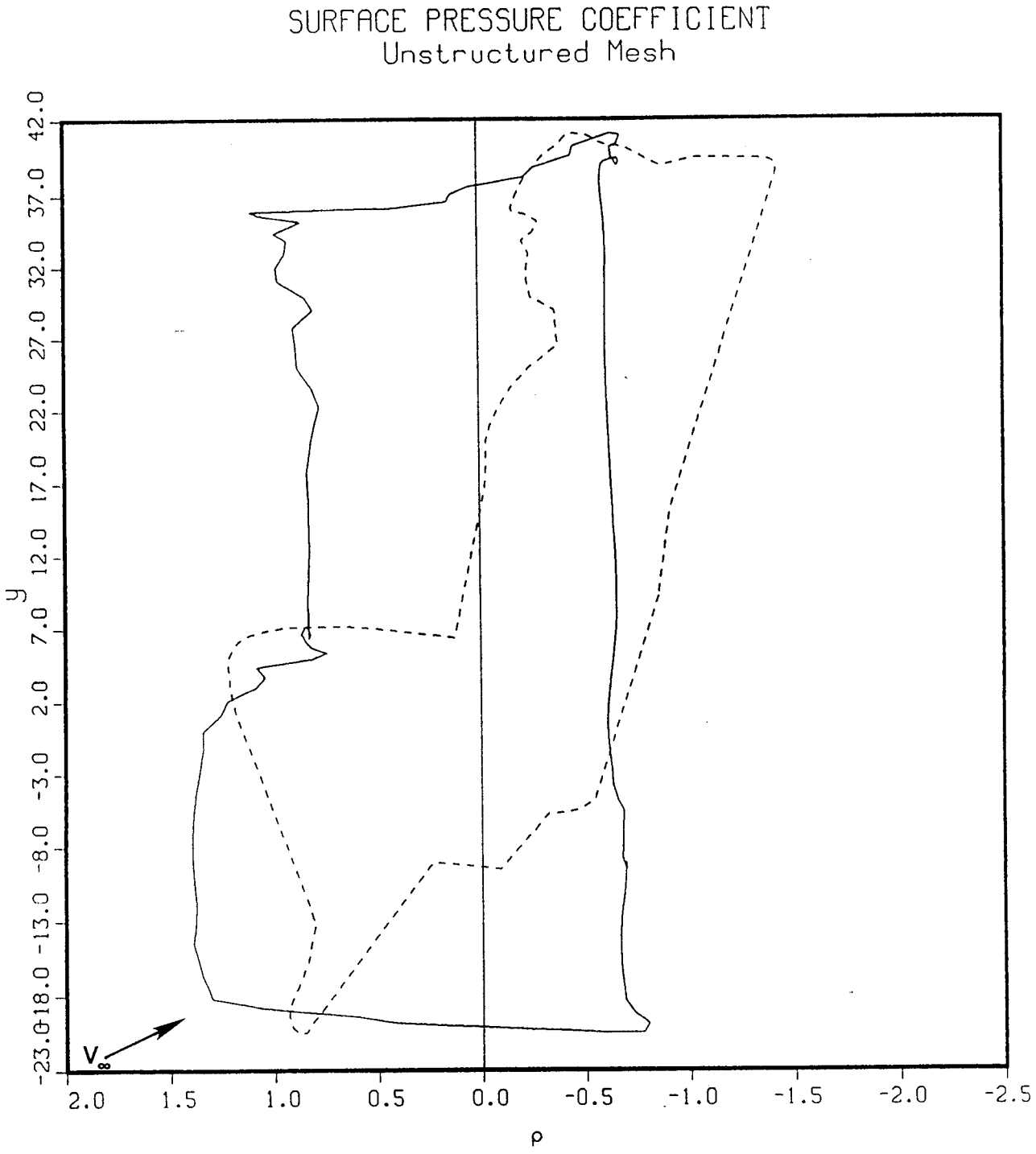

Figure 21. - Predicted surface pressure distribution on the SIIIS-3ER ejection seat modeled with an unstructured grid, $M_\infty = 1.2$, $\alpha = 25°$.

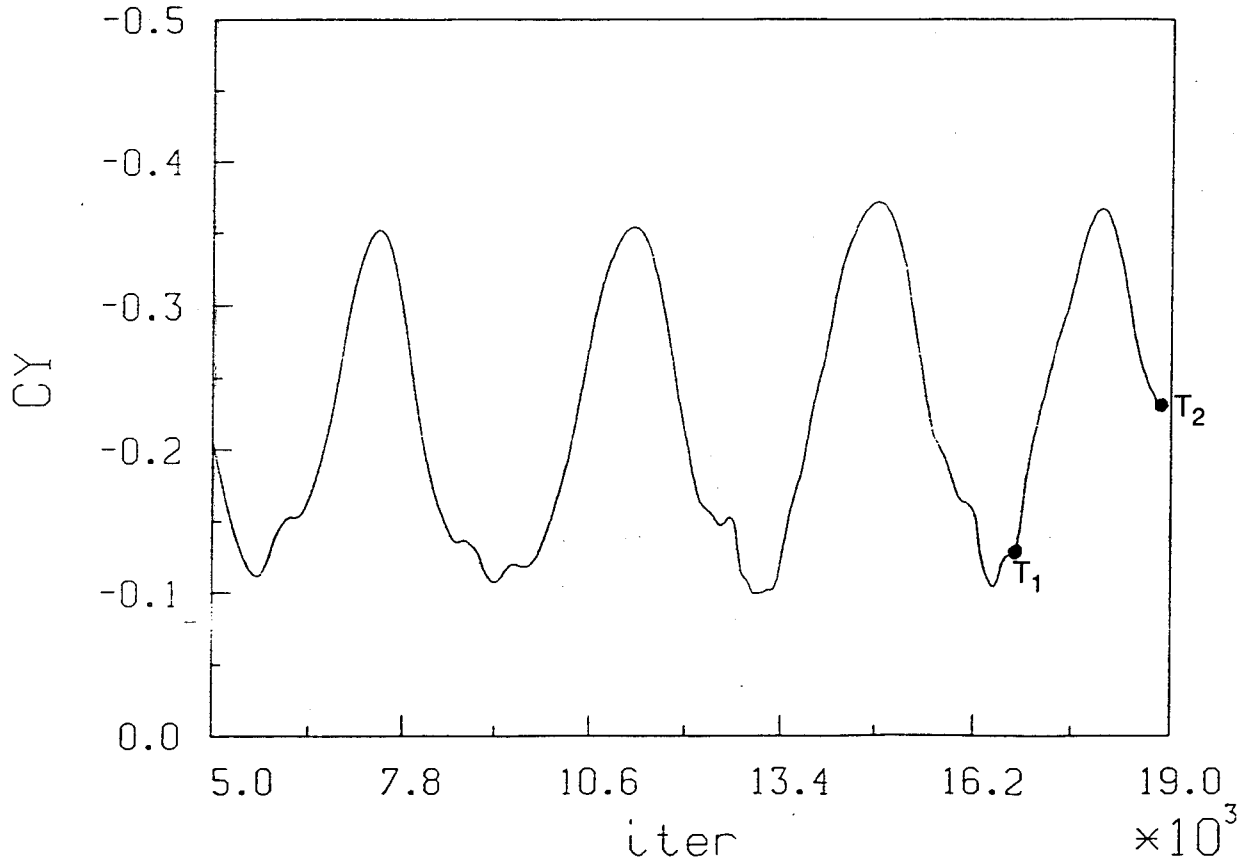

(a) Normal force coefficient

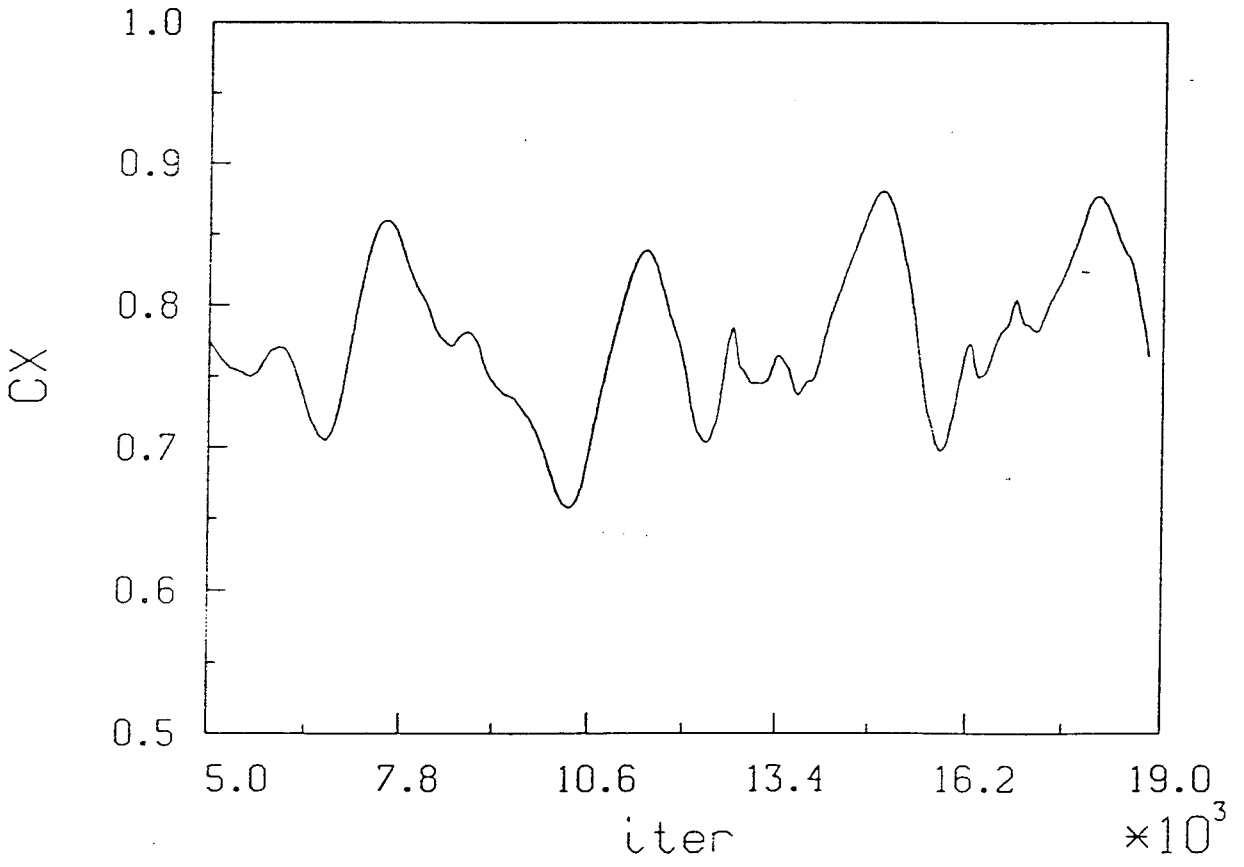

(b) Axial force coefficient

Figure 22. - Predicted unsteady forces on the SIIIS-3ER ejection seat, $M_\infty = 0.75$, $\alpha = 0°$.

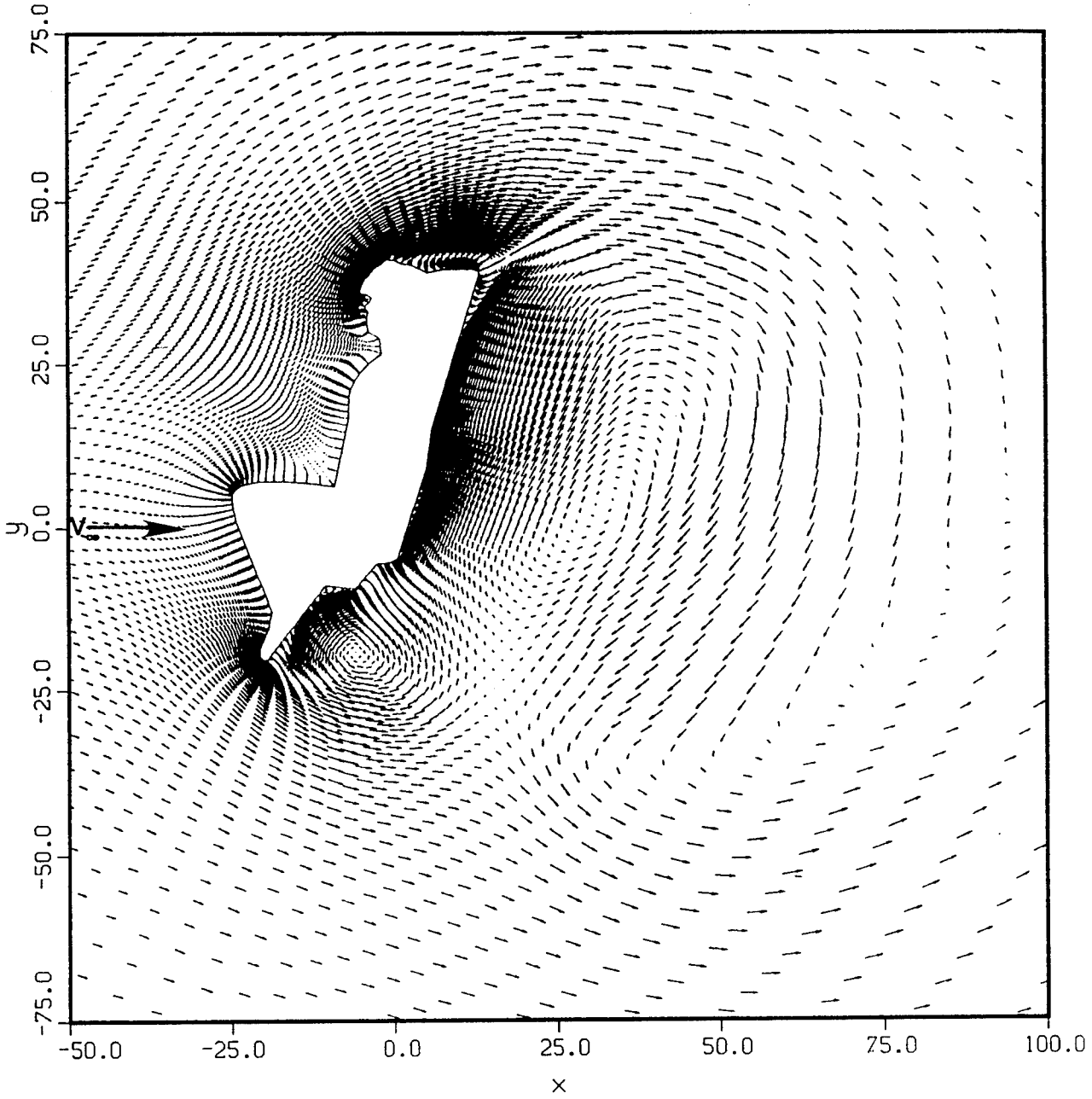

(a) Iteration 16,800

Figure 23. - Predicted velocity field near the SIIIS-3ER ejection seat, $M_\infty = 0.75$, $\alpha = 0°$.

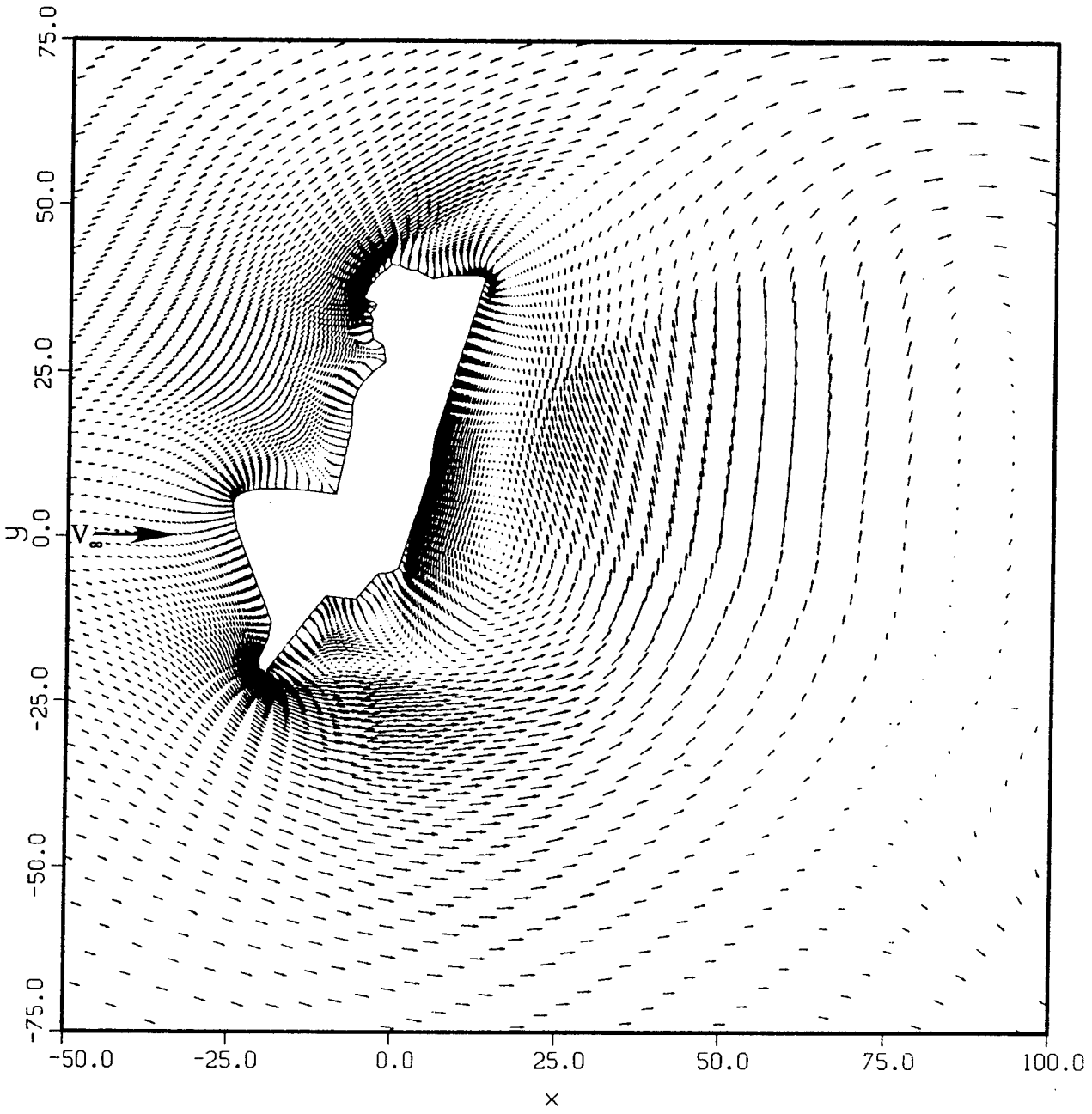

(b) Iteration 18,200

Figure 23. - Concluded.

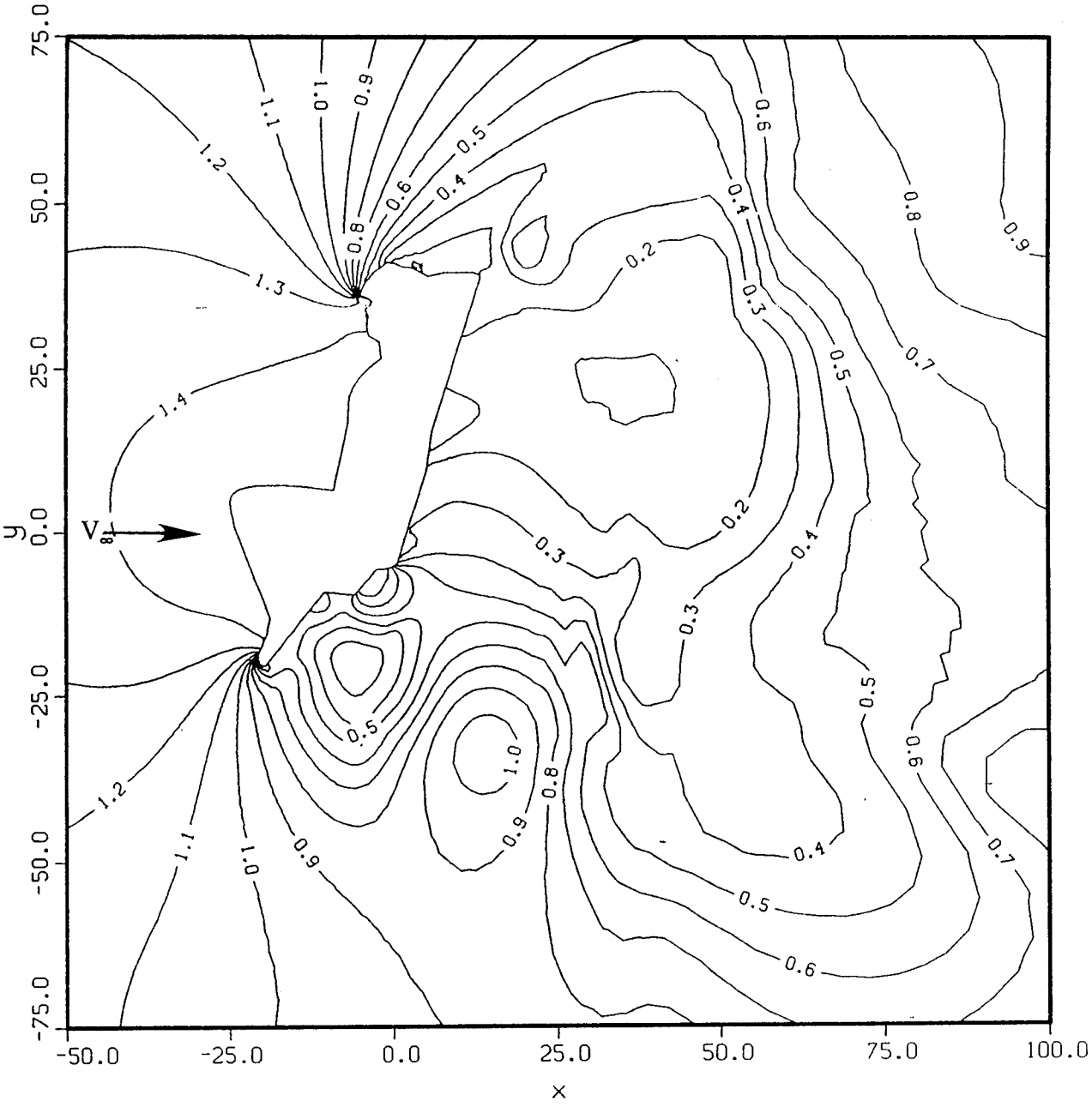

(a) Iteration 16,800

Figure 24. - Predicted pressure contours near the SIIIS-3ER ejection seat, $M_\infty = 0.75$, $\alpha = 0°$.

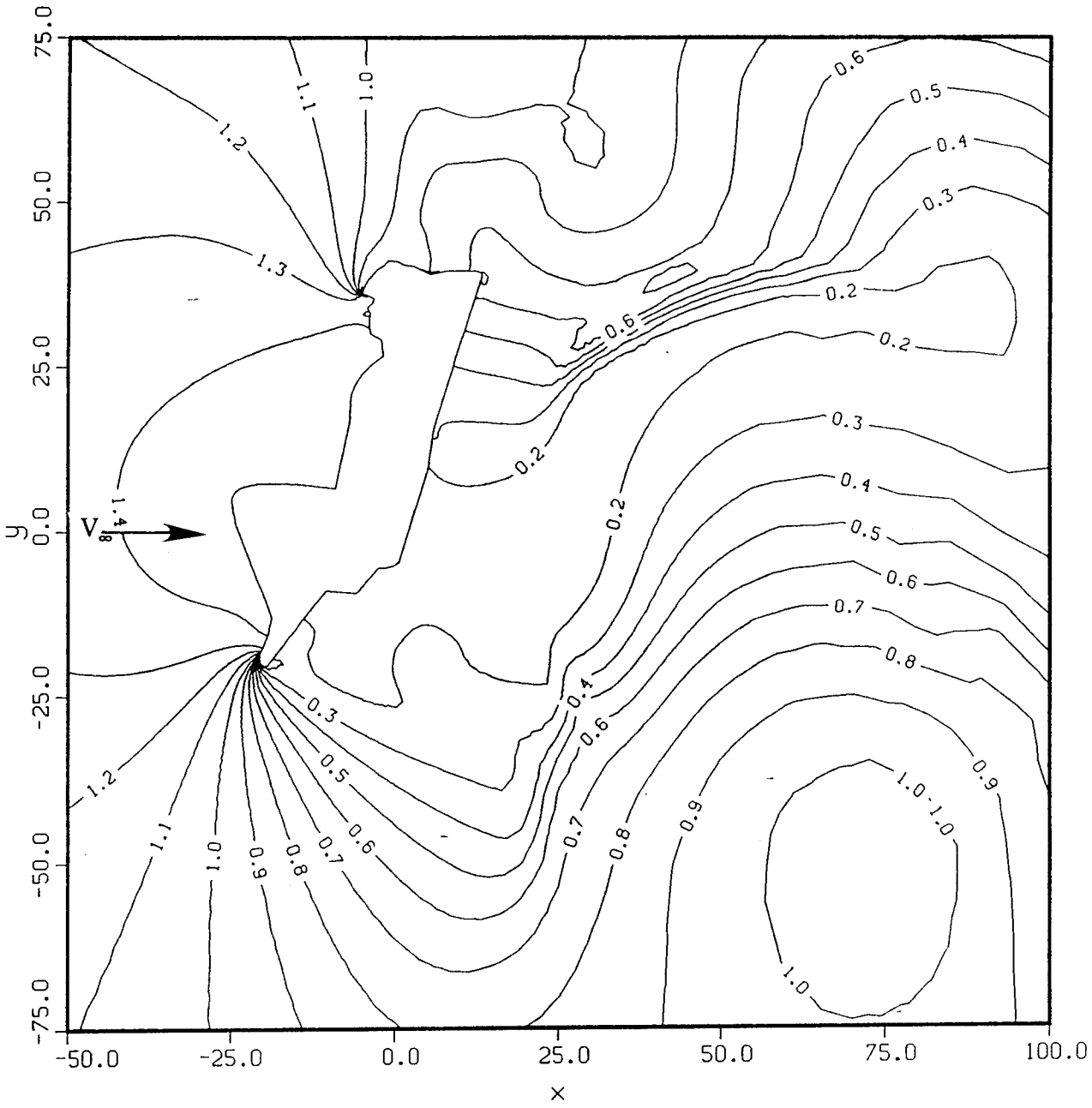

(b) Iteration 18,200

Figure 24. - Concluded.

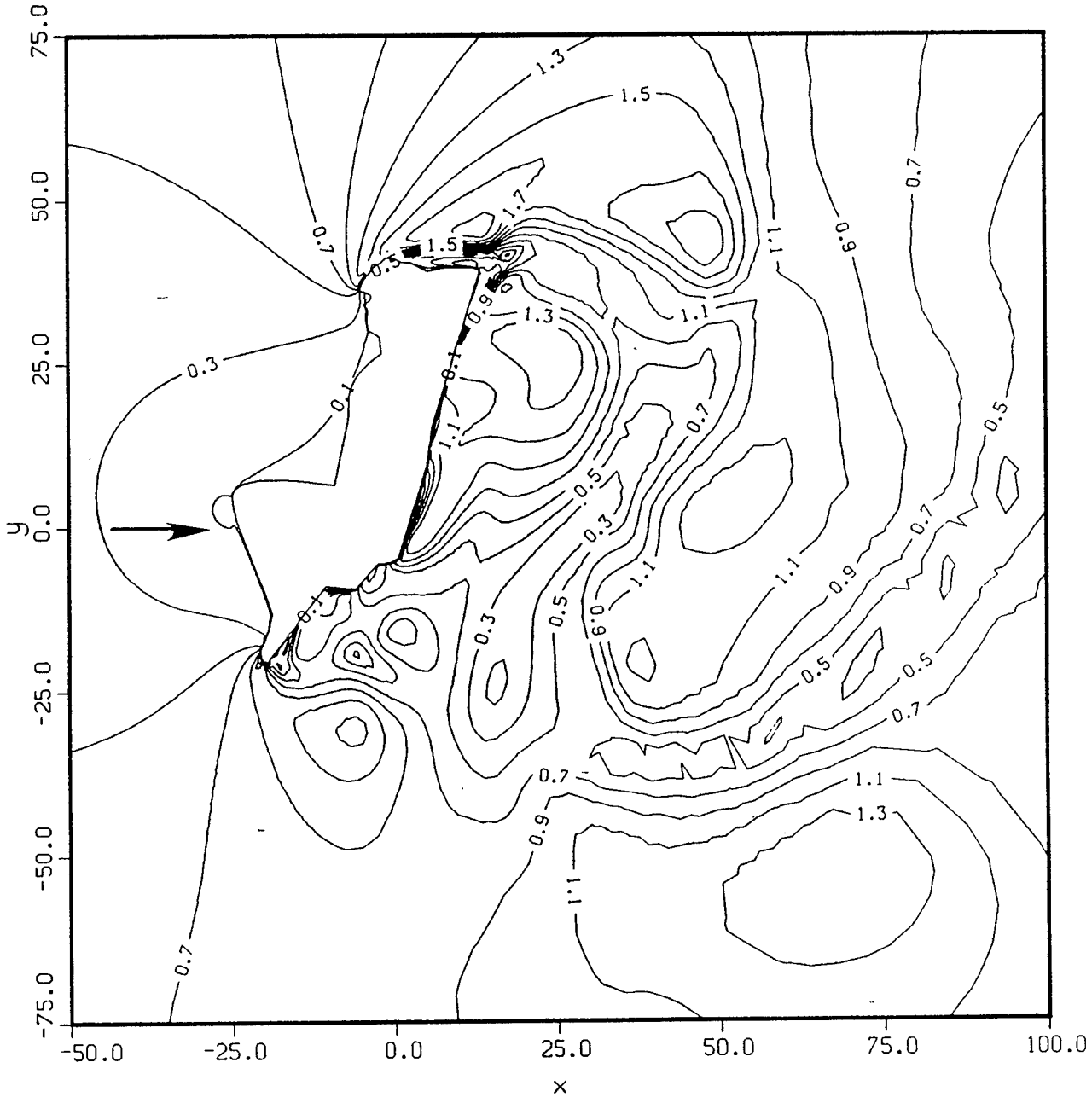

(a) Iteration 16,800

Figure 25. - Predicted Mach number contours near the SIIIS-3ER ejection seat, $M_\infty = 0.75, \alpha = 0°$.

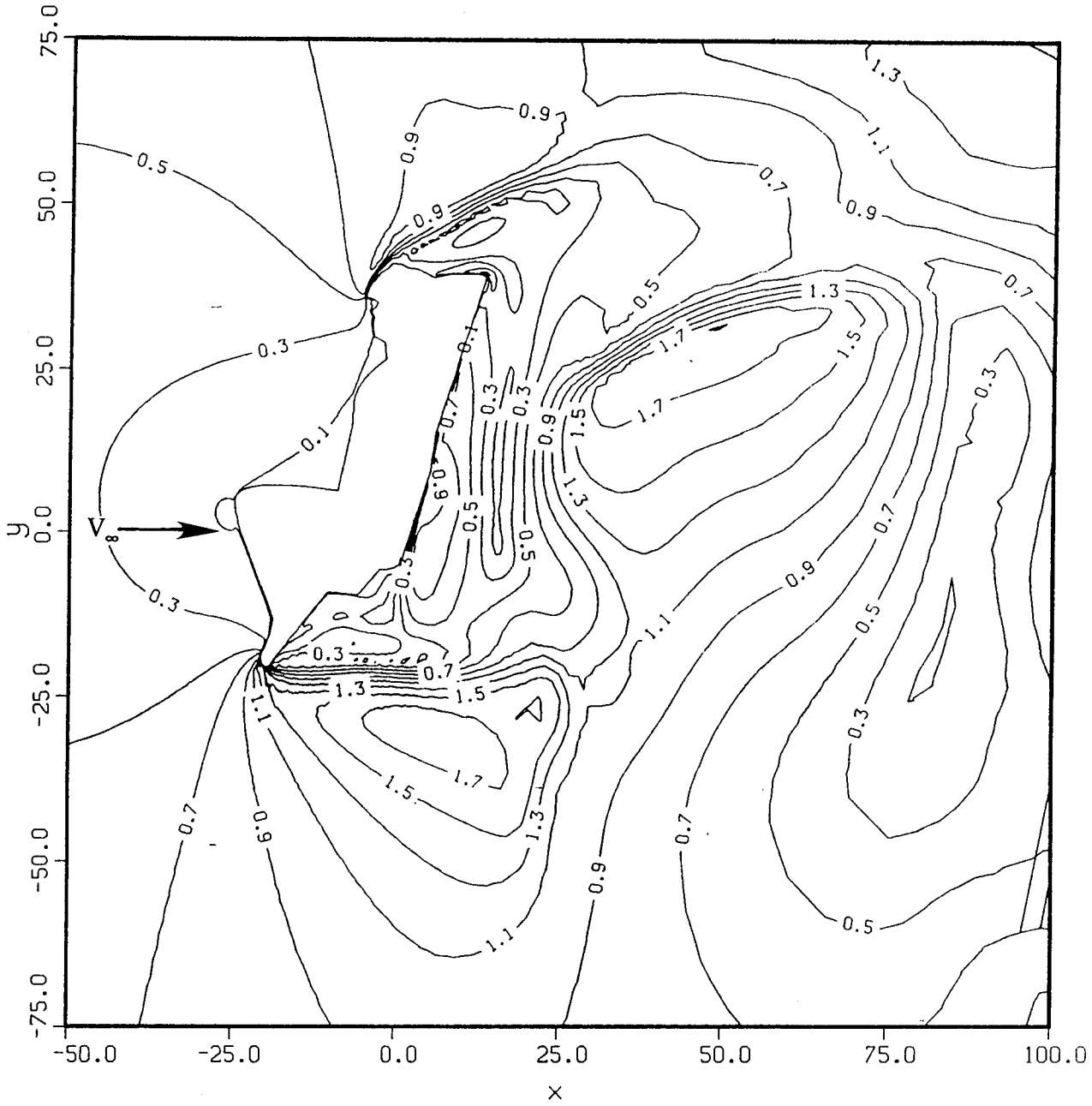

(b) Iteration 18,200

Figure 25. - Concluded.

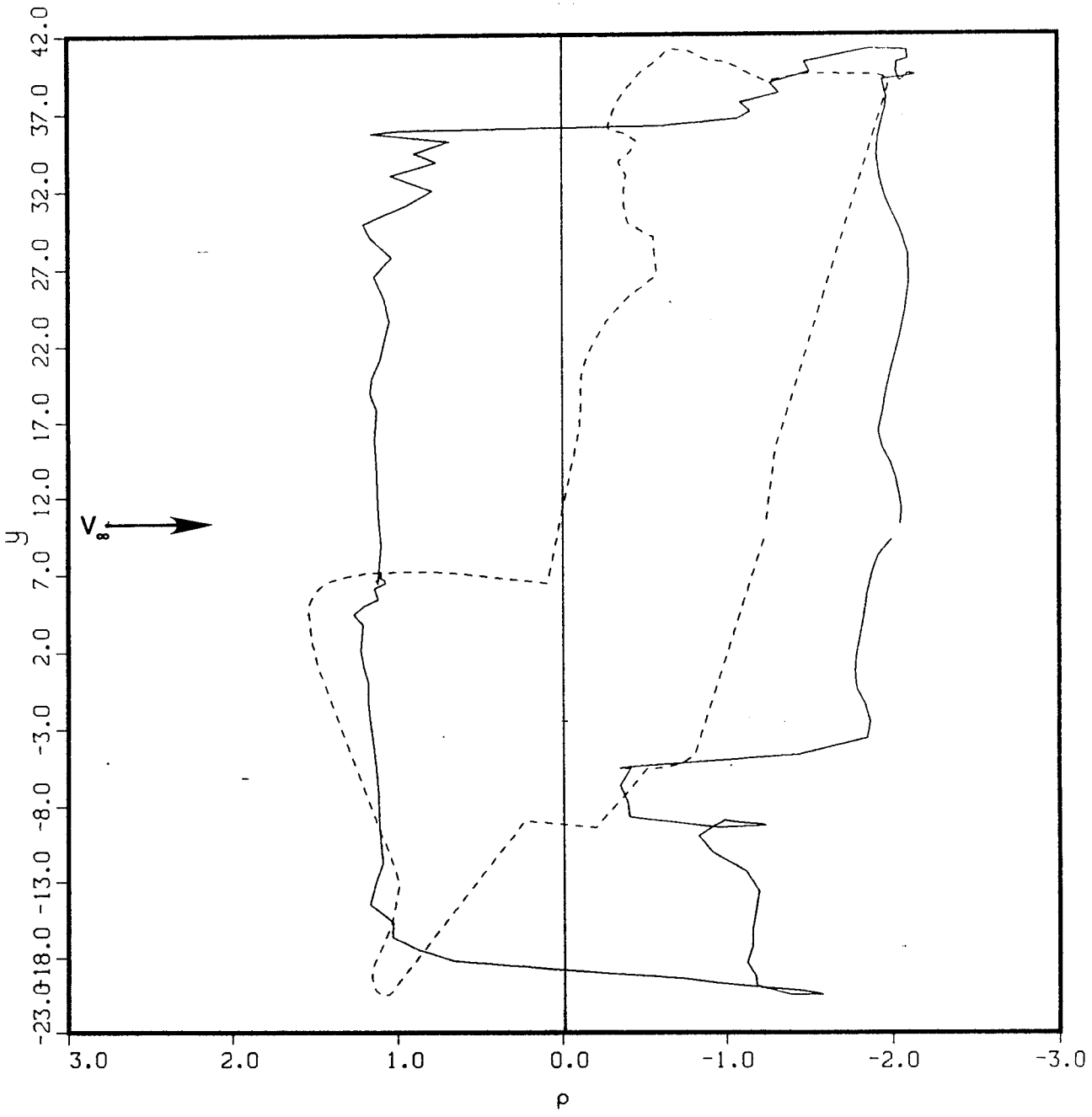

(a) Iteration 16,800

Figure 26. - Predicted surface pressure distribution on the SIIIS-3ER ejection seat, $M_\infty = 0.75$, $\alpha = 0°$.

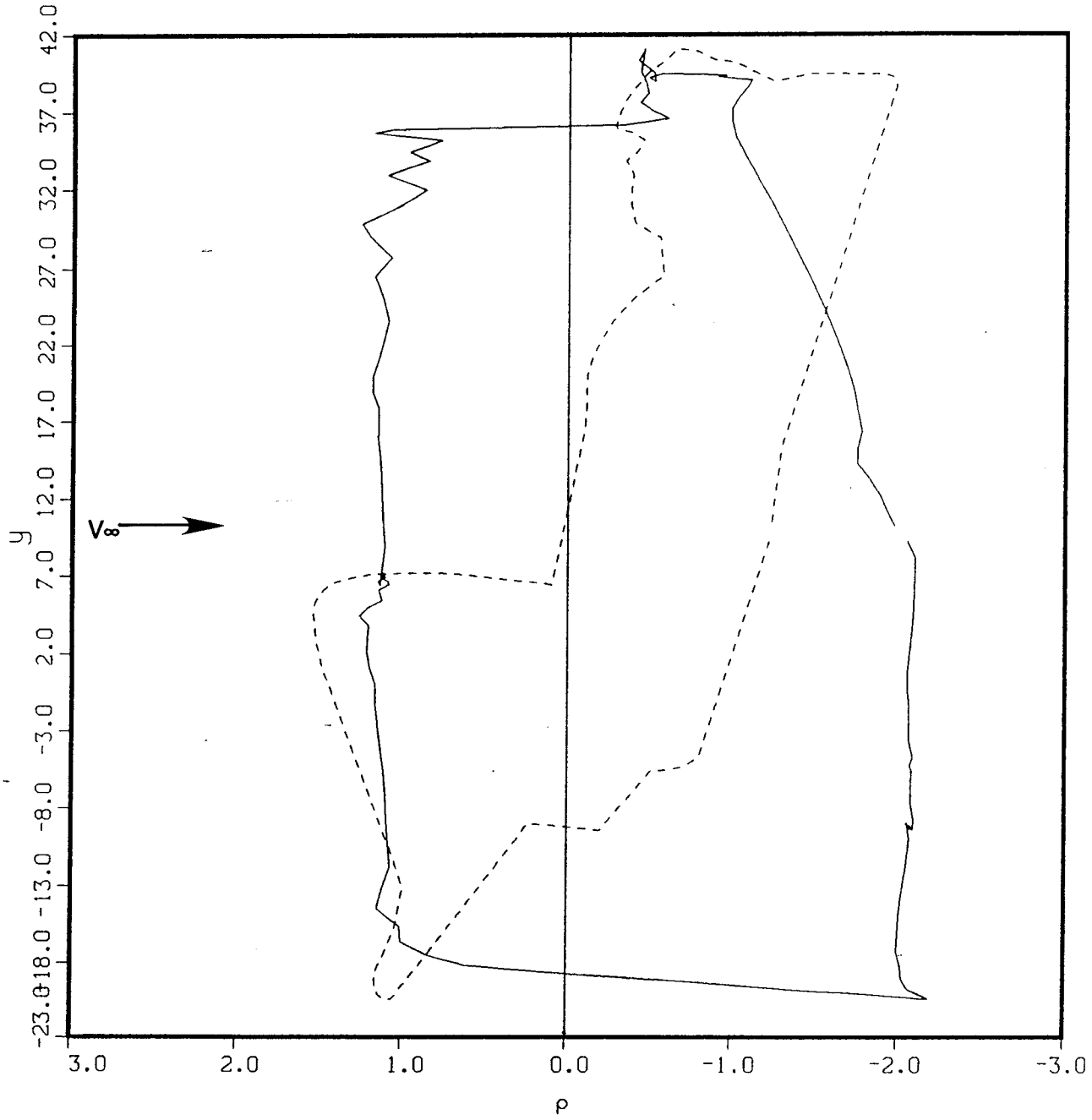

(b) Iteration 18,200

Figure 26. - Concluded.

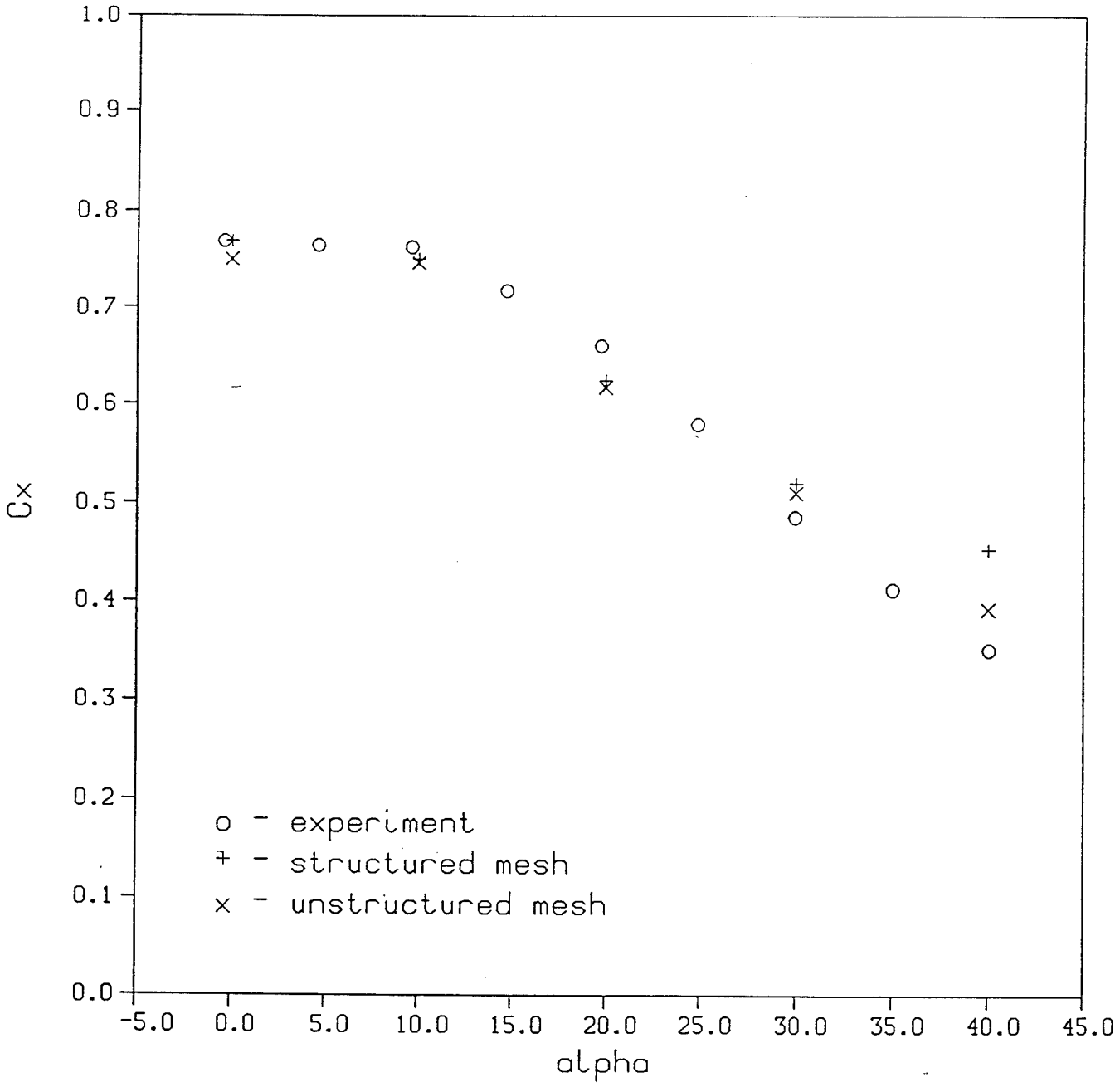

(a) Axial force coefficient

Figure 27. - Measured and predicted force on the SIIIS-3ER ejection seat, $M_\infty = 0.75$.

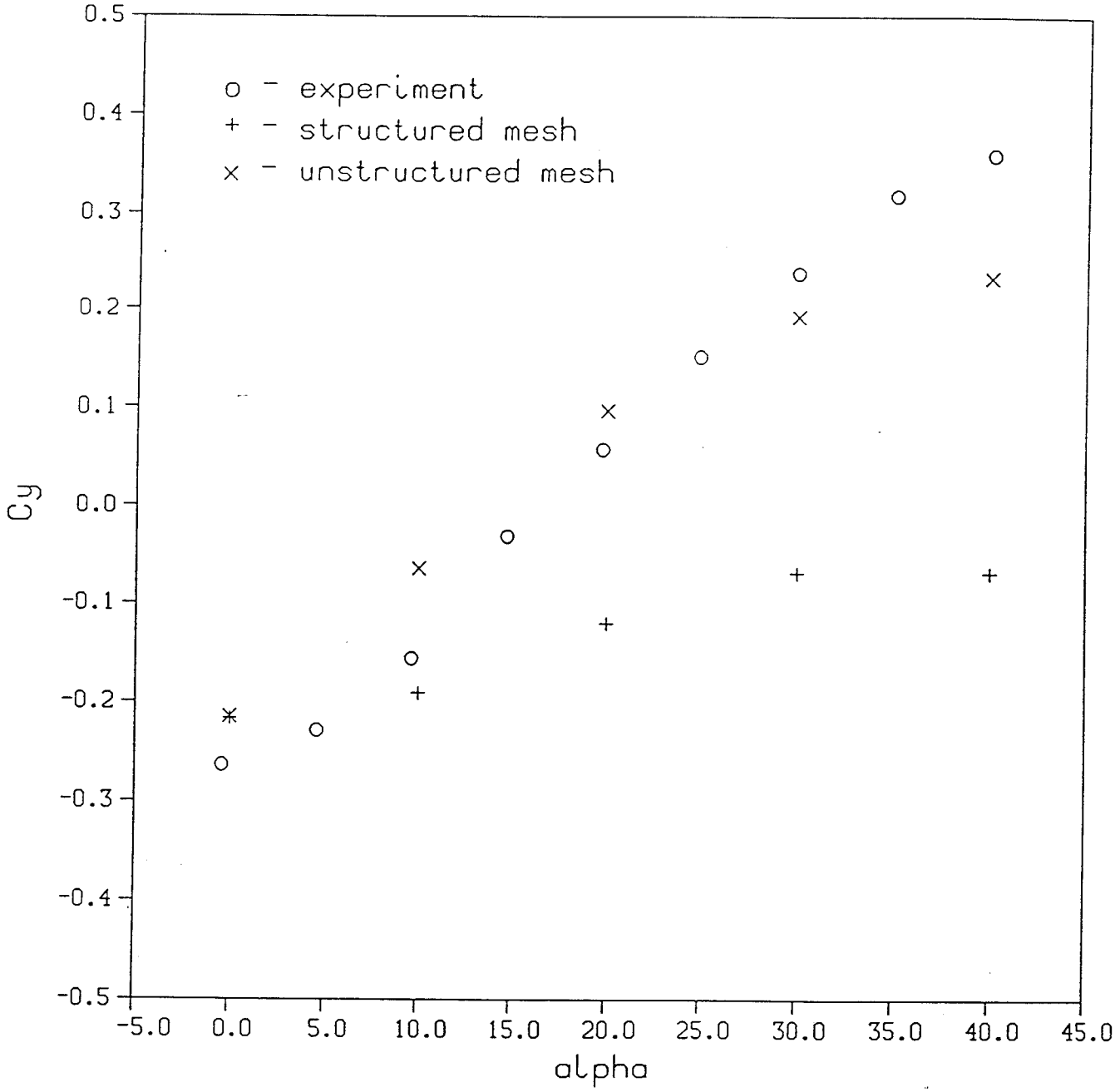

(b) Normal force coefficient

Figure 27. - Concluded.